

EVALUATION OF THE *IN VIVO* ROLE OF P-GLYCOPROTEIN IN
THE MAINTENANCE OF CHOLESTEROL HOMEOSTASIS

by

Stephen D. Lee

B.Sc. University of Victoria, 2002

A THESIS SUBMITTED IN PARTIAL FULFILLMENT OF
THE REQUIREMENTS FOR THE DEGREE OF

DOCTOR OF PHILOSOPHY

in

The Faculty of Graduate Studies

(Pharmaceutical Sciences)

THE UNIVERSITY OF BRITISH COLUMBIA

(Vancouver)

October 2012

© Stephen D. Lee, 2012

Abstract

Removal of cholesterol from the body is the final step in reverse cholesterol transport, the process by which excess cholesterol is moved from peripheral tissues to the liver for excretion. Several provocative studies led us to probe the contributions of P-glycoprotein (Pgp), an ATP-dependent transporter with broad range of hydrophobic substrates, to the removal of cholesterol and its bile acid metabolites from the body. We used knockout mice lacking both isoforms of Pgp (*Abcb1a*^{-/-}/*1b*^{-/-}) fed test diets containing elevated fat and/or cholesterol to determine if Pgp deletion affects murine cholesterol homeostasis. The knockout mice had the same cholesterol phenotype as wild-type mice, measured by cholesterol absorption, circulating lipoproteins, and hepatic storage of cholesterol.

We examined the activation of two key regulatory pathways that maintain cholesterol homeostasis, Sterol Regulatory Element Binding Protein-2 (SREBP-2) and Liver X Receptor (LXR), to determine if the knockout mice maintain cholesterol balance through compensatory mechanisms. The knockout mice had decreased expression of SREBP-2-target genes in the jejunum and increased expression of LXR-target genes in the liver. These perturbations to cholesterol regulatory networks are indirect evidence that the knockout mice lacked a cholesterol efflux mechanism.

We evaluated efflux of bile acids from the liver to the gallbladder in mice after nine weeks on the test diets. Knockout mice fed elevated fat or cholesterol had a 30-50% reduction in bile acid efflux capacity compared to wild type mice, suggesting that

Pgp contributes to murine bile acid efflux. Subsequent analysis revealed that Pgp did not display specificity for a particular class of bile acids.

In summary, we provide evidence that deletion of Pgp did not alter the cholesterol phenotype of mice; however, compensatory shifts in cholesterol regulatory networks maintained homeostasis in the knockout. Additionally, we show that Pgp knockout mice had a reduced capacity to efflux bile acids to the gallbladder. The nature of the changes to the cholesterol regulatory networks and the perturbations to bile acid efflux suggest that Pgp is a non-specific efflux transporter that recognizes both cholesterol and bile acids as substrates.

Preface

- At the time of writing, none of the work presented in this thesis has been published. We will submit two papers while the thesis is in external review:
 - (1) Chapters 3, 4, 5 will be submitted as a single paper. The authors are: Mr. Stephen Lee (designed all the experiments and performed all the work described in this thesis with the exceptions denoted below), Dr. Sheila Thornton (designed the *in vivo* experiments, assisted with the surgeries, co-investigator on the CIHR grant that funds this project), Dr. Kishor Wasan (advisor, principal investigator on the CIHR grant that funds this project).
 - (2) Chapter 6 will be submitted as a paper with three authors: Mr. Stephen Lee (performed all the work described in the thesis, designed all experiments, evaluated the data, will write the paper) Ms. Jo-Ann Osei-Twum (conducted studies evaluating the activity of Pgp using the model established in this thesis, she will assist with the writing), Dr. Kishor Wasan (advisor, principal investigator on the grant that funds this project).
- All protocols involving *in vivo* research described in this thesis were reviewed and approved by the University of British Columbia Animal Care Committee (Certificate number A05-0032).
- Some of the work presented in this thesis was performed in collaboration with David Cohen's laboratory at the Harvard Center for Digestive Diseases. For both the FPLC analysis of serum lipoproteins and the HPLC analysis of gallbladder bile acids, Stephen Lee collected and prepared the samples, the members of Dr.

Cohen's lab performed the analytical work in a blinded manner and sent the raw data back to Stephen for analysis.

Table of contents

Abstract	ii
Preface	iv
Table of contents	vi
List of tables	x
List of figures	xii
List of symbols and abbreviations	xiv
Acknowledgments	xvii
Dedication	xviii
Chapter 1: Literature review	1
1.1 Introduction	1
1.2 Cholesterol and cardiovascular disease	2
1.3 Lipoprotein biology	3
1.3.1 LDL-cholesterol and cardiovascular disease	6
1.3.2 HDL-cholesterol and cardiovascular disease.....	9
1.4 Reverse cholesterol transport	10
1.4.1 Cholesterol efflux from macrophages	11
1.4.2 Transport to the liver.....	13
1.4.3 Cholesterol trafficking in the liver	16
1.4.4 Cholesterol uptake and transport in the enterocyte.....	19
1.5 ABC transporters	22
1.5.1 P-glycoprotein.....	23

1.5.2 ABC transporters in cholesterol and bile acid homeostasis.....	27
1.5.3 P-glycoprotein as a cholesterol transporter	30
1.5.4 P-glycoprotein as a bile acid transporter.....	32
1.6 Transcriptional regulation of intracellular cholesterol	33
1.6.1 Liver X receptor responds to increased intracellular cholesterol	34
1.6.2 SREBP-2 is activated by low intracellular cholesterol.....	38
1.7 Bile acid homeostasis.....	43
1.7.1 Regulation of bile acid synthesis	43
1.7.2 Efflux of bile acids from the liver.....	46
1.7.3 Enterohepatic recycling of bile acids	47
1.8 Specific hypotheses tested in this thesis.....	50
1.9 Specific aims	51
Chapter 2: Methodology.....	52
2.1 Methods used in chapter 3	52
2.1.1 Animals.....	52
2.1.2 Reagents	52
2.1.3 Test diets.....	53
2.1.4 Cholesterol absorption studies	53
2.1.5 Quantification of circulating lipids.....	57
2.1.6 Lipoprotein profile determination	57
2.1.7 Quantification of fecal radiolabeled cholesterol and β -sitostanol.....	57
2.2 Methods used in chapter 4	59

2.2.1 Reagents	59
2.2.2 RNA isolation.....	59
2.2.3 Reverse transcription	60
2.2.4 Real time PCR.....	60
2.3 Methods used in chapter 5	66
2.3.1 Gallbladder bile acid quantification	66
2.3.2 Gallbladder lipid analysis.....	66
2.4 Methods used in chapter 6	66
2.4.1 Reagents	66
2.4.2 Culture conditions	67
2.4.3 Transfection.....	68
2.4.4 Characterization of the Caco-2 cells	69
2.4.5 Cholesterol uptake and esterification.....	71
2.4.6 Cholesterol synthesis	73
2.5 Data analysis.....	74
Chapter 3: Cholesterol phenotype of the <i>Abcb1a</i>^{-/-}/<i>1b</i>^{-/-} knockout mouse	75
3.1 Results	76
Discussion	83
3.1.1 Conclusions	88
Chapter 4: The effect of diet and P-glycoprotein deletion on cholesterol regulatory networks	89
4.1 Results	89

4.2 Discussion	98
Chapter 5: P-glycoprotein and the efflux of bile acids.....	104
5.1 Results.....	104
5.2 Discussion.....	114
Chapter 6: Transient knockdown of <i>ABCB1</i> in Caco-2 cells.....	119
6.1 Results.....	119
6.2 Discussion.....	129
Chapter 7: Conclusions and future directions	135
7.1 Summary of key findings.....	135
7.2 Summary of unanswered questions.....	136
7.3 Future studies.....	138
References	142

List of tables

Table 1-1: Lipid homeostasis genes up-regulated by LXR.....	38
Table 1-2: Genes that are up regulated by the SREBP-2 transcription factor.	42
Table 2-1: Composition of the test diets.	53
Table 2-2: Summary of the TaqMan gene expression assays	63
Table 2-3: Efficiency, limit of quantification and reproducibility of the PCR reaction...	64
Table 2-4: Summary of controls in the RT-qPCR experiments.....	65
Table 2-5: Western blot antibodies	71
Table 3-1: Plasma cholesterol in the pilot study mice.....	77
Table 3-2: Plasma cholesterol levels after 12 weeks on the HFHC diet (Study#2).....	80
Table 3-3: Effect of diet and deletion of P-glycoprotein on serum cholesterol parameters after nine weeks on the test diets.....	81
Table 3-4: Accumulation of cholesterol in the livers of wild type and knockout mice.	83
Table 4-1: Summary of changes to the transcriptional networks in the jejunum of wild type FVB mice induced by dietary conditions.....	91
Table 4-2: Summary of changes to transcriptional networks in the jejunum of <i>Abcb1a^{-/-}/1b^{-/-}</i> mice induced by dietary conditions.....	92
Table 4-3: Summary of the changes to transcriptional networks in the livers of wild type FVB mice induced by dietary conditions.....	93
Table 4-4: Summary of the changes to transcriptional networks in the livers of <i>Abcb1a^{-/-}/1b^{-/-}</i> mice induced by dietary conditions.....	94
Table 4-5: Accumulation of cholesterol in the jejunum.	98

Table 5-1: Assessment of global homology between the amino acid sequence of murine P-glycoprotein (ABCB1A: *Mus musculus*) and members of the ABC transporter superfamily associated with drug resistance..... 112

Table 5-2: Assessment of global homology between the amino acid sequence of human P-glycoprotein (ABCB1: *Homo sapiens*) and members of the ABC transporter superfamily associated with drug resistance..... 113

List of figures

Figure 1-1: General structure of a lipoprotein.....4

Figure 1-2: Lipoprotein metabolism.....8

Figure 1-3: Models for Pgp-mediated transport of drugs..... 26

Figure 1-4: The role of ABC transporters in the macrophage reverse cholesterol
transport pathway..... 28

Figure 1-5: Endogenous production of cholesterol and oxysterols..... 35

Figure 1-6: SREBP-2 is activated by low intracellular cholesterol..... 41

Figure 1-7: Overview of murine bile acid synthesis. 45

Figure 1-8: Effects of FXR on the enterohepatic circulation of bile acids..... 48

Figure 3-1: Cholesterol absorption calculated from the pilot study (Study #1). 78

Figure 3-2: Plasma dual isotope cholesterol absorption assay (Study #2)..... 79

Figure 3-3: Effect of diet and P-glycoprotein deletion on fractional cholesterol
absorption. 80

Figure 3-4: Effects of P-glycoprotein deletion on lipoprotein cholesterol. 82

Figure 4-1: Effects of diet on the expression of *Abcb1a* in the jejunum. 95

Figure 4-2: Effects of diet on the expression of *Abcb1a* in the liver. 95

Figure 4-3: Effect of *Abcb1a/1b* deletion on SREBP-2 and LXR activity in the jejunum. 96

Figure 4-4: Effect of *Abcb1a/1b* deletion on SREBP-2 and LXR activity in the liver..... 97

Figure 4-5: Intracellular responses to increased cholesterol. 102

Figure 5-1: Effects of *Abcb1a/1b* deletion and diet on the molar composition of bile
constituents. 106

Figure 5-2: Effect of <i>Abcb1a/1b</i> deletion on gallbladder bile phospholipid content. .	107
Figure 5-3: Effect of <i>Abcb1a/1b</i> deletion on bile acid efflux to the gallbladder.	108
Figure 5-4: Effects of <i>Abcb1a/1b</i> deletion on the molar composition of the bile acid pool.....	109
Figure 5-5: Cumulative fecal excretion of polar ¹⁴ C derived from [¹⁴ C]-cholesterol.	110
Figure 5-6: Mass of gallbladders after a 60min ligation of the common bile duct.....	111
Figure 6-1: Dose response of the <i>ABCB1</i> -targeting siRNA construct HSS182278.	121
Figure 6-2: Dose response of the <i>ABCB1</i> -targetting siRNA construct HSS107919.....	122
Figure 6-3: Dose response of the <i>ABCB1</i> -targeting siRNA construct HSS107918.	123
Figure 6-4: Representative figure showing formation of a confluent Caco-2 monolayer with tight junctions within 4 days growth on a polycarbonate membrane.....	124
Figure 6-5: Time dependent silencing of Pgp using the HSS182278 siRNA construct.	125
Figure 6-6: Time dependent silencing of Pgp using the HSS107919 siRNA construct.	126
Figure 6-7: Detection of sucrase-isomaltase in Caco-2 cells treated with the HSS182278 siRNA construct.....	127
Figure 6-8: Detection of sucrase-isomaltase in Caco-2 cells treated with the HSS107919 siRNA construct.....	127
Figure 6-9: Cholesterol uptake and esterification in silenced Caco-2 cells.	128
Figure 6-10: Cholesterol synthesis and esterification in silenced Caco-2 cells.	129

List of symbols and abbreviations

A note on nomenclature: I have endeavored to follow the official nomenclature rules for genes and proteins published by the HUGO gene nomenclature committee(1) and the International Committee for Standardized Genetic Nomenclature in Mice(2).

Consequently, all genes symbols are in italics, those from *Homo sapiens* use all capital letters while only the first letter of the symbol is capitalized for *Mus musculus*. For both species, the protein symbol is denoted in capital letters (no italics). The official gene and protein symbols, obtained from the Genbank database(3), are used throughout this thesis with two notable exceptions:

- The official name for P-glycoprotein is ABCB1 (encoded by *ABCB1* in humans and *Abcb1a* and *Abcb1b* in mice), for clarity, this protein is abbreviated as Pgp throughout the thesis
- The official name for the Bile Salt Export Pump is ABCB11 (encoded by the *ABCB11* gene in humans and the *Abcb11* gene in mice), for clarity this protein is abbreviated as BSEP throughout the thesis

Acronym	Explanation
ABC	ATP-binding cassette
ACAT	Acyl-CoA cholesterol acyltransferase
APO	Apolipoprotein
ASBT	Apical sodium-dependent bile acid transporter
BCA	Bicinchoninic acid assays
BSA	Bovine serum albumin
BSEP	Bile salt export pump (encoded by <i>ABCB11</i>)
CE	Cholesteryl ester
CETP	Cholesteryl ester transfer protein
Ct	Threshold cycle - the calculated number of PCR cycles required for the fluorescence of the cleaved TaqMan probes to increase beyond background. This corresponds to the beginning of the exponential phase of the PCR reaction.
CVD	Cardiovascular disease
CYP7A1	Cytochrome P450 isoform 7A1
DAPI	4',6-Diamidino-2-phenylindole, dihydrochloride - a fluorescent DNA stain
DMEM	Dulbecco's modified eagle medium
DR4	Direct repeat 4 sequence: a six base pair DNA sequence that is repeated after separation by four base pairs
EDTA	Ethylenediaminetetraacetic acid
EL	Endothelial lipase
FBS	Fetal bovine serum
FC	Free cholesterol
FGF	Fibroblast growth factor
FGFR	Fibroblast growth factor receptor
FPLC	Fast protein liquid chromatography
FXR	Farnesoid X receptor
HDL	High-density lipoprotein
HFHC	High fat high cholesterol diet (45% kcal derived from fat with 0.2% w/w cholesterol)
HFNC	High fat normal cholesterol diet (45% kcal derived from fat with 0.02% w/w cholesterol)
HL	Hepatic lipase
HMGCR	3-Hydroxy-3-methylglutaryl-CoA reductase
HNF-4 α	Hepatocyte nuclear factor 4 α
HRP	Horseradish peroxidase
IDOL	Inducible degrader of the LDL receptor
INSIG	Insulin induced gene
JNK	c-Jun NH(2)-terminal protein kinases

KO	Knockout mice (<i>Abcb1a^{-/-}1b^{-/-}</i> backcrossed onto an FVB background for 12 generations)
LCAT	Lecithin cholesterol acyltransferase
LDL	Low-density lipoprotein
LDLR	LDL receptor
LPL	Lipoprotein lipase
LRH-1	Liver receptor homolog-1
LXR	Liver X receptor
MGAT	Acyl-CoA monoacylglycerol acyltransferase
miR	Micro RNA
MTP	Microsomal triacylglycerol transfer protein
NFHC	Normal fat high cholesterol diet (25% kcal derived from fat with 0.2% w/w cholesterol)
NFNC	Normal fat normal cholesterol diet (25% kcal derived from fat with 0.02% w/w cholesterol)
NTCP	sodium taurocholate cotransporting peptide
OATP	Organic anion transporting polypeptide
OST	Organic solute transporter
PBS	Phosphate buffered saline (0.9% w/w) pH 7.4
PFIC	Progressive familial intrahepatic cholestasis
Pgp	P-glycoprotein (encoded by <i>ABCB1</i>)
PLTP	Phospholipid transfer protein
PPAR	Peroxisome proliferator-activated receptor
PXR	Pregnane X receptor
RCT	Reverse cholesterol transport
RXR	Retinoid X receptor
SCAP	SREBP cleavage activating protein
SCARB1	Scavenger receptor class B type 1
SHP	Small heterodimer partner
SREBP	Sterol regulatory element binding protein
TBS-T	Tris buffered saline containing 0.1% (v/v) tween-20.
TE buffer	10mM Tris-HCl, 1mM EDTA buffer; pH 7.5
TEER	Transepithelial electrical resistance
VLDL	Very low-density lipoprotein
WT	Wild type mice (FVB strain)

Acknowledgments

My passion for science comes from having had some wonderful academic mentors. Without the inspiration from my undergraduate advisor, Dr. Ed Ishiguro, I would never have contemplated graduate school. My graduate advisor, Dr. Kishor Wasan, helped me to transition from an undergraduate student to technician and finally to a Ph.D. student. His constant enthusiasm and support have made this an enjoyable and fruitful process.

I would like to thank my advisory committee, Dr. John Hill, Dr. Marc Levine, Dr. Gordon Francis and Dr. Wayne Riggs. You have helped guide me and given me the intellectual and moral support that I needed over the past six years. I have thoroughly enjoyed the discussions that I have had with each of you.

Finally I would like to thank the people in Dr. Wasan's laboratory. I will always be thankful to Dr. Kristina Sachs-Barrable and Dr. Sheila Thornton for showing me on a daily basis what it means to be a good scientist and a good friend. Without Jackie Fleischer, Alexis Twiddy, and Jo-Ann Osei-Twum I don't think that I would have survived the failed experiments, contradictory data, and all the other frustrating moments that are part of the graduate school experience. Each of you is an amazing person and I consider myself quite fortunate to know you. Finally, I would like to thank all the other people in Dr. Wasan's lab and in the Faculty of Pharmaceutical Sciences who made my time here such a positive experience.

Dedication

This is dedicated to my parents and my wonderful wife, Tracy. Without your support and faith in me, I would not be the person I am today.

Chapter 1: Literature review

1.1 Introduction

Maintaining cholesterol homeostasis *in vivo* is achieved through the coordinated interplay of trafficking, biosynthesis, absorption, and efflux of cholesterol. The liver regulates the movement of cholesterol through the circulatory system and removes excess cholesterol from the body, either through the catabolism into bile acids or direct secretion into bile via ATP-binding cassette (ABC) transporters(4, 5). The dimer formed by the half transporters ABCG5 and ABCG8 is the primary efflux mechanism for cholesterol from cells of the small intestine and the liver. In the absence of ABCG5/ABCG8, there is unregulated cholesterol uptake by enterocytes in the jejunum(6). Similarly, deletion of AGCG5 and ABCG8 in mice demonstrates that the dimer is responsible for up to 90% of the secretion of cholesterol from hepatocytes to bile. Interestingly, cholesterol efflux from the liver is diminished but not completely ablated in *Abcg5^{-/-}/g8^{-/-}* mice, (7) suggesting that a secondary mechanism for the removal of cholesterol must exist(8). This idea is supported by a clinical observation in a small cohort(9). Similarly, excess cholesterol that is converted to bile acids in the liver is removed at the apical face of hepatocytes through the ABC transporter encoded by *ABCB11*, commonly referred to as the Bile Salt Efflux Pump (BSEP). Deletion of *Abcb11* reduces bile acid output by 70% but an unidentified secondary mechanism maintains sufficient bile acid transport to prevent cholestasis(10). There are several lines of evidence suggesting that the ABC

transporter encoded by the *ABCB1* gene, P-glycoprotein (Pgp), may be the secondary removal mechanism postulated for both cholesterol and bile acids(10-12). The purpose of the experiments described in this thesis is to determine if Pgp contributes to the efflux of cholesterol and/or bile acids after chronic exposure to a range of physiologically relevant diets.

1.2 Cholesterol and cardiovascular disease

From the original discovery that atherosclerotic plaques contain >20-fold more cholesterol than a healthy aorta to the discovery of the importance of mutations to the LDL-receptor in the rare genetic disease, Familial Hypercholesterolemia, cholesterol has been studied for its links to cardiovascular disease (CVD). The complexity of studying cholesterol comes from the paradox: cholesterol is crucial for normal biological functions including hormone synthesis, bile acid synthesis and maintaining cell membrane fluidity; however, excess circulating cholesterol, hypercholesterolemia, is associated with CVD. The evidence linking cholesterol to heart disease comes from epidemiology studies(13-15), genetic linkages(6, 16, 17), experimental models(18, 19), and therapeutic intervention(20). Despite tremendous gains in our understanding of CVD, it remains the leading cause of mortality worldwide(21, 22). CVD is a complex disease with a range of etiologies and ischemic heart disease, the clinical manifestation of atherosclerosis, accounts for the majority of CVD-related deaths in Canada(23). Atherosclerosis is the gradual formation of lipid-rich plaque accompanied by thickening of the arterial wall, a complex process that spans decades and involves lipid deposition, oxidative stress and inflammation(24,

25). Hypercholesterolemia, elevated circulating cholesterol, is an important predictor of CVD, but a patient's lipoprotein profile gives a better prediction of risk(26-29).

Cholesterol is hydrophobic and requires specialized carriers for transportation through the aqueous circulatory system. These macromolecular vehicles, called lipoproteins (see Figure 1-1), are composed of a hydrophobic core of cholesteryl esters and triacylglycerol surrounded by a polar phospholipid coat and scaffold proteins called apolipoproteins (APO). Apolipoproteins confer structure to the lipoprotein and act as ligands for receptors and enzymes, which are important to the disposition of the lipoprotein (Figure 1-2).

1.3 Lipoprotein biology

Lipoproteins are spherical or discoidal particles with diameters ranging from 3.6nm to 6 μ m that carry lipids and lipid soluble chemicals through the aqueous environment of the circulatory system(30, 31). The core of a lipoprotein consists of hydrophobic molecules including triacylglycerol and esterified cholesterol. The outer surface of a lipoprotein is composed of a phospholipid monolayer (with polar head groups that facilitate solubilization) interspersed with amphiphilic molecules, such as unesterified cholesterol and specialized proteins called apolipoproteins (Figure 1-1).

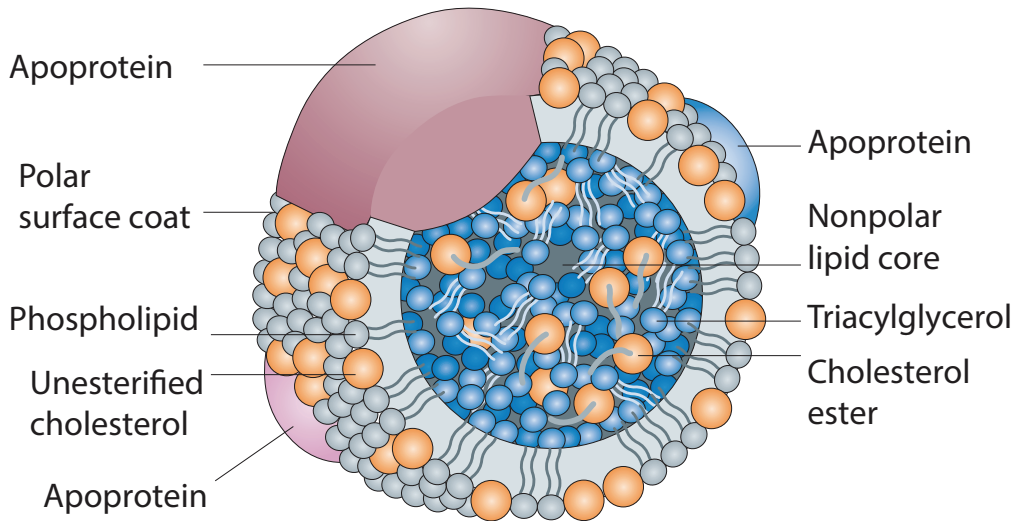


Figure 1-1: General structure of a lipoprotein.

The core is primarily composed of triacylglycerol and cholesterol esters. They are encased by a phospholipid monolayer. Apolipoproteins embedded in the phospholipid layer confer structural and functional properties to the molecule. Reprinted by permission from Macmillan Publishers Ltd: Nature Reviews Drug Discovery (32), copyright 2008 (<http://dx.doi.org/10.1038/nrd2353>)

There are two classification systems for lipoproteins. The density of the particles most commonly defines them, but historically they were also distinguished by electrophoretic mobility. The density nomenclature includes high-density lipoprotein (HDL: $1.063 < \delta < 1.21$ g/mL), low-density lipoprotein (LDL: $1.006 < \delta < 1.063$ g/mL), very low-density lipoprotein (VLDL: $0.94 < \delta < 1.006$ g/mL), and the largest of the particles, the chylomicron ($\delta < 0.94$ g per mL). Lipoproteins have additionally been classified by their electrophoretic mobility as α (HDL), pre- β (VLDL) and β (LDL) (chylomicrons do not exhibit electrophoretic mobility)(31, 33-35).

Chylomicrons are produced and secreted from the intestinal tract. They are primarily composed of triacylglycerol (80–88% weight by weight). Each chylomicron contains a truncated form of APOB, referred to as APOB-48 (a unique RNA editing

process creates a peptide that is 48% of the size of the mature APOB) (36).

Chylomicrons are secreted containing an exchangeable apolipoprotein, APOA1, which is immediately transferred to the HDL particles. Chylomicrons are rapidly cleared from the bloodstream by lipoprotein receptors in the liver, where the triacylglycerol content is repackaged into nascent VLDL particles.

VLDL begins with the synthesis, lipidation, and secretion of a single APOB polypeptide that moves triacylglycerol from the liver to the peripheral tissues. Consequently, they are primarily composed of triacylglycerol (45–50% w/w), but also contain both free and esterified cholesterol. VLDL has a particle size ranging from 30–80nm in diameter. Up to 90% of the VLDL triacylglycerol content is cleaved by lipases in the endothelium for use by peripheral tissues. The VLDL remnants are partially cleared by hepatic lipoprotein receptors, but the majority (~70%) remain in the plasma for subsequent conversion to LDL through the loss of APOE and remodeling by lipid transfer proteins in circulation (37, 38) (Figure 1-2). LDL is the stable product of VLDL catabolism. LDL particles range in size from 22 to 28 nm in diameter(27, 39, 40) and are cleared from the system by the LDL-receptor(LDLR) (17). Each LDL particle is composed primarily of cholesterol and cholesteryl esters and contains a single molecule of APOB-100.

HDL is a heterogeneous mixture of lipoproteins with particle size <12nm. The defining characteristic of HDL is the relatively high apolipoprotein content (35–56% w/w), primarily composed of APOA1 and APOA2. HDL contains relatively high esterified cholesterol, due to the circulating enzyme lecithin–cholesterol acyltransferase (LCAT) (41, 42). Some of the cholesteryl ester content is exchanged for

triglycerides from VLDL or LDL through the actions of the cholesteryl ester transfer protein (CETP) (43, 44). HDL-cholesterol is cleared by the liver through the actions of scavenger receptor class B type 1 (SCARB1, commonly abbreviated as SR-B1: Figure 1-2) (45-47).

***Please note that the preceding section was taken from my contributions to the Wasan *et al.* review paper with permission from the publisher(32).

1.3.1 LDL-cholesterol and cardiovascular disease

There is strong evidence linking elevated LDL-cholesterol with increased risk of CVD. High levels of LDL-cholesterol in a population increases the risk of CVD(13, 14, 48-50), genetic diseases that raise LDL levels increase risk of CVD(24), and pharmacological lowering of LDL-cholesterol reduces the risk of CVD(20, 51-59). Based on these findings, medical researchers have used a variety of techniques to elucidate causative mechanisms by which LDL-cholesterol contributes to CVD. As shown in Figure 1-2, LDL carries cholesterol from the liver, depositing it in peripheral tissues as part of the “forward cholesterol transport” pathway. The initial formation of an atherosclerotic lesion involves lipid deposition and retention of APOB-containing lipoproteins in the endothelium(25). The findings of several clinical studies suggest that measuring small dense LDL particles may better predict CVD risk than simply measuring LDL-cholesterol, though the mechanism through which these particles increase the risk of CVD remains to be explained(27, 39, 60). Oxidation of circulating LDL creates epitopes recognized by scavenger receptors on macrophages in the endothelial space. Because oxidized LDL is recognized by more receptors, there is

increased uptake and retention leading to the formation of lipid-laden macrophages, called foam cells(61-63). Lipid overloading in foam cells induces the cells to produce pro-inflammatory cytokines, initiating an inflammatory state (24, 64).

Pharmacological reduction of LDL-cholesterol is most commonly achieved by treatment with statins, a class of drugs that inhibit HMG CoA Reductase, the enzyme that catalyzes the rate-limiting step in the biosynthesis of cholesterol (see Figure 1-5). Large clinical trials with statins demonstrate that pharmacological intervention can improve life expectancy and reduce the risk of serious coronary events(52-55, 57-59, 65). A meta-analysis of >100000 patients in 14 studies demonstrates that there is a 22% reduction in risk of a major coronary event for every 1mmol/L reduction in circulating LDL-cholesterol(20). As the evidence linking LDL-cholesterol levels with CVD risk becomes clearer, there is a clinical imperative for further reductions in LDL-cholesterol(51). Consequently, current clinical guidelines call for reductions in LDL cholesterol to less than 2.5mmol/L (100mg/dL) for patients with moderately high risk or high risk for CVD(28, 29, 66). Although treatment with statins reduces mortality rates due to CVD, up to 67% of patients receiving treatment continue to have CVD-related events(67). Thus, further research is needed to understand the biological nature of these events and to develop effective treatments to work as adjuncts with statin therapy to further reduce CVD mortality and morbidity.

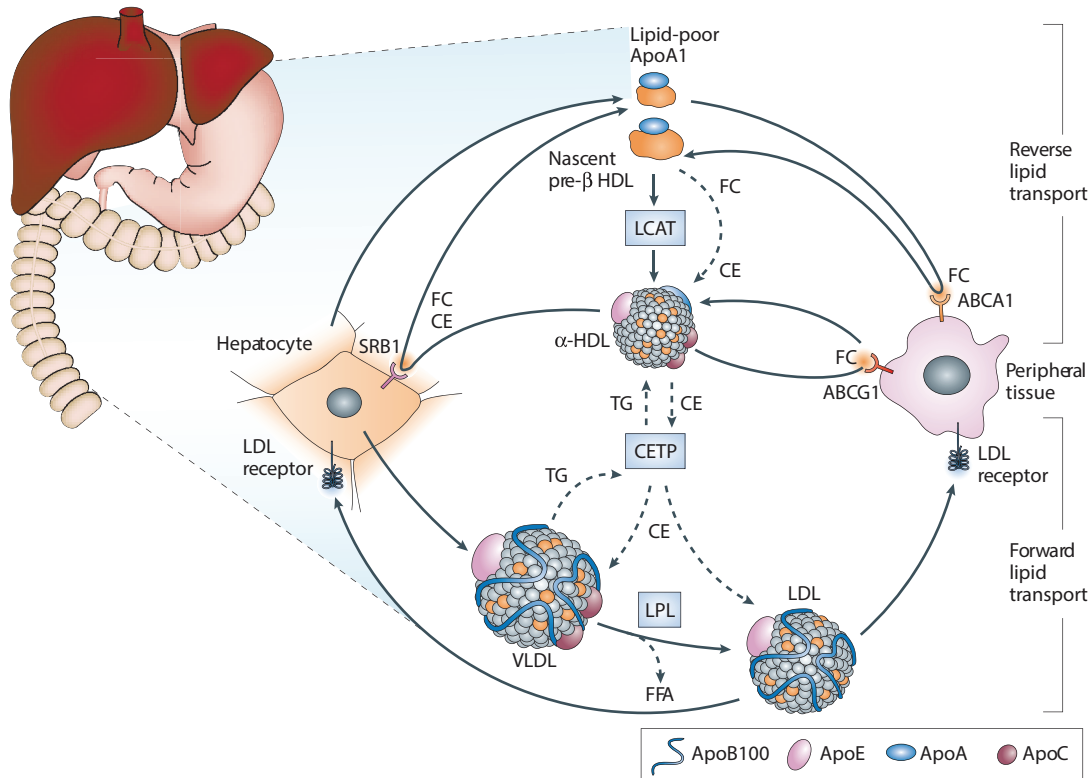


Figure 1-2: Lipoprotein metabolism.

During reverse lipid transport, apolipoprotein A1 (APOA1) synthesized in hepatocytes and enterocytes is released as lipid-poor APOA1. These particles bind to ATP-binding cassette transporter A1 (ABCA1) located on the surface of peripheral cells, leading to the transfer of unesterified (free) cellular cholesterol (FC). As the discoidal lipid-poor APOA1 accumulates cholesterol, the particles become nascent pre-β high-density lipoproteins (HDL). Remodeling by lecithin-cholesterol acyltransferase (LCAT), phospholipid transfer protein (PLTP) and cholesteryl ester transfer protein (CETP) completes the transformation to α-HDL. The mature HDL particles continue to collect free cholesterol from peripheral tissues through the action of ATP binding cassette transporter G1 (ABCG1). HDL-cholesterol is cleared from the bloodstream by scavenger receptor B1 (SR-B1) on the surface of hepatocytes. In forward lipid transport, very low-density lipoproteins (VLDL) are secreted from the liver as vehicles to transport triglycerides to the peripheral tissues. The lipolytic action of lipoprotein lipase (LPL) results in the release of free fatty acids (FFA) and monoacylglycerol from the VLDL particles. As the VLDL particles are remodeled, they become the target of lipid transfer proteins such as CETP, which complete the transformation to a stable intermediate known as low-density lipoproteins (LDL). LDL particles are removed from circulation by LDL receptors. Solid lines represent lipoprotein pathways; dashed lines represent the transfer of lipids. CE, cholesterol ester; TG, triglyceride. Reprinted by permission from Macmillan Publishers Ltd: Nature Reviews Drug Discovery ((32)), copyright 2008 (<http://dx.doi.org/10.1038/nrd2353>)

1.3.2 HDL-cholesterol and cardiovascular disease

In contrast with LDL, population studies demonstrate that HDL-cholesterol levels are inversely associated with cardiovascular risk(13, 26, 50, 68-75). Consequently, HDL-cholesterol levels of less than 1.00mmol/L (38.7mg/dL) are defined as an independent risk factor for CVD by the National Cholesterol Education Program in the U.S.A. (28). The first evidence of the cardioprotective role of HDL was a small case-control study published in 1975 by Miller *et al.* (76). There has been considerable interest in understanding the mechanisms by which HDL may reduce CVD risk. Several theories for this phenomenon include anti-inflammatory activity, anti-oxidant activity, vasoprotective actions and inhibition of the coagulation cascade. Each of these mechanisms may contribute to a reduction in CVD risk but the primary mechanism by which HDL is thought to protect the cardiovascular system is through the movement of cholesterol from peripheral tissues, including atheroma, to the liver for removal from the body in a process called Reverse Cholesterol Transport (RCT):

Figure 1-2. Testing whether HDL is cardioprotective or simply a biomarker for reduced CVD risk has been challenging due to the lack of pharmacological interventions that raise levels of functional HDL. *Scarb1*^{-/-} mice bred with *ApoE*^{-/-} or *Ldlr*^{-/-} mice demonstrate the importance of increasing functional HDL-cholesterol. These mice develop premature atherosclerosis and mortality, despite having significant increases to HDL-cholesterol levels(77-79).

Current HDL-raising therapies can only achieve modest increases to HDL-cholesterol: Niacin (15-30% increase), Fibrates (10-15% increase), and Thiazolidinediones (5-10% increase) (24, 80, 81). Clinical trials with these compounds

have failed to clearly demonstrate reduced risk of CVD associated with increased HDL-cholesterol levels. Recent clinical trial results with CETP inhibitors demonstrate that HDL-cholesterol levels can be raised by >100%, accompanied by decreases to LDL-cholesterol(82). Other approaches to increase HDL-cholesterol include infusions with APOA1(83-85), *APOA1* up regulation(86), or treatment with glitazars, agonists of multiple isoforms of the nuclear receptor peroxisome proliferator-activated receptor (PPAR) (87, 88). It is hoped that subsequent studies using these new pharmacological agents will demonstrate that intervention can replicate the cardioprotective effects of HDL seen in epidemiology studies(43, 81).

1.4 Reverse cholesterol transport

The hypothesized cardioprotective role of HDL-cholesterol is derived from the role of HDL in the flux of cholesterol from atherosclerotic lesion for eventual excretion into feces. This concept that HDL was responsible for the net flux of cholesterol from the body was first hypothesized in 1968 and remains an area of active investigation nearly half a century later(43, 89, 90). Although the RCT pathway involves the net flux of cholesterol from all peripheral tissues to the liver, recent research has focused specifically on the flux of cholesterol from macrophages to feces(25). This occurs in four continuous phases: **(A)** unesterified cholesterol is abstracted from the macrophage in the atherosclerotic plaque by HDL, **(B)** cholesterol is transported through the circulatory system to the liver, **(C)** cholesterol is processed by the liver for

excretion, and (D) some of the cholesterol is taken up by absorptive cells in the jejunum for transport back into the body, while the remainder is excreted in feces.

1.4.1 Cholesterol efflux from macrophages

After lipoprotein deposition, one of the first stages of atherosclerotic development is the migration of monocytes into the intima, the small space between the endothelium and the smooth muscle of the vessel wall(25). In the intima, monocytes differentiate into macrophages and take up APOB-containing lipoproteins by phagocytosis. Cholesteryl esters taken up from lipoproteins are hydrolyzed to free cholesterol and fatty acids in the late endosome, excess free cholesterol is trafficked to the endoplasmic reticulum, where it is re-esterified for storage in lipid droplets(91). These lipid-laden macrophages, called foam cells due to their appearance, continue to engulf lipoproteins and oxidized lipoproteins, eventually releasing inflammatory cytokines and chemokines, initiating an inflammatory response(64, 92). The removal of cholesterol from macrophages and foam cells is deemed to be a key step in the prevention and perhaps regression of atherosclerosis(44, 93). Excess cholesterol can be effluxed by one of four known mechanisms: ABCA1-mediated, ABCG1-mediated, SCARB1-mediated, or aqueous diffusion(93, 94).

Mutations in *ABCA1* cause Tangier disease, a rare autosomal disease characterized by an absence of HDL-cholesterol and increased atherosclerosis(95-97). Studies using fibroblasts from Tangier disease patients demonstrate that while flux of cholesterol to mature HDL is only diminished by 30-50%, the cells are completely unable to efflux cholesterol to lipid poor APOA1(98, 99), suggesting that ABCA1 is

responsible for the flux of cholesterol to nascent lipid poor APOA1 (Figure 1-2). The importance of ABCA1 to macrophage cholesterol efflux was confirmed using macrophages isolated from *Abca1*^{-/-} mice(100, 101).

The half transporter ABCG1 was proposed to account for the ABCA1-independent flux of cholesterol to HDL (102). Knockout mice lacking *Abcg1* have unchanged circulating lipid levels but have accumulations of cholesterol in their macrophages, apparently confirming the role of ABCG1 in macrophage efflux to mature HDL(103). Further analysis revealed that ABCG1 effluxes cholesterol to a range of acceptor molecules, with varying affinity including phosphatidylcholine vesicles > LDL > reconstituted HDL > spherical HDL particles(104, 105). New studies suggest that ABCG1 is an intracellular protein(106), suggesting that it is an intracellular sterol transporter, consistent with the high affinity for phosphatidylcholine membrane acceptors. Additional studies are required to determine the precise mechanism by which ABCG1 facilitates cholesterol efflux to HDL.

The scavenger receptor SCARB1 has been implicated in cholesterol efflux using *in vitro* models(94) but these findings are not consistent with *ex vivo* studies using knockout mice(100, 107). This discrepancy is perhaps explained by the bi-directional nature of SCARB1-mediated sterol flux. Expressing *SCARB1* in cell culture increases the efflux of free cholesterol in a phospholipid dependent manner(108, 109). The flux of cholesterol, similar to aqueous diffusion, is bidirectional, down the concentration gradient(94, 110). Using precise growth conditions, SCARB1-mediated cholesterol efflux is observed in a range of cell types but this observation may lack physiological

relevance as the influx of cholesterol is 2-3-fold higher than efflux when the cells are incubated with human serum(111).

Aqueous diffusion is the final mechanism for the efflux of cholesterol. Like SCARB1-mediated efflux, this passive model is driven by a concentration gradient. Cholesterol is only sparingly soluble in water (4.7 μ M) and spontaneously self assembles at 25nM(112, 113). Consequently, while aqueous diffusion is possible, the process is limited by the desorption rate from the membrane and has only been characterized *in vitro*. Up to 35% of the total cholesterol efflux has been attributed to aqueous diffusion(90), though this value was derived after subtracting the efflux attributable to ABCA1, ABCG1, and SCARB1 rather than direct measurement of aqueous diffusion(107). Until aqueous diffusion can accurately be determined to account for the unexplained efflux, the possibility remains that other active mechanisms for macrophage cholesterol efflux may yet be discovered.

1.4.2 Transport to the liver

The formation of HDL begins with the synthesis of APOA1 in hepatic and intestinal cells. As APOA1 is secreted, the hydrophobic regions of the polypeptide are lipidated with phospholipid and cholesterol. The precise mechanisms involved in the biogenesis of HDL are still being investigated and may include the lipid transfer activity of ABCA1. Poorly lipidated APOA1 is secreted from the cells as a discoidal, pre- β migrating, HDL particle. Nascent HDL acts as an acceptor for ABCA1-mediated efflux of unesterified cholesterol and phospholipid in a multistep process described in section 1.4.1. Five different enzymes in the circulatory system modify HDL in the

process of macrophage RCT, only two of which are shown in Figure 1-2. The free cholesterol content of HDL is esterified in circulation by LCAT, an enzyme synthesized primarily in the liver(114). LCAT binds to phospholipid in HDL before interacting with APOA1, with preferential association to small HDL molecules(115). It catalyzes the cleavage of the *sn*-2 fatty acid from phosphatidylcholine and the subsequent esterification of the 3-hydroxyl group of cholesterol with the fatty acid released in the cleavage reaction(114).

As the cholesteryl ester content increases in the HDL particle, its shape becomes more spherical and it is recognized by CETP. CETP catalyzes the exchange of cholesteryl ester from HDL for triacylglycerol from APOB-containing lipoproteins. The actions of CETP contribute to the remodeling of HDL to more spherical shape as well as aiding in the maturation of intermediate density VLDL to LDL. The cholesteryl ester content in LDL may contribute to RCT if it is cleared by hepatic LDL receptors; alternately, it may be deposited back into peripheral tissues including the atherosclerotic lesion. CETP has been targeted pharmacologically because it decreases HDL-cholesterol levels. Although CETP inhibition can raise HDL-cholesterol levels by 70-100%(82, 116), there is considerable debate whether the HDL molecules formed in this manner will be dysfunctional and whether CETP inhibition will reduce atherosclerosis(44, 117-119).

HDL is further remodeled by actions of another lipid transfer protein, PLTP. In circulation PLTP facilitates the transfer of phospholipids from triacylglycerol rich lipoproteins to HDL(120). This transfer produces two types of HDL particles: small phospholipid rich (pre- β) HDL and relatively large spherical α -HDL. Two mechanisms

are proposed by which PLTP produces both particle types(121). The first involves the dissociation of phospholipid-rich ApoA1 upon PLTP binding leading to the fusion of unstable PL-depleted HDL particles into a stable α -HDL(122). The second proposed mechanism begins with the formation of an unstable fusion of HDL particles, from which small, stable pre- β HDL dissociates with the stabilization of a large HDL particle(123). The production of more pre- β HDL provides additional acceptors for ABCA1-mediated cholesterol efflux, thereby increasing the capacity for RCT(124). In addition to remodeling HDL in circulation, PLTP may stabilize the association between ABCA1 and APOA1, thereby increasing the flux of cholesterol onto nascent HDL(125).

HDL particles are also remodeled by several lipases that are tethered to the cell walls of the endothelium by heparan sulfate proteoglycans. Macrophages and endothelial cells produce Endothelial Lipase (EL). The phospholipase activity of EL cleaves the fatty acid from the *sn*-1 position of HDL phospholipids. EL is considered pro-atherogenic because increased circulating levels correlate with increased adiposity and increased CVD(126). However, further analysis indicates that EL protein levels are induced in response to inflammation(127), making it difficult to determine whether the increased EL was secondary to an undetermined causative factor. Interestingly, *in vitro* studies demonstrate that EL may enhance cholesterol efflux from macrophages, suggesting that it may contribute to macrophage RCT(128).

Hepatic lipase (HL) is produced in the liver, and is bound to heparan-sulfate proteoglycans on the sinusoidal membranes of hepatocytes. HL has both phospholipase and triacylglycerol lipase activities: it cleaves the *sn*-1 fatty acid from phospholipids and both the *sn*-1 and *sn*-3 fatty acids from triacylglycerol. The

triacylglycerol content that HDL acquires through the actions of CETP is released by the lipase activity of HL, returning HDL to a pre- β size. Low HL activity is associated with increased CVD in humans but this may be a consequence of higher circulating triacylglycerol and the resulting alterations to APOB-containing lipoprotein metabolism(129, 130). Further studies are needed to determine whether HL contributes to RCT. Although lipoprotein lipase does not target HDL directly, its actions on triacylglycerol rich APOB lipoproteins are proposed to release phospholipid, cholesterol and exchangeable apolipoproteins to HDL(120). Genetic studies in humans show that lipoprotein lipase deficient homozygotes and heterozygotes have reduced HDL-cholesterol (131), potentially explained by increased CETP activity(120).

1.4.3 Cholesterol trafficking in the liver

The liver plays a central role in maintaining whole body cholesterol homeostasis, potentially because it is the only established route of elimination of cholesterol(5). Circulating cholesterol is removed from the bloodstream by one of two pathways. The members of the LDL receptor family bind APOB and APOE apolipoproteins, and internalize the lipoprotein in a process called receptor-mediated endocytosis(17, 132). The identification of a receptor for LDL came from studying lipoprotein uptake in cells isolated from familial hypercholesterolemia patients(133). LDLR-LDL complexes are internalized by the “pinching” of the clathrin-coated pit and the vesicle enters the endocytic trafficking pathway. In the early endosome, the acidic pH causes the lipoprotein to dissociate from the receptor(134), which is returned to

the cell surface for re-use within ten minutes(135). LDL in the endosome continues to be trafficked to the late endosomes which fuse with lysosomes for degradation of the endosome contents(136). Acid hydrolase in the lysosome hydrolyzes the cholesteryl ester content of the lipoprotein to free cholesterol.

There is a significant gap in knowledge explaining how cholesterol traffics from the late endosome to other organelles. Genetic studies of the cholesterol storage disease, Niemann Pick C, identified two genes likely involved: *NPC1* and *NPC2*. The proteins from both these genes bind cholesterol, with different rates of binding and release(137). Brown and Goldstein hypothesize that the aqueous protein NPC2 binds cholesterol released in the degradation of LDL and transfers it to NPC1, an integral membrane protein, which inserts the cholesterol into the organelle wall for transport to other intracellular membranes(133, 138). The membranes of the endocytic compartment represent a pool of cholesterol important to the ABCA1-mediated formation of nascent HDL(91). Lipoprotein-derived cholesterol not removed from the cell as lipid-poor HDL reaches the endoplasmic reticulum, where it is re-esterified by ACAT either for storage in lipid droplets or incorporation into nascent VLDL(139).

The second, less well characterized, pathway for hepatic lipoprotein uptake is the HDL-cholesterol clearance by SCARB1. Unlike the receptor-mediated pathway described above, HDL does not enter the cell but rather interacts with a scavenger receptor at the cell surface, allowing the lipid content of the lipoprotein to be internalized. Studies in cell culture demonstrate that both SCARB1 and another scavenger receptor, CD36, bind HDL with high affinity but only SCARB1 facilitates the “selective lipid uptake” of cholesteryl ester into the cell(45). APOA1 binding to SCARB1

facilitates a unidirectional transport of cholesteryl ester from the lipoprotein into the cell in addition to the bidirectional transport of free cholesterol described in section 1.4.1. The importance of SCARB1 to HDL cholesterol and RCT has been demonstrated using mouse models. Disruption of *Scarb1* increases HDL-cholesterol levels(140, 141) but also increases atherosclerosis(77-79). Conversely, overexpression of *Scarb1* reduces HDL-cholesterol levels(47, 142) but reduces atherosclerosis and increases macrophage to feces RCT(143). Although the precise mechanism by which HDL-derived cholesterol is moved to the canalicular membrane has not been determined, in humans it is the preferred source of cholesterol for removal by biliary excretion(144).

The third mechanism by which the liver accumulates cholesterol is biosynthesis. Cholesterol is synthesized from acetate in a complicated process requiring >26 steps(139, 145-147). The rate-limiting step in the reaction is the conversion 3-hydroxymethylglutaryl CoA to mevalonate, catalyzed by the enzyme HMG CoA Reductase (encoded by *HMGCR*). Cholesterol synthesis in the liver is carefully regulated and fluctuates to maintain balance between uptake from lipoproteins and removal by catabolism or excretion(5).

Excess cholesterol is removed from the liver by one of two mechanisms: catabolism into bile acids or direct secretion into bile. The use of cholesterol as a precursor in the synthesis of bile acids is predicted to be the primary means of cholesterol removal in the liver. This will be discussed in section 1.7. The heterodimer of ABCG5/G8 is crucial for normal biliary secretion of cholesterol in mice(148, 149). Recently, ABCG5/G8-independent pathways have been postulated to contribute to

the biliary secretion of cholesterol(8, 150) but the molecular mechanisms responsible for this flux remain to be elucidated.

1.4.4 Cholesterol uptake and transport in the enterocyte

The processes that govern the trans-cellular movement of cholesterol across the absorptive cells of the intestinal tract determine the absorption of cholesterol from the gastrointestinal lumen. In order for cholesterol to be transported into the body, it is packaged in a unique lipoprotein produced by the intestine called a chylomicron. Three complementary pathways must converge for the synthesis of these lipoproteins. (A) Cholesterol must be taken up by the cell and packaged in nascent chylomicrons for secretion into the lymphatic system. (B) Dietary fats must be taken up by the enterocyte, assembled into triacylglycerol, and packaged onto the nascent chylomicron. (C) APOB-48, the protein scaffold for chylomicrons, must be synthesized in the endoplasmic reticulum and traffic to the Golgi apparatus for assembly of the mature chylomicron prior to secretion into the lymph. Disruption of any of these pathways will affect the efficiency and magnitude of cholesterol absorption.

Cholesterol is taken up into the brush border of columnar absorptive cells, called enterocytes, as a monomer from mixed micelles in the gastrointestinal lumen. Upon uptake into the plasma membrane, cholesterol is subjected to competing molecular pathways. Two hemi ABC transporters, ABCG5 and ABCG8, dimerize to form a complete hetero-transporter that recognizes and actively effluxes both cholesterol and plant-derived sterols back into the intestinal lumen(6, 148). The importance of

ABCG5/G8 as a barrier that regulates the absorption of cholesterol is demonstrated in the rare autosomal recessive human disease sitosterolemia. These patients have unregulated absorption of cholesterol leading to the formation of xanthomas and premature cardiovascular disease(6, 151).

In opposition to the actions of ABCG5/G8 is the absorptive pathway mediated by Niemann Pick C 1 Like 1 (NPC1L1). This integral membrane protein contains extracellular sensing domains, a sterol sensing domain and extensive N-linked glycosylation, all properties predicted of a cholesterol transporter. Knockout mice lacking NPC1L1 have an ~80% reduction in the absorption of cholesterol and are insensitive to treatment with the potent cholesterol absorption inhibitor, ezetimibe(152, 153). Cholesterol is moved from the plasma membrane to the endoplasmic reticulum by a clathrin-mediated vesicular pathway that requires NPC1L1. Ezetimibe and its glucuronide metabolite bind to an extracellular loop of NPC1L1 preventing the movement from the plasma membrane to the endoplasmic reticulum(154, 155). In the endoplasmic reticulum cholesterol is made more hydrophobic through an esterification reaction with fatty acids catalyzed by ACAT(156, 157). The cholesteryl esters and some unesterified cholesterol associate with newly assembled triacylglycerol molecules into lipid droplet-like micro-organelles prior to assembly into nascent chylomicrons.

Dietary fats are absorbed by the enterocyte as monoacylglycerol and as free fatty acids. Once in the intestinal cell, they are repackaged as triacylglycerol molecules through the subsequent actions of Acyl CoA: MonoacylGlycerolAcylTransferase (MGAT), and Acyl CoA: diacylglycerol acyl transferase. The conversion from

monoacylglycerol to diacylglycerol catalyzed by MGAT is predicted to be the rate limiting step in this process(158) . The repackaged triacylglycerol molecules bind to a transfer protein called Microsomal Triacylglycerol Transfer Protein (MTP) (159). MTP transports triacylglycerol, cholesteryl ester, cholesterol, and phospholipid between membranes, however it has higher affinity for neutral lipids like triacylglycerol and cholesteryl ester(160). The essential nature of MTP-mediated lipid transfer was revealed when Wetterau *et al.* discovered that mutations in *MTTP*, the gene encoding MTP, were responsible for the rare autosomal recessive disease abetalipoproteinemia(159). Patients with this disease have no circulating APOB, and consequently very low levels of circulating triacylglycerol and cholesterol. The triacylglycerol transfer activity of MTP adds lipid to the APOB-48 polypeptide as it is being translated, helping the protein fold correctly. The precise molecular role that MTP plays in the transfer of triacylglycerol to newly synthesized APOB-48 has yet to be determined, efforts to do so are reviewed in detail by Hussain *et al.* (161)

The third pathway required for chylomicron assembly is the synthesis of APOB-48. This is a truncated form of the APOB-100 gene, produced by a RNA editing pathway, unique to the enterocyte, that introduces a stop codon after ~48% of the amino acids have been translated(36). Ingestion of fat does not appear to regulate production of APOB-48, as evidenced by the secretion of small dense lipoproteins containing APOB-48 in the fasted state(162). Rather, the enterocyte retains a store of small dense chylomicron precursors for rapid response to feeding(163). Mechanistic studies on the regulation of assembly of APOB-containing lipoproteins demonstrate that production of APOB is controlled through degradation of the protein rather than

transcription(164). As APOB is translated, neutral lipid is required for proper folding of the polypeptide. In the absence of sufficient lipid, the polypeptide chain is ubiquitinated and degraded in the endoplasmic reticulum(165). Additionally, the nascent APOB-containing lipoprotein may be degraded either by re-uptake via lipoprotein receptors or through autophagy pathways(166).

Most of the mechanistic studies on APOB production have been performed in hepatocytes, with the assumption that similar processes occur in enterocytes. The complexity of this process has been the subject of a recent review and readers are directed to reference(167) for further reading. Post translation, there is an accumulation of high-density form of chylomicrons in the smooth endoplasmic reticulum. Upon ingestion of dietary lipid, the nascent chylomicrons are transported to the Golgi apparatus via a vesicle-mediated pathway that requires the actions of the Fatty Acid Binding Protein(168). Once in the Golgi apparatus, the neutral lipid core of the lipoproteins is rapidly expanded and the mature chylomicrons are secreted into the lymphatic system(169, 170). An alternate pathway for cholesterol transport, recently described in mice, shows that free cholesterol in the basolateral plasma membrane is effluxed to lipid poor APOA1 in the portal vein, bypassing the lymph(171). The contributions of this alternate route to cholesterol absorption have not been determined in humans.

1.5 ABC transporters

The ATP-binding cassette superfamily is the largest family of transmembrane proteins containing >600 members in organisms ranging from prokaryotes to

eukaryotes(172, 173). Prokaryotic ABC proteins can be import transporters, mediators of cellular processes, and export transporters. Conversely, all known eukaryotic ABC transporters are efflux transporters(172, 174). The human ABC transporter family contains 48 proteins split into 7 subfamilies labeled A-G with key roles in a diverse set of physiological functions(173, 175). A full ABC transporter contains 12 transmembrane domains and 2 nucleotide binding regions, called Walker regions(172). The active transport of substrates is accompanied by hydrolysis of ATP and can take place against a chemical gradient. The precise mechanism by which these transporters function has not been determined but it is likely accomplished by conformational changes associated with the binding and hydrolysis of ATP(176).

1.5.1 P-glycoprotein

P-glycoprotein is the first member of the ABC transporter family discovered. Victor Ling and colleagues were studying CHO cells selected for colchicine resistance that displayed reduced permeability of to a number of other drugs, resulting in a multidrug resistant phenotype(177). The authors named the protein P-glycoprotein for its role in limiting permeability and the extensive surface glycosylation. Soon afterwards, Pgp was identified in human tumors and the authors determined that increased tumor levels of Pgp was associated with resistance to chemotherapy(178). In 1986, the gene for Pgp was cloned by two groups, who named it *MDR1* for its ability to confer multidrug resistance. The gene encodes a 1280 amino acid protein containing two nucleotide binding domains and six pairs of putative transmembrane regions, with glycosylation sites on the N-terminus(179, 180). Pgp is not solely

expressed in tumors but rather it is found in a number of healthy human tissues, with specific subcellular localization on the apical face of polarized cells of the liver, digestive tract, kidney, and blood brain barrier(181-183). Pgp is also highly expressed on mature adrenal glands but not fetal or neonate(182). Rodents have two isoforms of Pgp, encoded by *Abcb1a* and *Abcb1b*. The proteins have 84% homology (Table 5-1) and are differentiated by tissue distribution. The ABCB1A isoform is distributed similarly to human Pgp while ABCB1B is only found in the pregnant uterus, ovaries, and adrenal gland(184).

The ability of Pgp to confer multi-drug resistance to cells and tumors is derived from its recognition and efflux of a range of structurally diverse chemicals. At present, Pgp has been implicated in the efflux of over 100 drugs including anticancer drugs, HIV protease inhibitors, anti-histamines, steroids, antibiotics, immunosuppressives, and more(174, 185-187). There are commonalities to Pgp substrates: they have a molecular weight in the range of 300-1000Da, they usually contain ring structures, and their hydrophobicity causes them to partition to the lipid bilayer, though many substrates are amphipathic. The “promiscuity” of Pgp with respect to substrate recognition may be a result of multiple drug binding pockets(188), or a single large pocket that can bind drugs with a differing affinities(174, 176). A number of models have been proposed to explain the efflux function of Pgp, including a classical pump, a hydrophobic “vacuum cleaner”, and a flippase as shown in Figure 1-3. In 2009, Aller *et al.* solved the crystal structure of murine Pgp at a resolution of 3.8Å in the absence of bound nucleotide. Based on the x-ray structures of two prokaryote orthologs of Pgp, (189, 190) Aller *et al.* speculated that mammalian Pgp adopts a different

conformation when ATP is bound. The X-ray data support the hydrophobic vacuum cleaner model for Pgp function. There are a number of pores between the transmembrane helices allowing substrates access to a large central compartment. The binding of ATP is proposed to cause a conformational change that exposes the drug binding pocket to the extracellular space, while hydrolysis of ATP returns Pgp to its native state(176), see Figure 1-3.

Multidrug resistance in cancer cells is a key reason for the failure of chemotherapy. Although resistance is mediated by several mechanisms, the most commonly encountered is increased levels of Pgp, causing reduced accumulation of the cytotoxic drug(192, 193). Due to the prevalence of Pgp-mediated chemoresistance, significant research has been focused on the creation of pharmacological modulators of Pgp activity. The first generation inhibitors of Pgp are drugs that were developed against other targets that also inhibit Pgp. Because of this search strategy, each drug has at least one off-target effect. Second-generation inhibitors were designed for specificity to Pgp. Unfortunately, they also inhibit other ABC transporters and induce drug detoxification processes, such as the cytochrome P450 enzymes, leading to drug-drug interactions(192). Third generation inhibitors do not induce drug degradation pathways and have improved specificity but still exhibit some off-target inhibition(192).

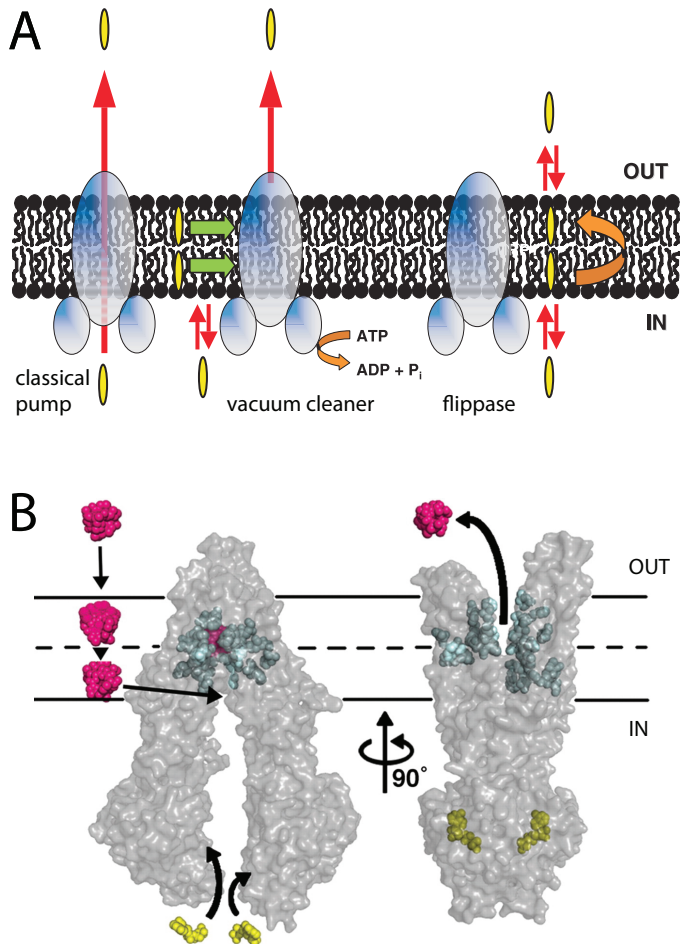


Figure 1-3: Models for Pgp-mediated transport of drugs.

(A) In the classical pump model Pgp moves a substrate (yellow) from the cytosol to the extracellular face, accompanied by the hydrolysis of ATP. Under the hydrophobic vacuum cleaner model Pgp takes up lipophilic substrates in the lipid bilayer followed by efflux induced by a conformational change linked to the hydrolysis of ATP. The flippase model is a variant of the hydrophobic vacuum cleaner model. In this scheme hydrolysis of ATP causes Pgp to move the substrate from the inner leaflet of the bilayer to the outer leaflet. Reproduced with permission, from Sharom, F. J. Shedding light on drug transport: structure and function of the P-glycoprotein multidrug transporter (ABCB1). *Biochem. Cell Biol.* 84, 979–992 (2006). © 2008 Canadian Science Publishing or its licensors. (191)

(B) Proposed model of Pgp-mediated transport of a model substrate. The configuration on the left is based on the x-ray crystal structure of Pgp bound to a test substrate (in pink). Substrates enter the drug-binding pocket (labeled in blue) from the lipid bilayer through pores in the transmembrane regions. ATP (yellow) binding causes a conformational shift in Pgp, leading to the efflux conformation based on the x-ray structure of two prokaryotic orthologs of Pgp (MsbA and Sav1866). From Aller, S. G. *et al.* Structure of P-glycoprotein reveals a molecular basis for poly-specific drug binding. *Science* 323, 1718–1722 (2009). Reprinted with permission from AAAS(176)

Due to these off-target effects, elucidating the role of Pgp in cell biology has required the use of multiple inhibitors and the observation of conserved changes. When studying the role of Pgp in cholesterol and bile acid homeostasis, the majority of the published studies have relied on first and second generation Pgp inhibitors. New techniques, such as RNA interference are beginning to be used more frequently; however these approaches rely on careful use of controls to ensure specificity silencing and appropriate interpretation of the results(194).

1.5.2 ABC transporters in cholesterol and bile acid homeostasis

Members of the ABCA, ABCB, and ABCG families have well-established roles in maintaining cholesterol homeostasis, as summarized in Figure 1-4. The roles of ABCA1, ABCG1, ABCG5, and ABCG8 in cholesterol efflux have been discussed in section 1.4 and will not be discussed further in this section. The ABCB family of transporters contributes to the formation of bile. BSEP (*ABCB11*) and ABCB4 mediate bile acid and phospholipid efflux respectively. Although the role of Pgp (*ABCB1*) as a protective measure against xenobiotics is well established, no endogenous function for Pgp has been conclusively determined, though there are provocative preliminary studies suggesting its role in cholesterol and bile acid homeostasis.

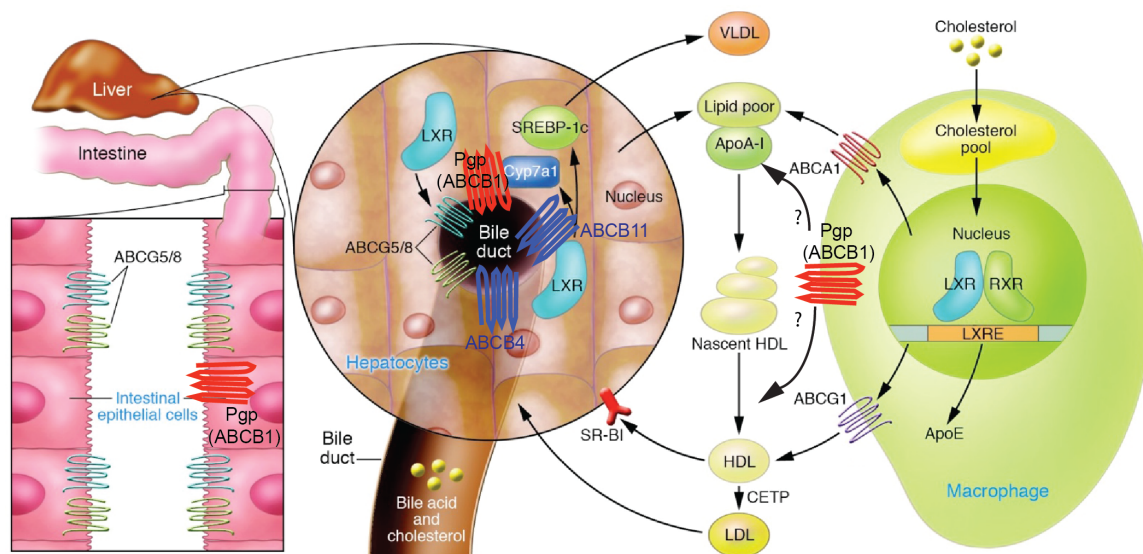


Figure 1-4: The role of ABC transporters in the macrophage reverse cholesterol transport pathway. ABCA1 and ABCG1 contribute to the efflux of cholesterol from macrophages to HDL. In the liver ABCG5/G8 is responsible for the efflux of cholesterol, ABCB4 is the phospholipid transporter and ABCB11 (BSEP) is the bile salt export pump. In the enterocyte, ABCG5/G8 prevent the uptake of cholesterol and plant sterols. P-glycoprotein (ABCB1) is found on macrophages, on the canalicular face of hepatocytes, and on the apical face of enterocytes but its role in RCT has not been determined. Figure adapted from the Journal of Clinical Investigation (195) with permission (<http://dx.doi.org/10.1172/JCI27883>). © 2006, American Society for Clinical Investigation.

The *ABCB4* gene (formerly referred to as *MDR2* or *MDR3* in humans and *Mdr2* in mice) was first identified due to its sequence homology to the multidrug resistance transporter, P-glycoprotein(196); however studies in cell culture failed to identify a role in drug resistance(197). Knockout mice homozygous for *Abcb4* deletion have pronounced liver disease and no phospholipid in the gallbladder clearly demonstrating the role of murine *ABCB4* to phospholipid efflux(197). The human ortholog, encoded by *ABCB4*, is also a phospholipid transporter in cell culture(198, 199). Mutations in *ABCB4* are linked to several inherited human diseases including

Type III Progressive Familial Intrahepatic Cholestasis (PFIC) (200), pregnancy related intrahepatic cholestasis(201), and cholelithiasis(202).

BSEP was also discovered due to its homology with *ABCB1* and was initially named sister of Pgp, though unlike Pgp it is only found in the liver(203). The role of BSEP in bile salt efflux wasn't discovered until the human gene, *ABCB11*, was linked to type 2 PFIC(204). Recent publications summarize 82 mutations in this gene associated with the disease(205, 206). Surprisingly, *Abcb11* knockout mice do not have signs of cholestasis(10) unless challenged with a diet containing 0.5% cholic acid(207) despite reductions in bile salt efflux, specifically of hydrophobic bile acids. BSEP has a high affinity for bile salts with comparable K_m values for taurocholate transport between human(208) and rat(209) orthologs (4.3 μ M and 5.3 μ M, respectively) and slightly lower affinity in the mouse ortholog (11 μ M) (210). The relative affinity of murine BSEP for specific bile acids has been estimated either by direct measurement(211) or by inhibiting taurocholate transport using other bile acids(210). Transport of taurocholate was most effectively inhibited by taurodeoxycholic acid > chenodeoxycholic acid > taurochenodeoxycholic acid > cholic acid > ursodeoxycholic acid(210). From this data, it appears that the more hydrophobic a bile acid is(212) the more effective it is as an inhibitor of murine BSEP. Similar results are reported for direct measurement of affinity(211). The finding that *Abcb11*^{-/-} mice do not spontaneously develop cholestasis lead to research probing for a secondary mechanism for bile acid efflux, summarized in section 1.5.4.

1.5.3 P-glycoprotein as a cholesterol transporter

Pgp function is intricately linked with membrane cholesterol content, though the details of the association are controversial(213, 214). Studies using purified Pgp reconstituted in lipid membranes with precise cholesterol content demonstrate the direct binding of cholesterol to Pgp(215). Cholesterol content alters the biophysical properties of the membranes, which affects Pgp function in proteoliposomes(213, 215, 216) and in cell culture(217, 218), perhaps due to the preferential localization of Pgp in cholesterol rich microdomains(219). In 2002, Garrigues *et al.* proposed that cholesterol is responsible for the basal ATPase activity of Pgp. They demonstrate in proteoliposomes that Pgp functions as an ATP-dependent cholesterol flippase, moving cholesterol from the inner leaflet to the outer leaflet, consistent with an efflux mechanism(216).

Studies in cell culture probed whether the association between Pgp and cholesterol affects the trafficking and homeostasis of cholesterol. The majority of these studies utilized non-specific pharmacological inhibitors to reduce the activity of Pgp. Despite the non-specific nature of the inhibitors used, a number of consistent changes to cholesterol homeostasis were observed, including altered trafficking of cholesterol from the plasma membrane to the endoplasmic reticulum, reduced synthesis, and reduced esterification of cholesterol without directly inhibiting ACAT(220-224). Similar findings are reported when these experiments were repeated using more specific inhibitors(225).

Two groups have used specific overexpression of *ABCB1* as part of their experimental design(226, 227). One group presented data suggesting that cholesterol

uptake and trafficking correlates with overexpression of *ABCB1*(226), while the other group found that transient overexpression had no effect on cholesterol trafficking(227). Le Goff *et al.* used a fibroblast cell culture system with an inducible *ABCB1* promoter region that responds to tetracycline(227). Unfortunately, tetracycline is an established substrate of Pgp(228) and by treating the cells with 2000ng/mL tetracycline, the authors may have saturated the efflux capacity of Pgp, obscuring the effects of Pgp overexpression on cholesterol trafficking.

These studies are countered by equally compelling negative results. Recently, the reproducibility of the cholesterol flippase activity of Pgp was questioned when attempts to repeat the experiment using fluorescently labeled or unlabeled cholesterol were unsuccessful(213). The use of drug-selection to isolate cell lines that over-express *ABCB1* has been called into question, as there are multiple changes to these cells that confer multi-drug resistance. The inability to control for the multitude of changes that occur make it challenging to draw conclusions about the role of Pgp in the altered cholesterol trafficking seen in these cells(227). These findings do not refute the association of Pgp with cholesterol, but conclude that it is the biophysical characteristics of cholesterol-rich microdomains that are required for Pgp function that drive the association rather than the protein acting as a cholesterol flippase(213).

Despite the data collected from *in vitro* studies, only two preliminary studies have been published investigating the role of Pgp in cholesterol homeostasis *in vivo*. Luker *et al.* studied the role of murine *Abcb1a/1b* in cholesterol absorption. Although they did not observe changes to cholesterol absorption, they noted a reduction in dietary cholesterol reaching the liver. The authors speculated that diets enriched in fat

or cholesterol would be required to elucidate the role of murine Pgp(229). Our group published a pilot study in 2008 demonstrating that knockout of *Abcb1a/1b* did not affect levels of circulating cholesterol after chronic administration of normal chow or high fat diets but found that there was increased cholesterol in the feces of the knockout mice, perhaps explained by increased liver X receptor in the liver(230). These two preliminary studies suggest that cholesterol homeostasis is perturbed in *Abcb1a^{-/-}/1b^{-/-}* knockout mice but neither study demonstrates a definitive role for Pgp in cholesterol balance.

1.5.4 P-glycoprotein as a bile acid transporter

The removal of bile acids from the liver is a protective mechanism against hepatic cholestasis, a liver disease caused by reduced bile flow(231). Several closely related members of the ABC transporter family mediate the efflux of bile components from the canalicular membrane of hepatocytes. Studies in knockout mice clearly demonstrate the role of ABCB4 in phospholipid efflux(197) and of the heterodimer ABCG5/G8 in cholesterol efflux into bile(7). In humans, mutations in *ABCB11* (the gene encoding the Bile Salt Export Pump (BSEP)) are linked to the development of Type 2 Progressive Familial Intrahepatic Cholestasis; however, mice lacking *Abcb11* do not show signs of cholestasis(10). While *Abcb11^{-/-}* mice have a reduced capacity to efflux hydrophobic bile acids, a secondary mechanism maintains sufficient bile acid output to prevent cholestasis. The increases in hepatic Pgp protein levels in response to both *Abcb11* knockout and dietary cholic acid suggests that Pgp may be responsible for the flux of bile acids in the BSEP knockout(11). In addition, triple knockout mice lacking

BSEP and both isoforms of Pgp (*Abcb11*^{-/-}/*Abcb1a*^{-/-}/*1b*^{-/-}) have severe cholestasis and increased mortality when fed a diet fortified with 0.5% (w/w) cholic acid(12). This finding confirms that P-glycoprotein is required for bile acid efflux in the absence of functional BSEP, especially when the mice were challenged with a cholic acid fortified diet. The inherent capacity of Pgp to bind and transport cholic acid has been demonstrated using an *in vitro* assay of membrane vesicles(11); however, the role of this transporter in maintaining bile homeostasis *in vivo* using physiologically relevant diets has not been defined.

1.6 Transcriptional regulation of intracellular cholesterol

Cholesterol is required for a range of cellular functions; however, at high concentrations it is toxic to cells. Consequently, cells have elaborate cholesterol sensing pathways that maintain optimal intracellular levels. The ability to sense and adapt to changing cholesterol content is achieved primarily through the opposing actions of two transcription factors: the Sterol Response Element Binding Protein-2 (SREBP-2) and the Liver X Receptor (LXR). Decreased cellular cholesterol activates the SREBP 2 transcription factor, which induces the expression of genes that increase cholesterol levels through increased synthesis and uptake from lipoproteins(17, 197, 232, 233). Conversely, elevated cellular cholesterol results in the formation of oxidized derivatives of cholesterol. These metabolites, called oxysterols, activate the LXR transcription factor that increases the expression of efflux transporters and cholesterol catabolizing enzymes to reduce cellular cholesterol levels(234, 235).

1.6.1 Liver X receptor responds to increased intracellular cholesterol

1.6.1.1 Formation of oxysterols

Oxysterols are oxygenated derivatives of cholesterol with important roles in the maintenance of cellular cholesterol homeostasis. Oxysterols are precursors for bile acids and mediators of sterol transport, they also activate cholesterol efflux pathways while repressing cholesterol biosynthesis(236). All oxysterols have a short half-life relative to cholesterol and are, consequently, 10^3 - 10^6 -fold less abundant within cells(237, 238). The oxygenation of cholesterol to an oxysterol is the first step in the catabolism of cholesterol to bile acid; consequently, oxysterol formation is catalyzed by a number of cytochrome P450 enzymes involved in bile acid synthesis(236). Oxysterols can also form spontaneously in the presence of reactive oxygen species. The primary routes of oxysterol formation are shown in Figure 1-5. One additional oxysterol, 24(S),25-epoxycholesterol, is synthesized directly in a shunt from the cholesterol biosynthetic pathway(239). Oxysterols formed either by enzymatic catalysis or by auto oxidation have important roles in the transcriptional and post-transcriptional regulation of intracellular cholesterol homeostasis.

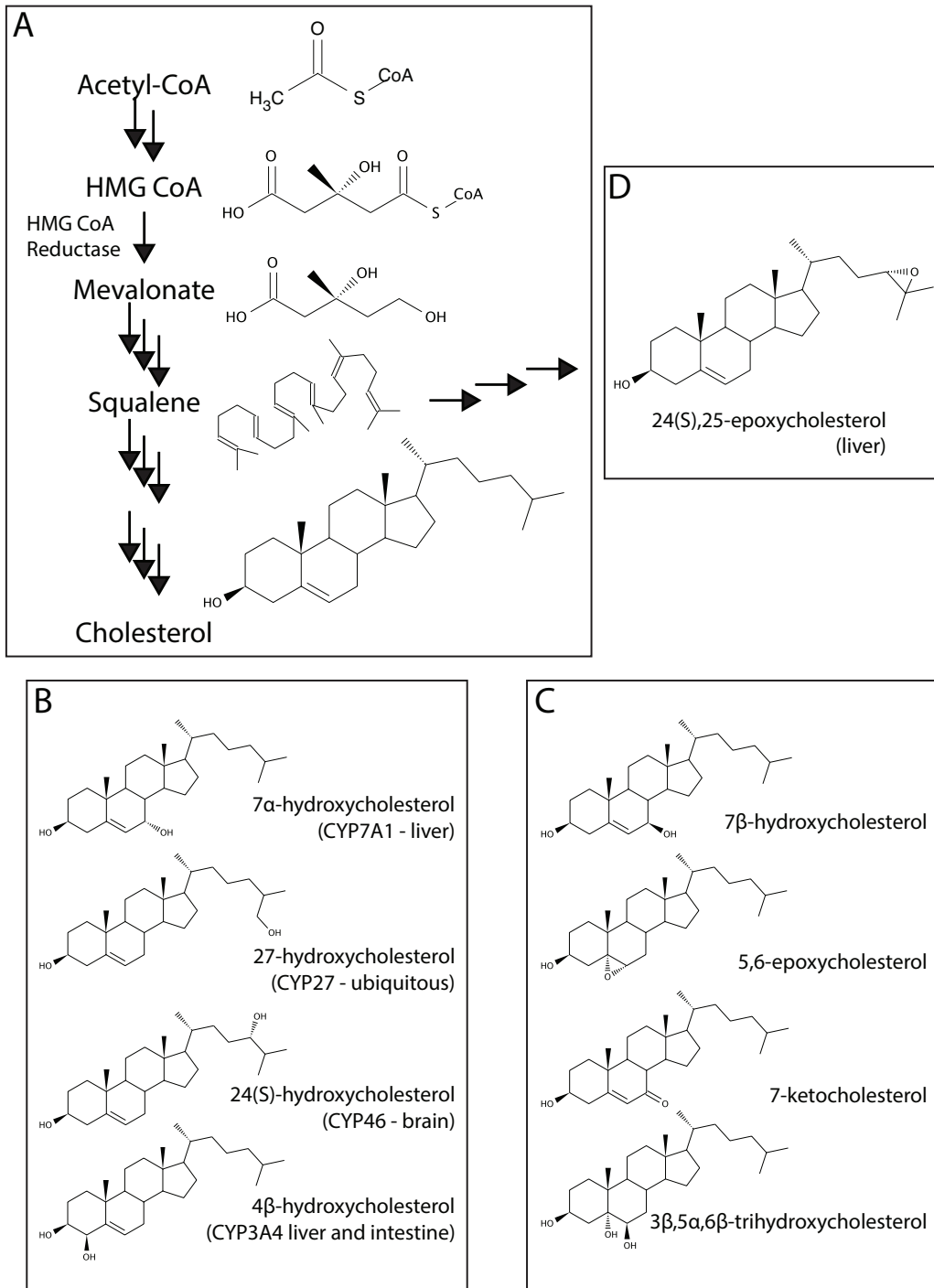


Figure 1-5: Endogenous production of cholesterol and oxysterols.

(A) Simplified schematic of the biosynthesis of cholesterol from acetyl-CoA with several key intermediates displayed. (B) Oxysterols produced from cholesterol in reactions catalyzed by cytochrome P450 enzymes, including the primary site of synthesis in the body. (C) Oxysterols produced by autoxidation in the presence of reactive oxygen species, (D) 24(S)-25-epoxycholesterol is produced from squalene 2,3,22,23-dioxide in a shunt from the cholesterol biosynthetic pathway (146, 147, 237, 240, 241).

1.6.1.2 Activation of LXR

The liver X Receptor is a member of the “orphan nuclear receptors”, a family of genes first identified by their homology with the steroid hormone receptors rather than by known ligands and function(242). There are two highly homologous isoforms of LXR, differentiated by tissue expression. LXR β (*NR1H2*) is ubiquitously expressed while LXR α (*NR1H3*) is highly expressed in liver, adipose and macrophages. Studies using knockout mice clearly demonstrate that LXR α is required for hepatic elimination of cholesterol(243) while deletion of LXR β has no effect on cholesterol homeostasis in mice(244), suggesting differing physiological roles for the each isoform. Further studies using a combination of LXR α and LXR β knockout mice bred on the *APOE*^{-/-} background demonstrate that both isoforms do contribute to RCT but confirm that LXR α is quantitatively more important to RCT as well as reducing atherosclerosis(245, 246).

LXR forms an obligate heterodimer with Retinoid X Receptor (RXR) to form a transcription factor that is activated by endogenously-produced oxysterols, including 22(*R*)-hydroxycholesterol, 24(*S*)-hydroxycholesterol, 24(*S*),25-epoxycholesterol, and 27-hydroxycholesterol(247-249). Under low cholesterol conditions, the heterodimer is inactivated through the binding of a corepressor complex. The LXR-RXR heterodimer is permissive(250), in that binding of ligands for either LXR or RXR induces a conformational change in the heterodimer, releasing the corepressors and recruiting coactivators(235, 251). Nuclear receptors induce transcription of target genes through a DNA binding zinc finger motif that recognizes a specific motif in the promoter region of the target gene. The LXR response element is a direct repeat 4 (DR4) motif:

the repeat of a sequence of six base pairs (GGTTTA) separated by four base pairs(252). Although it is possible to screen genome databases for the putative LXR response element, most of the known LXR target genes were identified in experiments using LXR agonists(235).

1.6.1.3 Genes induced by LXR

LXR is the primary transcriptional activator for genes involved in cholesterol efflux and catabolism. New data also suggest that LXR has a pivotal role in inflammation responses(253). The focus of this thesis is on cholesterol homeostasis, so the role of LXR in inflammation will not be explored in this chapter. The altered hepatic storage of cholesterol in LXR α knockout mice provided the first *in vivo* evidence that LXRs are important to cholesterol catabolism and removal(243). Subsequent studies, both *in vitro* and *in vivo* demonstrate that LXR activates a host of genes involved in lipid homeostasis, summarized in Table 1-1.

Table 1-1: Lipid homeostasis genes up-regulated by LXR.

This collection of genes was assembled from my own literature reviews as well as two excellent review papers(254, 255).

Gene	Notes	Reference(s)
<i>ABCA1</i>	Efflux	(234, 256)
<i>ABCG1</i>	Efflux	(102, 104, 257)
<i>ABCG5</i> and <i>ABCG8</i>	Efflux	(6, 258)
<i>Apod</i>	Adipocyte biology. The hepatic form was not induced by LXR agonism	(259)
<i>APOE</i>	Lipoprotein metabolism	(260)
<i>CETP</i>	Lipoprotein metabolism	(261)
<i>PLTP</i>	Lipoprotein metabolism	(262)
<i>SCARB1</i>	Uptake and Efflux	(263)
<i>APOC1/CIV/CII</i>	Lipoprotein metabolism	(264)
<i>Cyp7a1</i>	Human <i>CYP7A1</i> is not a LXR target, only murine <i>Cyp7a1</i>	(243, 248, 265)
<i>LPL</i>	Lipoprotein metabolism	(266)
<i>NR1H3</i> (LXR α)	Auto regulation does not occur in murine macrophages or pre-adipocytes	(267)
<i>IDOL</i>	Degradation of the LDL Receptor	(268)
<i>SREBF1C</i> and other lipogenic genes including <i>SCD1</i> , <i>FASN</i> , <i>ANGPTL3</i> , <i>THRSP</i> .	SREBP-1C is a transcription factor that induces the expression of lipogenic genes but LXR can also induce transcription directly.	(259, 269-272)

1.6.2 SREBP-2 is activated by low intracellular cholesterol

Intracellular cholesterol sensing occurs in the endoplasmic reticulum, a relatively cholesterol-poor cellular compartment. When intracellular cholesterol levels drop, homeostasis is maintained by up-regulating biosynthesis, increasing uptake from lipoproteins and reducing efflux of cholesterol, all regulated transcriptionally by

the SREBP-2 transcription factor(233). SREBP-2 itself lacks sterol sensing capability, its activity is regulated through SREBP Cleavage Activating Protein (SCAP), a chaperone protein that contains the sterol sensing motif (273). SREBP-2 is synthesized as a membrane-bound, inactive, form in the endoplasmic reticulum where it immediately associates with SCAP. Under low endoplasmic reticulum cholesterol conditions, the SCAP-SREBP-2 complex buds from the endoplasmic reticulum in vesicles coated with COPII proteins, which target the vesicle to the Golgi Apparatus(274). This selective budding is accomplished by binding of a hexapeptide domain in SCAP (MELADL) to SEC24, a member of the COPII complex(275). In the Golgi Apparatus, SREBP-2 is processed by two sequential proteases to cleave first the c-terminus-SCAP portion, then release the aqueous N-terminus, which contains the DNA binding motif(276). Mature SREBP is then free to travel to the nucleus and induce transcription of genes containing a sterol regulatory element sequence in the promoter region(277).

When endoplasmic reticulum cholesterol levels are high, two changes impact the SREBP-2 pathway: increased cholesterol in the endoplasmic reticulum and increased intracellular oxysterol levels. Increased cholesterol in the endoplasmic reticulum increases the direct binding of SCAP to cholesterol(278). This induces a conformational change in SCAP(279), which promotes binding to an endoplasmic reticulum anchoring protein, INSIG (INSulin Induced Gene) (280). Simultaneously, 25-hydroxycholesterol binds to INSIG, altering its conformation to increase binding to SCAP. The binding of INSIG to SCAP prevents SCAP from associating with COPII proteins and acts as an anchor holding the SREBP-2-SCAP complex in the endoplasmic reticulum. By treating CHO cells with cholesterol and/or cyclodextrin, Radhakrishnan

et al. demonstrate that SREBP-2 is deactivated by small increases to the endoplasmic reticulum cholesterol content in a switch-like mechanism (Figure 1-6) (232).

Furthermore, by adjusting the expression of INSIG, the threshold for SREBP-2 activation can be raised or lowered, suggesting a mechanism by which different tissues can maintain optimal intracellular cholesterol content.

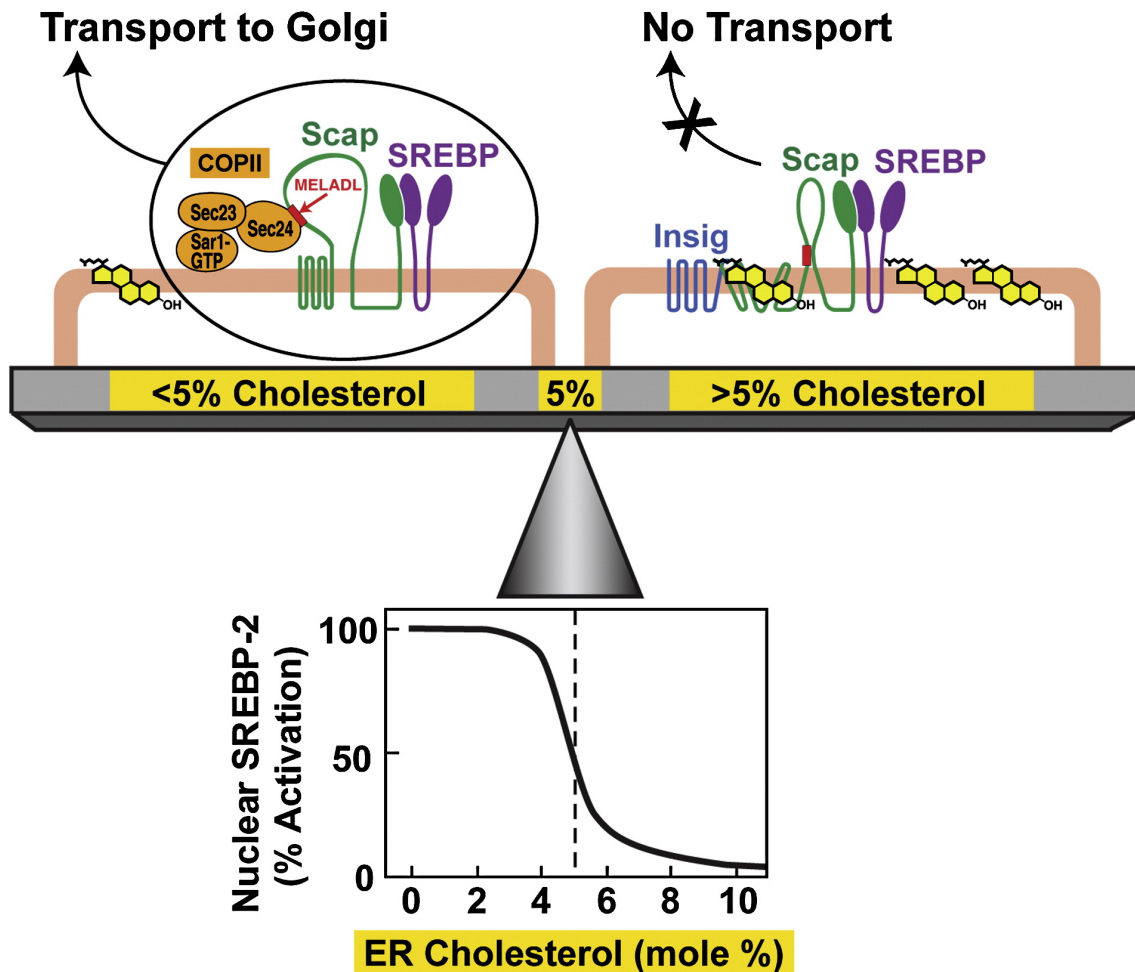


Figure 1-6: SREBP-2 is activated by low intracellular cholesterol. SREBP-2 is synthesized in the endoplasmic reticulum as a membrane-bound inactive precursor. Low levels of endoplasmic reticulum cholesterol trigger conformational change in the chaperone protein SCAP, releasing the SCAP-SREBP-2 complex from the anchoring protein INSIG for transport to the Golgi for proteolytic activation of SREBP-2. The relative amount of intracellular SREBP-2 in active (nuclear) or inactive (membrane-bound) forms is dependent on the cholesterol content of the endoplasmic reticulum. The activation of SREBP-2 responds to small changes in cholesterol content in a “switch-like mechanism”. Reprinted with permission from Elsevier (*Cell Metabolism* **8**, Radhakrishnan, A, Goldstein, JL, McDonald, JG & Brown, MS, Switch-like control of SREBP-2 transport triggered by small changes in ER cholesterol: a delicate balance 512–521. Copyright 2008) (232).

1.6.2.1 Genes induced by SREBP-2

SREBP-2 is the master regulator for all enzymes involved in cholesterol biosynthesis and uptake(233). The list below is not an exhaustive summary but rather summarizes genes that are relevant to the research presented in this thesis.

Table 1-2: Genes that are up regulated by the SREBP-2 transcription factor.

Gene	Notes	Reference
<i>HMGCR</i> and 19 other enzymes in the cholesterol biosynthetic pathway	Biosynthesis of cholesterol	(233)
<i>LDLR</i>	Clearance of LDL from the bloodstream, increases intracellular cholesterol levels	(281)
<i>SCARB1</i>	Influx and efflux of cholesterol	(282)
<i>NPC1L1</i>	Uptake of cholesterol in enterocytes and hepatocytes	(283)
<i>miR33</i>	Micro RNA that silences LXR-target genes	(284)

New data suggest that in addition to up regulating genes, both SREBP-2 and LXR can exert negative regulation on the opposing pathway. Treatment of macrophages with LXR agonist reduces LDL binding and uptake, explained by a reduction in LDL receptor protein levels. The degradation of LDLR is achieved by up regulation of *IDOL* (inducible degrader of LDLR), a gene encoding a novel ubiquitin ligase that targets members of the LDL receptor family for proteolytic degradation(268, 285-288). Similarly, when *SREBP2* (the gene encoding SREBP-2) is expressed, two micro RNAs encoded in the first intron are also expressed. These micro RNA molecules (miR33a and miR33b) target and repress the expression of a number of

LXR target genes, including *ABCA1*, *ABCG1*, and *NPC1*(284). Subsequent studies demonstrated that inhibition of miR-33a/b improved cholesterol efflux and reduced atherosclerosis in mice(289) and non-human primates(290). The recent discoveries that both LXR and SREBP-2 can regulate the each other's pathways demonstrates the complexity of cholesterol homeostasis and provides interesting avenues for future research.

1.7 Bile acid homeostasis

1.7.1 Regulation of bile acid synthesis

Synthesis of bile acids by the liver is the dominant cholesterol catabolism mechanism in humans, followed by production of steroid hormones. The human liver produces an average of 500mg of bile acids per day by one of two biochemical pathways involving catalysis by 17 different enzymes (291). The synthesis of bile acids occurs in four distinct steps: initiation by hydroxylation of the 7-carbon, ring structure modification, side chain oxidation and shortening, and conjugation. These steps lead to the synthesis of primary bile acids. In humans these are cholic acid and chenodeoxycholic acid(291, 292) whereas mice produce a more hydrophilic bile acid pool, comprised primarily of muricholic acid and cholic acid(293, 294) (Figure 1-7). The primary bile acids are further modified by bacteria in the digestive tract to secondary and tertiary bile acids, including deoxycholic acid and lithocholic acid(295).

The initial, rate limiting, step in the classical pathway is the oxidation of cholesterol to 7 α -hydroxycholesterol catalyzed by CYP7A1. Deletion of *Cyp7a1* in mice causes a 75% reduction in bile acid pool size(296) leading to a range of pathologies

and neonatal mortality consistent with malabsorption of fat and fat-soluble vitamins(297). Supplementing the diets of the pregnant mice with vitamins and cholic acid increases the survival rate to match wild type mice. Interestingly, *Cyp7a1*^{-/-} mice that reach 21 days can produce 7 α -hydroxylated bile acids, explained by a secondary pathway whereby oxysterols are the substrate for an oxidation reaction at the 7-carbon(298). Subsequent studies demonstrate that two different oxysterol precursors can be used for the synthesis of primary bile acids as shown in Figure 1-7 (299).

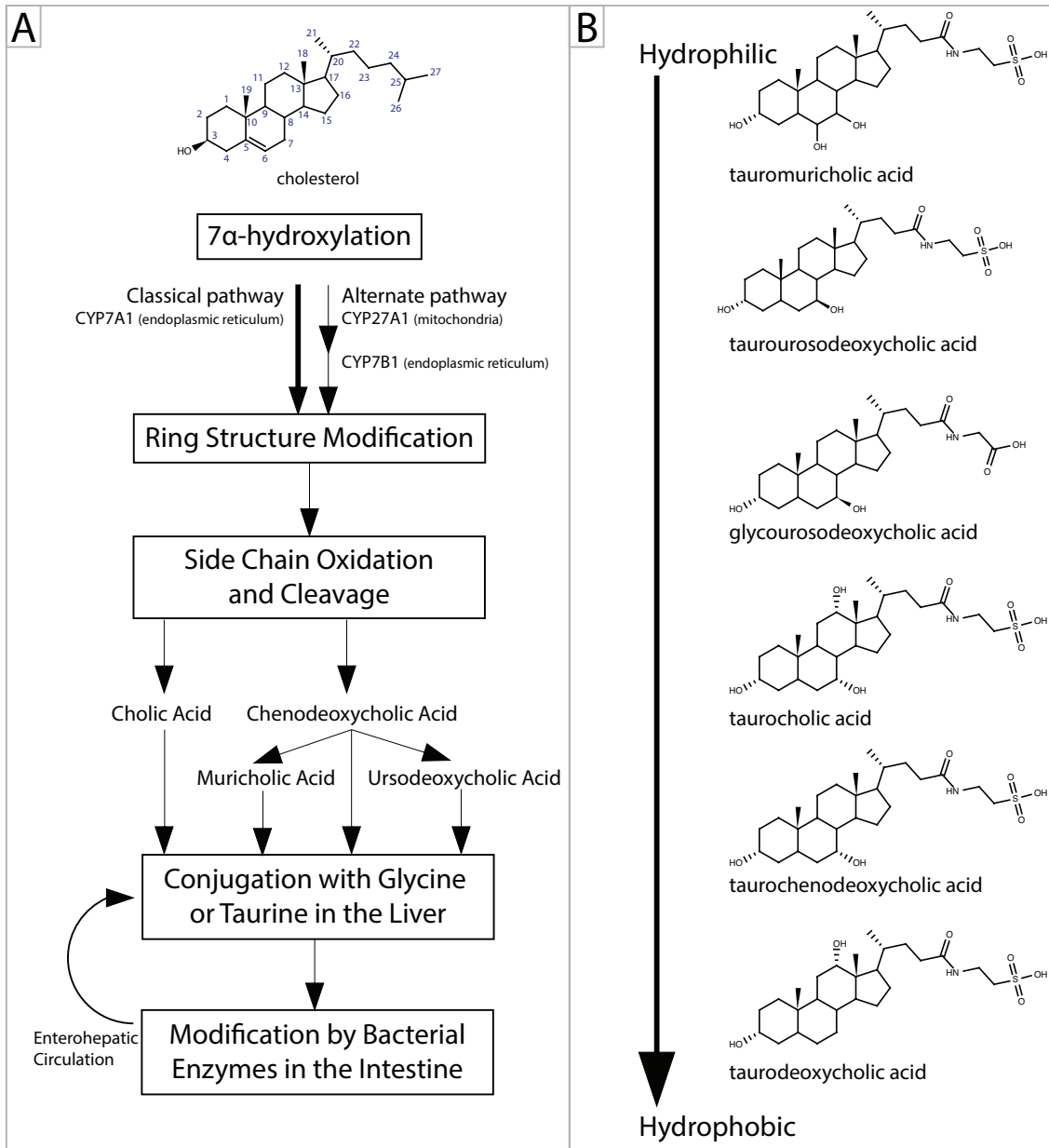


Figure 1-7: Overview of murine bile acid synthesis.

(A) The classical and alternative pathways for bile acid synthesis involve initiation by hydroxylation of the 7-carbon followed by sterol ring modifications, side chain modification and cleavage, followed by conjugation. Primary bile acids are further modified into secondary bile acids by bacterial enzymes and reabsorbed by enterohepatic circulation(291, 295). (B) The six most prevalent conjugated murine bile acids are arranged by increasing hydrophobicity(212).

The regulation of bile acid synthesis occurs primarily in the liver. Bile acids are toxic to cells due to their surfactant properties; consequently accumulation of bile acids triggers negative feedback of synthesis. The discovery that bile acids are endogenous ligands for the Farnesoid X Receptor (FXR) stimulated research into how this nuclear receptor negatively regulates bile acid synthesis(300, 301). FXR activation in the liver stimulates the expression of *NR0B2*, the gene encoding Small Heterodimer Partner (SHP). SHP binds to and represses the activity of two transcription factors that up regulate bile acid production(255, 291, 302, 303), Liver Receptor Homolog 1 (LRH-1) and Hepatocyte Nuclear Factor 4 α (HNF4 α) (304). The bile acid pool size in SHP knockout mice is increased, as is the fecal excretion of bile acids, suggesting that synthesis is increased. Deletion of SHP did not completely ablate negative feedback of bile acid synthesis, suggesting the existence of another negative feedback mechanism(305). The intestine is an important site for hepatic bile acid regulation. FXR activation in the intestine induces the expression of Fibroblast Growth Factor 19 (FGF19 – the murine ortholog is FGF15) (306). FGF15/19 produced in the intestine is transported to the liver where it interacts with the FGF receptor 4 (FGFR4). FGFR4 suppresses the expression of *CYP7A1* in a SHP-dependent and independent manner. The SHP-independent repression of *CYP7A1* is predicted to involve the JNK pathway, a stress response pathway, though the mechanistic details have not been clearly identified(4, 307, 308).

1.7.2 Efflux of bile acids from the liver

This is covered in section 1.5.2 (Page 27)

1.7.3 Enterohepatic recycling of bile acids

Bile acids are crucial for the absorption of fat, cholesterol, and fat-soluble vitamins, all of which are absorbed in the proximal small intestine. Passive uptake of bile acids occurs the length of the digestive tract; however, active uptake only occurs in the ileum(309). Up to 95% of the bile acids that enter the distal ileum are taken up by the apical sodium-dependent bile acid transporter (ASBT, encoded by *SLC10A2*) for recycling back to the liver. In all cells, the details of the intracellular trafficking of bile acids have yet to be discovered(291, 309, 310). Bile acids enter the portal vein at the basolateral face of the enterocyte, mediated by a dimer of organic solute transporter (OST) α and β (309). Bile acids are taken up at the sinusoidal face of hepatocytes primarily by the sodium taurocholate cotransporting peptide (NTCP, encoded by *SLC10A1*) and OST α -OST β as well as by a family of non-specific organic anion transporting polypeptides (OATP, encoded by *SLC21A* genes).

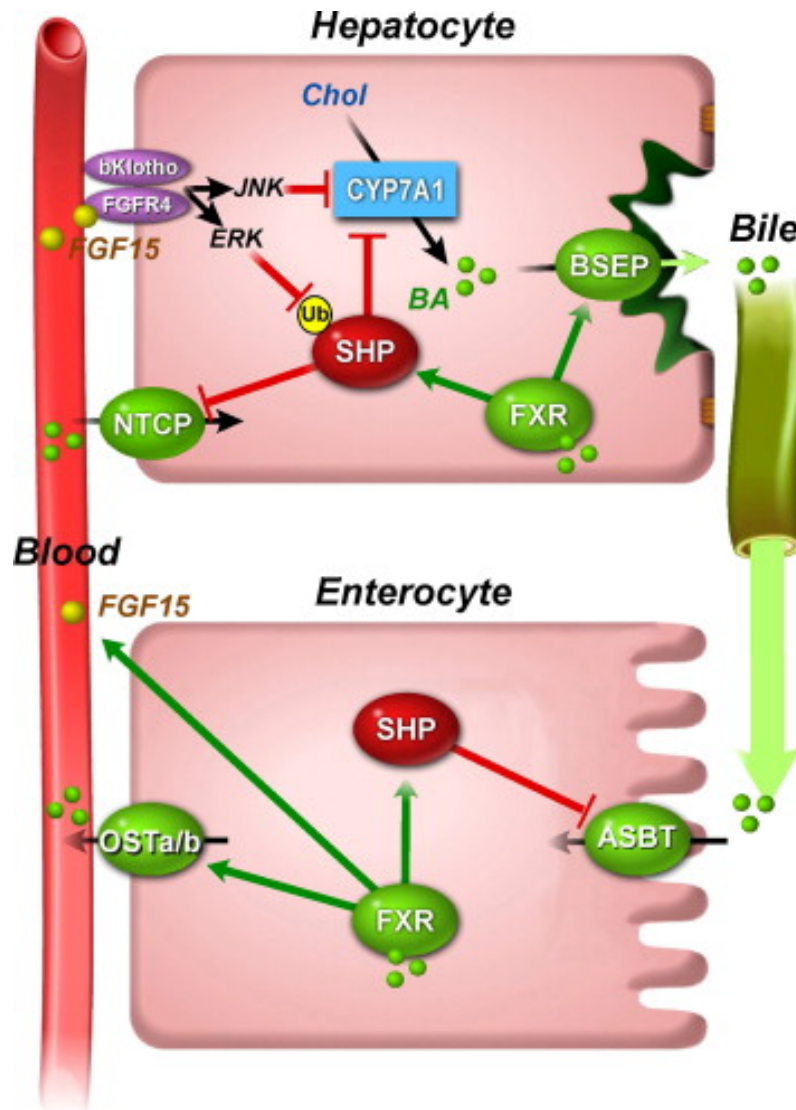


Figure 1-8: Effects of FXR on the enterohepatic circulation of bile acids. Bile acid accumulation activates the Farnesoid X Receptor (FXR), which reduces intracellular levels of bile acids. In the hepatocyte FXR induces the expression of small heterodimer partner (SHP), which represses the formation of new bile acids by inhibiting CYP7A1. SHP also reduces the uptake of bile acids from the bloodstream by inhibiting the sodium taurocholate cotransporting polypeptide (NTCP). In the intestine, FXR activation reduces bile acid accumulation by increasing efflux by inducing the organic solute transporters (OST). SHP reduces uptake from the gastrointestinal lumen mediated by the apical sodium dependent bile acid transporter (ASBT). FXR also stimulates FGF15/19, a hormone that traffics to the liver where it indirectly affects CYP7A1 to reduce the production of new bile acids. Reprinted from reference (311) with permission from Elsevier © 2011.

As seen with bile acid synthesis, FXR exerts negative feedback on enterohepatic circulation. Bile acid accumulation activates FXR, which represses hepatic uptake of bile acids through SHP-mediated inhibition of *NTCP* expression(4). In the enterocyte, FXR activation reduces uptake of bile acids by repressing the expression of *SLC10A2* (the gene encoding ASBT) (255, 312), while inducing the expression of *OST α* and *OST β* (309). Bile acid sequestrants disrupt the enterohepatic circulation of bile acids leading to increased bile acid synthesis and are effective at decreasing circulating LDL-cholesterol. Unfortunately, administration of bile acid sequestrants is often accompanied by gastrointestinal distress and treatment is discontinued(313). Further research into the molecular mechanisms that mediate enterohepatic circulation of bile acids may provide new therapies to reduce circulating cholesterol.

1.8 Specific hypotheses tested in this thesis

This purpose of this thesis is to seek answers to several key unanswered questions involving the endogenous function of P-glycoprotein. As discussed in the literature review, several provocative studies link Pgp with cholesterol and bile acid trafficking; however, the precise role that Pgp plays *in vivo* remains to be determined. In this project I sought to answer three key questions: (A) what role does Pgp play in the gastrointestinal absorption of cholesterol? (B) Does Pgp contribute to the efflux of cholesterol? (C) Does Pgp have a role in bile acid efflux in the presence of functional Bile Salt Export Pump? Based on evidence in the literature as well as pilot studies within the lab, I present the following hypotheses:

1. Deletion of Pgp will increase cholesterol absorption after chronic administration of diets rich in fat and/or cholesterol.
2. Cholesterol regulatory pathways will be perturbed in *Abcb1a^{-/-}/1b^{-/-}* mice relative to wild type mice.
3. P-glycoprotein is required, in addition to BSEP, for the maintenance of bile acid homeostasis.

1.9 Specific aims

1. Establish a physiologically relevant model to assess cholesterol absorption in mice
2. Determine if deletion of *Abcb1a* and *Abcb1b* affects the fractional absorption of cholesterol in mice after chronic feeding with diets enriched in fat, cholesterol, or the combination of fat and cholesterol
3. Characterize the cholesterol phenotype of wild type and *Abcb1a*^{-/-}/*1b*^{-/-} knockout mice after chronic exposure to the four diets by assessing circulating lipids, lipoprotein profiles, and hepatic storage of cholesterol
4. Determine if alterations to the LXR and SREBP-2 cholesterol regulatory networks may be compensating for the deletion of *Abcb1a* and *Abcb1b*
5. Determine if the loss of Pgp affects bile formation in mice after chronic exposure to the test diets
6. Establish an *in vitro* model of the absorptive cells of the gastrointestinal tract after down-regulation of *ABCB1* using RNAi to probe the contributions of Pgp to cholesterol trafficking with a specificity that is not possible using existing Pgp inhibitors

Chapter 2: Methodology

2.1 Methods used in chapter 3

2.1.1 Animals

All animal studies were conducted after the University of British Columbia Animal Care Committee reviewed and approved the protocols (certificate #A05-0032). All studies compared wild type FVB mice with congenic male mice lacking both isoforms of P-glycoprotein(184) backcrossed for 12 generations on the FVB background (FVB.129P2-*Abcb1a*^{tm1Bor}*Abcb1b*^{tm1Bor} N12). All mice (knockouts and FVB wild types) were from Taconic Farms (Hudson, NY).

2.1.2 Reagents

Intralipid™ and NaOH (ACS grade) and was purchased from Sigma Aldrich (St. Louis, MO). Soybean oil (USP grade) was purchased from Xenex Labs (Burnaby, BC). [4-¹⁴C]-cholesterol and [1,2-³H]-cholesterol were purchased from GE Healthcare (Waukesha, WI). [5,6-³H]-β-sitostanol was purchased from American Radiolabeled Chemicals (St. Louis, MO). The Animal Resource Unit at the University of British Columbia provided all anesthetics. The Healthy Heart Clinic at St. Paul's Hospital generously provided Ezetimibe. PBS was prepared from dry chemicals (Life Technologies, Carlsbad, CA). Solvents (chloroform, methanol, petroleum ether) were of HPLC grade and were purchased from Thermo Fisher (Waltham, MA). Cytoscint ES liquid scintillation cocktail was purchased from MP Biomedicals (Solon, OH).

2.1.3 Test diets

The test diets were developed with the assistance of Research Diets (New Brunswick, NJ). The diets were based on the well-established high fat diet (D12451) (314). We used the diets summarized in Table 2-1 to test the effect of elevated fat and/or elevated cholesterol on the mice.

Table 2-1: Composition of the test diets.

The fat and cholesterol content were selected based on the high fat diet utilized by van Heek *et al.* to demonstrate the role of leptin in adiposity(314). The cholesterol content was either 0.02% or 0.2% (w/w) to match the cholesterol content in well-established mild atherogenic diets(19).

Dietary component	NFNC (D05092803)		HFNC (D12451)		NFHC (D08031901)		HFHC (D05092804)	
	g	kcal (%)	g	kcal (%)	g	kcal (%)	g	kcal (%)
Protein	21	20	24	20	21	20	24	20
Carbohydrate	58	55	41	35	57	55	41	35
Fat	12	25	24	45	12	25	24	45
Cholesterol	0.02%		0.02%		0.20%		0.20%	
kcal/g	4.2		4.7		4.2		4.7	
Total	100		100		100		100	

2.1.4 Cholesterol absorption studies

Three separate *in vivo* studies are described in this thesis:

1. A pilot study that was performed using the plasma dual-isotope cholesterol absorption assay. Due to inconsistent results, this method was not repeated.
2. A plasma dual-isotope cholesterol absorption study using a more reliable method.

3. A fecal dual-isotope cholesterol absorption study. This method was the most reliable. All subsequent analyses were performed using samples obtained in this study.

2.1.4.1 Pilot plasma dual isotope cholesterol absorption assay.

This method is based on the Luker *et al.* paper(229). Male 4 to 6-week old male mice arrived from Taconic Farms. The mice ate a standard chow diet for five days for acclimatization before they were assigned (random number generator assignment) to receive one of the NFNC, HFNC, or HFHC test diets for 12 weeks. On week 13, cholesterol absorption was assessed using the plasma dual isotope cholesterol absorption assay. The mice were restrained using a non-dominant one-hand hold a feeding needle was used to administer an oral gavage of 150 μ L of 10% Intralipid containing 1 μ Ci of [1,2-³H]-cholesterol. The mice were restrained and administered an intravenous bolus of 50 μ L of 10% Intralipid containing 0.1 μ Ci of [4-¹⁴C]-cholesterol to the tail vein. The mice recovered in their cages with free access to food and water. At 72h post-injection, the mice were anaesthetized (isofluorane) then euthanized them by cardiac puncture exsanguination and cervical dislocation. The heart, spleen, right kidney, liver and a sample of visceral adipose tissue were weighed then cleaned with PBS and frozen in liquid nitrogen. The small intestine was split into three segments approximating the duodenum, jejunum, and ileum. The medial segment of each section was cleaned in PBS and frozen in liquid nitrogen. All samples were subsequently stored at -80°C. Plasma was collected from the blood and analyzed for ³H and ¹⁴C radioactivity in scintillation cocktail. The radioactivity in the serum is

compared with the dose of radioactivity administered PO and IV to calculate the % cholesterol absorption, as shown in Equation 1.

Equation 1: Plasma dual label cholesterol absorption calculation

$$\% \text{ cholesterol absorption} = \left(\frac{\% \text{ Dose}_{\text{PO}} / \text{mL plasma}}{\% \text{ Dose}_{\text{IV}} / \text{mL plasma}} \right) \times 100\%$$

2.1.4.2 Plasma dual isotope cholesterol absorption assay

The plasma dual isotope method published by Luker *et al.* generated variable results caused by insufficient radiolabeled cholesterol remaining in serum at 72h. Consequently, this study was based on a protocol modified from a 2003 publication by Wang and Carey, in which the authors compare a range of methodologies for assessing cholesterol absorption(315). Five-week old male mice were fed the HFHC diet for 12-weeks. On week 13, each mouse received an oral gavage containing 150 μ L of 10% Intralipid containing 1 μ Ci of [4-¹⁴C]-cholesterol. The mice were immediately administered an intravenous bolus of 100 μ L of 10% Intralipid containing 2.5 μ Ci of [1,2-³H]-cholesterol. Groups of mice were euthanized at 8h, 24h, 48h, and 72h post-administration (n=5 at each time point). At the time of sacrifice, the mice were anaesthetized and terminated by cardiac puncture exsanguination and cervical dislocation. Serum was obtained from whole blood by incubation in serum collection tubes at room temperature for 1hr before centrifugation at 2000g for 20min to facilitate collection. The liver, spleen, right kidney, and heart were washed in PBS and frozen in liquid nitrogen. The small intestine was split into three segments

approximating the duodenum, jejunum, and ileum, the medial portion of each segment was washed in PBS and frozen in liquid nitrogen. The serum was assayed for radioactivity in scintillation cocktail.

2.1.4.3 Fecal dual isotope cholesterol absorption assay

Each five-week old male mouse received one of the four test diets (NFNC, HFNC, NFHC, or HFHC) for 8-weeks, (n=10). On the ninth week, the mice were administered a single oral bolus of either 75µL water or 75µL of ezetimibe solution (10mg/kg dose). After 60min each mouse received an oral bolus of 75µL of soybean oil containing a mixture of 1µCi of [4-¹⁴C]-cholesterol and 2µCi of [5,6-³H]-β-sitostanol. The mice were placed in metabolic-style cages for 96h containing shelter and enrichment items. Total fecal output was collected at 24h, 48h, 72h, and 96h post-administration. The mice recovered in conventional-style housing for 72-120h. The mice were anaesthetized (ketamine/xylazine) and the common bile duct was surgically ligated. The gallbladders filled for 60min prior to sacrifice. Each mouse's body temperature was maintained with heating pads. The mice were euthanized by cardiac puncture exsanguination and cervical dislocation. Serum was obtained from whole blood by incubation at room temperature for 60min before centrifugation at 2000g for 20min to facilitate collection. The gallbladder, liver, heart, spleen, and right kidney were removed, weighed and washed in PBS before being frozen in liquid nitrogen. The small intestine was removed and split into three segments approximating the duodenum, jejunum, and ileum. The medial portion of each segment was cleaned in PBS and frozen in liquid nitrogen.

2.1.5 Quantification of circulating lipids

Total serum (or plasma) cholesterol and unesterified cholesterol levels were measured by using cholesterol oxidase-based colorimetric assays from Wako Diagnostics (Richmond, VA). A two-step colorimetric assay from Wako Diagnostics determined the circulating triacylglycerol levels.

2.1.6 Lipoprotein profile determination

Pooled serum samples (300 μ L) were prepared from equal volumes of serum taken from 6-10 mice from each experimental group. The pooled serum was separated into lipoprotein classes by fast protein liquid chromatography (FPLC) on an HR10/30 column by Dr. David Cohen's laboratory (316). The column output was separated into 300 μ L fractions, which were analyzed for cholesterol concentration using a cholesterol oxidase-based colorimetric assay from Wako Diagnostics.

2.1.7 Quantification of fecal radiolabeled cholesterol and β -sitostanol

Feces were dried overnight in a 60°C oven, the mass recorded, and then ground to a fine powder with a pestle and mortar. The fecal powder was transferred to a pre-weighed borosilicate test tube and the mass of powder transferred was determined. The fecal matter was extracted with 19 volumes of 2:1 (v/v) chloroform:methanol with vigorous vortex mixing. The tubes were incubated for 3min in 60°C water bath for total lipid extraction before centrifugation (1000g for 5min at 4°C) to pellet the insoluble material. The supernatant was transferred to a new tube. The chloroform:methanol extraction was repeated on the insoluble material and the

supernatant pooled with the first extraction. Solvent was removed by drying under N₂ gas. The lipid films were saponified with 3mL of 1:1 (v/v) methanol:2N NaOH_(aq) for 60min in a 60°C water bath. The neutral sterols were isolated with sequential petroleum ether extractions: 3mL of petroleum ether was added to each tube, the tubes were vigorously mixed and the phases separated by centrifugation (1000g for 5min at 4°C), the upper, organic, phase was transferred to a scintillation vial. The petroleum ether extraction was repeated twice more on the aqueous phase. An aliquot (300µL) of the aqueous phase was transferred to a scintillation vial for determination of aqueous radiolabel. The contents of the scintillation vials were dried under N₂ before 5.4mL of liquid scintillation cocktail was added. The samples were incubated overnight before analysis in a liquid scintillation counter (Beckman LS6500). The radioactive cholesterol in the feces was compared to the dose given as an indirect measurement of cholesterol absorption. The dosing mixture also contained trace amounts of radiolabeled sitostanol, a derivative of cholesterol that is not absorbed as a dosing control. This method recovered 98.5% of the [5,6-³H]-sitostanol and 99.2% of the [4-¹⁴C]-cholesterol during method development experiments. The recovery of [5,6-³H]-sitostanol was 101.22% ± 18.87% (standard deviation) from the *in vivo* samples (Experiment #3). The variability observed is likely due to small changes in the dosing volume given to each animal. Cholesterol absorption was calculated using Equation 2, below.

Equation 2: Fecal dual isotope cholesterol absorption calculation

$$\% \text{ cholesterol absorption} = \left(\frac{\left(\frac{[^{14}\text{C}]}{[^3\text{H}]} \right)_{dose} - \left(\frac{[^{14}\text{C}]}{[^3\text{H}]} \right)_{feces}}{\left(\frac{[^{14}\text{C}]}{[^3\text{H}]} \right)_{dose}} \right) \times 100\%$$

2.2 Methods used in chapter 4

2.2.1 Reagents

TRIzol, Quant-iT RiboGreen RNA Assay, Quant-iT OliGreen ssDNA Assay, UltraPure DEPC-treated (RNase/DNase-free) water, Superscript III First Strand Synthesis SuperMix for RT-qPCR, and TaqMan gene expression assays were purchased from Life Technologies (Carlsbad, CA). Chloroform, and 2-propanol were purchased from Thermo Fisher Scientific (Waltham, MA). iTaq supermix with ROX was purchased from Bio-Rad (Hercules, CA)

2.2.2 RNA isolation

A ~50mg piece of frozen tissue (jejunum or liver) was placed in 1mL of TRIzol reagent in a borosilicate test tube. The tissue was homogenized using a Polytron™ homogenizer at speed 8 for 30 seconds from which we purified RNA. The RNA pellet was reconstituted in 50µL of 1x TE buffer (10mM Tris-HCl, 1mM EDTA, pH 7.5). An aliquot of the RNA solution (diluted 5000-fold) was used for quantification of the RNA using the Quant-iT RiboGreen RNA Assay according to the manufacturer's instructions. Each RNA solution was diluted to a final concentration of 0.2mg/mL with TE buffer.

2.2.3 Reverse transcription

cDNA was prepared from the RNA using the SuperScript III First Strand Synthesis SuperMix for RT-qPCR according to the manufacturer's instructions. Briefly, 5 μ L of RNA (0.2 μ g/ μ L) was mixed with 10 μ L of 2x Reaction Buffer, 2 μ L of RT Enzyme mix, and 3 μ L of DEPC-treated water in a thin-walled 0.2mL PCR tube. The tube was mixed, centrifuged briefly, and placed in a thermocycler programmed for the following steps: 25°C for 10min, 50°C for 30min, 85°C for 5min, then 4°C until the program was interrupted. The reaction was completed when 1 μ L of *E. coli* RNase I (2U) was added and mixed, then the tube was centrifuged it briefly and returned to the thermocycler for the following program: 37°C for 20min then 4°C until the program was interrupted. The concentration of cDNA in the solution was determined using the Quant-iT OliGreen ssDNA fluorescent assay in 200-fold dilutions of the RT product against an oligonucleotide standard. All samples were diluted to 10ng/ μ L in DEPC-treated water.

2.2.4 Real time PCR

2.2.4.1 Amplification efficiency

The minimal amount of cDNA required to maintain >90% amplification efficiency was determined for each gene assayed using a dilution curve analysis. These studies were conducted using pooled cDNA from the wild type NFNC samples. Each gene expression assay was tested with 8pg – 25ng of cDNA. The efficiency of the amplification was determined from the slope of the plot of threshold cycle (Ct) values vs. the logarithm of cDNA input (ng) according to Equation 3:

Equation 3: qPCR efficiency

$$\text{Efficiency} = \left(10^{(-1/\text{slope})} \right) - 1$$

The reproducibility of the replicates was measured by calculating the coefficient of determination as a measure of the variability in cycle threshold that is attributable to the amount of cDNA input.

2.2.4.2 Consistency of the reference gene amplification

Before analyzing any of the genes of interest, a plate was prepared probing the threshold cycle for *Actb* for all samples. For this assay 10ng of cDNA was input into each PCR reaction using the method described below.

2.2.4.3 No reverse transcription control

Two experiments were conducted to determine whether any contaminant genomic DNA affected the qPCR results. For all TaqMan gene expression assays except *Actb*, the primers were designed to flank an intron (>800kb). Consequently, the PCR products were separated on an agarose gel to determine whether any genomic DNA was amplified during the reaction. For the *Actb* analysis, a “No Reverse Transcription” control plate was prepared. The dilution factor for each RNA sample was calculated (the dilution due to the reverse transcription reaction and subsequent dilution of the cDNA). The RNA samples were diluted to the lowest dilution factor of all samples (highest potential concentration) then were subjected to a PCR reaction using the *Actb* TaqMan assay according to the method described below.

2.2.4.4 Final PCR method used to determine relative changes to gene expression

Each sample was analyzed for each gene in triplicate. Each plate contained triplicate *Actb* controls in addition to the TaqMan assays for the genes of interest. Two “no template control” wells were included on every plate. With the 96-well fast PCR plate in an ice bucket, the following reagents were added to each well: 10 μ L iTaq SuperMix, 1 μ L of TaqMan gene expression assay, and 4 μ L of DEPC-treated water followed by 5 μ L of the appropriate sample cDNA (2ng/ μ L). An optically transparent film sealed the plate prior to a brief centrifugation of the plate to draw all liquid to the bottom of the well. The plate was transported on ice to the ABI 7900HT real time thermocycler at the Centre for Drug Research and Development. The following settings were used to analyze the plates using the machine on standard mode:

- Total volume: 20 μ L
- Passive reference dye: ROX
- Stage 1: 95°C for 3:00 (to dissociate the inhibitory antibody from the *Taq* polymerase)
- Stage 2: 40 repeats of 95°C for 0:15 followed by 60°C for 1:00

The data were analyzed for relative gene expression using the $\Delta\Delta C_t$ method(317).

Table 2-2: Summary of the TaqMan gene expression assays

Gene	RefSeq	TaqMan Assay ID	Probe Sequence	Exon-Exon Boundary
<i>Abca1</i>	NM_013454.3	Mm01350760_m1	AGGAGACAAACATGTCAGCTGTTAC	2-3
<i>Abcb1a</i>	NM_011076.2	Mm00440761_m1	TCAAGTGAAAGGGGCTACAGGGTCT	20-21
<i>Abcb4</i>	NM_008830.2	Mm00435630_m1	GCAGCATCAGCAACCAAGGCAGAGA	2-3
<i>Abcb11</i>	NM_021022.3	Mm00445168_m1	GCTATGTTTTTCAGGGTGGTCTCTTC	23-24
<i>Abcg5</i>	NM_031884.1	Mm00446249_m1	TGTGTGTTATTGGACTCTGGGCTTG	10-11
<i>Abcg8</i>	NM_026180.2	Mm00445980_m1	TGGATAGTGCCTGCATGGATCTCCA	11-12
<i>Actb</i>	NM_007393.3	Mm00607939_s1	ACTGAGCTGCGTTTTACACCCTTTC	6-6
<i>Cyp7a1</i>	NM_007824.2	Mm00484152_m1	ACAACCTGCCAGTACTAGATAGCAT	4-5
<i>Hmgcr</i>	NM_008255.2	Mm01282499_m1	CCTGCCTGCAGATGCTAGGTGTTCA	18-19
<i>Ldlr</i>	NM_010700.2	Mm00440169_m1	GCGGAGCTGCCTCACAGAAGTCGAC	14-15
<i>Npc1l1</i>	NM_207242.2	Mm01191973_m1	CTCTACTGTGCCAATGCCCTCTCA	2-3
<i>Scarb1</i>	NM_016741.1	Mm00450234_m1	CTGTCAAGGGCATCGGGCAAACAGG	9-10

Table 2-3: Efficiency, limit of quantification and reproducibility of the PCR reaction

	Gene	Minimum cDNA input	Slope	Amplification efficiency	R ²
	Liver	<i>Abcg5</i>	200pg	-3.46	94.7%
<i>Abcg8</i>		200pg	-3.53	91.9%	0.9980
<i>Abcb4</i>		200pg	-3.49	93.5%	0.9988
<i>Abcb11</i>		200pg	-3.55	91.2%	0.9921
<i>Actb</i>		200pg	-3.30	101.0%	0.9716
<i>Cyp7a1</i>		200pg	-3.25	102.9%	0.9984
<i>Hmgcr</i>		200pg	-3.38	97.6%	0.9923
<i>Ldlr</i>		200pg	-3.32	100.1%	0.9961
<i>Scarb1</i>		200pg	-3.47	94.3%	0.9944
<i>Abcb1a</i>		1ng	-3.16	107.1%	0.9300
<i>Abcb1b</i>		>25ng	n/a	n/a	n/a
		Gene	Minimum cDNA input	Slope	Amplification efficiency
	Jejunum	<i>Abca1</i>	40pg	-3.48	93.9%
<i>Abcg5</i>		40pg	-3.53	91.9%	0.9985
<i>Abcg8</i>		200pg	-3.48	93.8%	0.9989
<i>Actb</i>		1ng	-3.48	93.7%	0.9992
<i>Nr1h4</i>		40pg	-3.47	94.3%	0.9980
<i>Npc1l1</i>		1ng	-3.47	94.0%	0.9997
<i>Hmgcr</i>		40pg	-3.55	91.5%	0.9708
<i>Ldlr</i>		40pg	-3.37	98.0%	0.9761
<i>Scarb1</i>		500pg	-3.57	90.8%	0.9909
<i>Abcb1a</i>		10ng	-3.58	90.1%	0.9937

Table 2-4: Summary of controls in the RT-qPCR experiments

RNA quality	Quantification of the RNA was performed using the RiboGreen assay, which has been demonstrated to recognize high quality RNA. Purity of the isolation was also assessed qualitatively using the ratio of UV absorption at 260nm and 280nm
Consistency of the RT reaction	The cDNA produced by the reverse transcription reaction was quantified using the OliGreen ssDNA assay. All samples were subsequently diluted to 2ng/μl prior to the PCR reaction.
PCR amplification efficiency	Dilution curves were run for each gene to determine the minimum input of cDNA that would result in amplification efficiency of >90% for all genes. This was found to be 0.2-1.0ng. To ensure that the reactions were above this threshold 10ng of template cDNA was used for all qPCR reactions.
Reproducibility	Each sample was analyzed for each gene in triplicate, additionally; the coefficient of determination was used to demonstrate that the Ct value correlates with cDNA input. The reference gene, encoding murine β-actin, was assayed for each sample on each plate in triplicate to ensure that there were no day to day variability
No Template Control	Duplicate No Template Control wells were assayed on each PCR plate
Genomic DNA control	The TaqMan assays for all genes except <i>Actb</i> were designed to flank an intron. Additionally, each RNA sample was assayed for <i>Actb</i> without a reverse transcription step – there was no evidence of interference by genomic DNA
Equal loading of wells	The equal loading of each well was confirmed using the passive dye ROX, which was incorporated into the iTaq SuperMix
Reference Gene	The reference gene (<i>Actb</i>) demonstrated consistent expression in all treatment groups. The slight plate-to-plate variability in Ct value for any given sample was greater than any differences between treatment groups

2.3 Methods used in chapter 5

2.3.1 Gallbladder bile acid quantification

The gallbladders were pierced and a 7 μ L aliquot of bile was sent to Dr. David Cohen's laboratory for analysis at the Harvard Digestive Diseases Center. The bile salt composition was determined by HPLC as previously reported(318). Briefly, gallbladder bile was extracted overnight in 50mL of ethanol at 60°C with glycocholate as an internal standard. The ethanolic extracts were dried under N₂ and re-solubilized in 1mL of methanol. The bile salt species were separated on a Beckman Ultrasphere reverse phase ODS column (250mm x 4.6 μ m internal diameter, 5 μ m particle size) using an isocratic mobile phase (3:1 v/v methanol : 10mM KH₂PO₄, pH 5.35).

2.3.2 Gallbladder lipid analysis

Gallbladder bile was analyzed for phospholipid content using a phospholipase D-choline oxidase based colorimetric assay; murine gallbladder bile contains only phosphatidylcholine, so not other assay is required(197). Cholesterol content in the gallbladder bile was determined using the Amplex Red Cholesterol Assay, a cholesterol oxidase based fluorometric assay.

2.4 Methods used in chapter 6

2.4.1 Reagents

Caco-2 cells (HTB-37) were purchased from the American Type Culture Collection (Manassas, VA). Dulbecco's Modified Eagle Medium (powdered high glucose without L-glutamine or NaHCO₃), L-glutamine, 100x Penicillin-Streptomycin

(10000U/mL, 10000µg/mL), Phosphate Buffered Saline (PBS), 0.25% Trypsin-50mM EDTA, Stealth™ siRNA silencing vectors, lot-matched Fetal Bovine Serum (qualified), TRIzol, Quant-iT RiboGreen RNA Assay, Quant-iT OliGreen ssDNA Assay, UltraPure DEPC-treated (RNase/DNase-free) water, Superscript III First Strand Synthesis SuperMix for qRT-PCR, and TaqMan gene expression assays, ZO-1 (N-terminus) rabbit polyclonal antibody, goat anti-rabbit-HRP488 monoclonal antibody, DAPI (4'-6-diamidino-2-phenylindole dihydrochloride), and Prolong AntiFade Gold were purchased from Life Technologies (Carlsbad, CA). HPLC-grade chloroform, methanol, hexanes, ethyl acetate, and 2-propanol were purchased from Thermo Fisher Scientific (Waltham, MA). iTaq supermix with ROX was purchased from Bio-Rad (Hercules, CA). Triton X-100 and bovine serum albumin (fatty acid free) were purchased from Sigma (St. Louis, MO).

2.4.2 Culture conditions

Caco-2 cells (passage 25-35) were grown in 75cm² tissue-culture treated flasks in Dulbecco's Modified Eagle Medium (DMEM) prepared as follows: 1 package of high glucose DMEM (no L-glutamine or NaHCO₃) was dissolved with 1.5g of NaHCO₃ in 1L of distilled water, and the pH adjusted to 7.2 ± 0.05. Under sterile conditions, 440mL of media was mixed with 50mL of heat inactivated fetal bovine serum (FBS), 5mL of 200mM L-glutamine, and 5mL of 100x Penicillin-Streptomycin (Final concentration: 10% heat inactivated FBS, 2mM L-glutamine, 100U/mL Penicillin, 100µg/mL streptomycin). The mixture was sterilized by filtration through a 0.22µm pore filter and stored at 4°C until needed.

Caco-2 cells were grown in tissue culture-treated flasks equipped with HEPA filters in a humidified 37°C incubator with a 5% CO₂ atmosphere. All experiments were conducted within passages 25-35. Cells were grown as a monolayer until they reached ~80 confluence. The cells were subcultured by washing with sterile PBS, then incubating with 2-3mL 0.25% Trypsin-EDTA to lift the cells from the flask (~5min). Washing the cells with media containing FBS inactivated the Trypsin. After centrifugation (125g for 5min) the supernatant was discarded and the cells were re-suspended in DMEM for counting and seeding onto new flasks.

2.4.3 Transfection

The transfection was set up so that the vector and lipid-based reagent cocktail was 10% of the total volume (50µL) while the cell suspension was 90% of the volume (450µL). Initial optimization experiments varied the lipid transfection reagent content while maintaining a constant siRNA concentration. The second step in the optimization experiments was to establish a dose-response of each siRNA construct. The final transfection protocol is as follows: in a sterile polystyrene plate siLentFect transfection reagent was diluted 4:21 with Opti-MEM 1. In a separate well, the siRNA construct was diluted from 20µM stock to a concentration 20x higher than the final desired concentration. After 5-10min of incubation at room temperature, equal volumes of diluted siLentFect and siRNA were mixed and incubated for 40-50min at room temperature. The cells from five tissue culture flasks were washed and lifted from the flask using Trypsin-EDTA, as described above. Washing the cell pellet three times with 10mL of additive-free Opti-MEM 1 media removed FBS and antibiotics.

After the final washing step, the cell pellet was re-suspended in 5mL of Opti-MEM 1 for counting prior to preparing a dilution of 933 333 cells/mL in Opti-MEM 1. In the apical chamber of the Transwell plate, 50 μ L of transfection reagent was mixed with 450 μ L of cell suspension (420000 cells). After filling the basolateral chambers with 1.5mL of Opti-MEM 1, the cells plate was incubated in a humidified 37°C incubator with a 5% CO₂ atmosphere. After 4h, the reagents were removed by aspiration and replaced with DMEM. Media was changed every 2d until the end of the experiment.

2.4.4 Characterization of the Caco-2 cells

Trans-epithelial electrical resistance (TEER) was used to measure the formation of a monolayer of cells linked by tight junctions. To qualitatively demonstrate the presence of tight junctions, representative monolayers were fixed and prepared for immunofluorescence microscopy to indirectly visualize the tight junction protein, ZO-1. The polycarbonate membrane was excised from the Transwell, washed for 20min in PBS with four changes of the PBS solution, and fixed in neutral buffered formalin. The membranes were washed for 3x5min in PBS (2mL each wash) and stored at 4°C until needed. A strip of membrane was washed in PBS, then “permeabilized” with 0.2% (v/v) Triton X-100 for 10min. The membrane strip was washed for 5x4min in 1mL of PBS. The strip was blocked with a 1% bovine serum albumin (BSA) solution for 60min then incubated with the primary antibody overnight at 4°C (1:100 dilution of polyclonal rabbit anti ZO-1 diluted in 1% BSA). The strip was washed for 3x5min in 0.5mL PBS and then incubated with secondary antibody for 3h at room temperature, protected from light (1:1000 goat anti rabbit-Alexa488 diluted in 1% BSA). The strip

was washed 3x5min in 0.5mL distilled water then stained for 60s with DAPI. The strip was immediately washed 3x1min in 0.5mL of distilled water and 1x15min in distilled water, protected from light. The strip was mounted on a microscope slide such that the apical face of the cells was facing away from the slide. Any residual water was removed by wicking, a drop of AntiFade Gold™ solution was added, and a coverslip was placed on top of the apical face of the cells. After curing for 24h in the dark, the cells were visualized using an Olympus FV10i confocal microscope.

The silencing of *ABCB1* was determined quantitatively using RT-qPCR. The polycarbonate membrane was excised from the Transwell, placed in a clean 12-well polystyrene plate and the total RNA was extracted from the Caco-2 cells using 1mL of TRIzol and a cell scraper. The TRIzol was transferred to a 2mL polypropylene centrifuge tube and the remaining RT-qPCR steps were performed exactly as described in section 2.2.4.4.

Protein levels were qualitatively observed using Western Blot techniques. The polycarbonate membrane was excised from the Transwell and placed in a clean 12-well polystyrene plate. The cells were lysed with the addition of 0.25mL of modified Radioimmunoprecipitation Assay (RIPA) buffer(50mM Tris-HCl pH 7.4, 1% NP-40, 0.25% Na deoxycholate, 150mM NaCl, 1mM EDTA, 1mM PMSF, 1mM Na₃VO₄, 1mM NaF, 1µg/mL Aprotinin, 1µg/mL leupeptin, 1µg/mL pepstatin). Bicinchoninic acid (BCA) assays quantified the protein content in the lysates. Aliquots (20-30µg protein) were reduced and denatured by the addition of 6x loading buffer containing β-mercaptoethanol followed by incubation at 60°C for 3min. The proteins were separated on 4-15% gradient polyacrylamide gels at constant current (15mA/gel

through the stacking gel and 20mA/gel through the resolving gel). The proteins were electrophoretically transferred to nitrocellulose in Towbin's buffer(319) at constant voltage (100V) for 90min with cooling. The membranes were blocked in 3% milk powder and 1% BSA diluted in tris-buffered saline containing 0.1% (v/v) Tween-20 (TBS-T) for 2h at room temperature. The membranes were cut along the 75kDa line into two strips and then incubated in primary antibody overnight at 4°C. The strips were washed 3x5min in TBS-T and then incubated with the appropriate secondary antibody for 1h at room temperature. The blots were washed 3x5min in TBS-T and visualized using SuperSignal West Pico substrate for the horseradish peroxidase (HRP) conjugated to the secondary antibodies in a CCD camera-equipped darkroom.

Table 2-5: Western blot antibodies

Target	Manufacturer	Host isotype	Dilution	MW
P-glycoprotein (C219 monoclonal)	Covance (sig-38710)	Mouse IgG ₁	1:20 (3.75µg/mL)	170kDa
Sucrase-Isomaltase (A-17)	Santa Cruz (SC-27603)	Goat polyclonal	1:100 (2µg/mL)	250kDa
Actin (I-19)	Santa Cruz (SC-1616)	Goat polyclonal	1:200 (1µg/mL)	42kDa
Goat IgG-HRP	Santa Cruz (SC-2020)	Donkey polyclonal	1:5000	n/a
Mouse IgG ₁	Santa Cruz (SC-2060)	Goat polyclonal	1:1000	n/a

2.4.5 Cholesterol uptake and esterification

The uptake and esterification experiments were conducted in Caco-2 cells five days post-transfection to allow for formation of tight junctions and differentiation of the cells. On day 4 post-transfection, a subset of cells were treated with 100nM

LY335979 (a third generation P-glycoprotein inhibitor) or 2.5% DMSO (as a vehicle control). Organic solutions of cholesterol (1mM in chloroform), oleoyl-*rac*-glycerol (300 μ M in chloroform), and sodium taurocholate (10mM in ethanol) were prepared in a fumehood. An aliquot of each organic solution (1.5mL each) was mixed with 450nCi of 14 C-cholesterol to prepare the micelle solution. The lipids were evaporated to dryness under N₂ and reconstituted in 5mL of DMEM using vortex mixing and sonication for ~10min until a clear solution was obtained. The medium from the apical chamber of the Transwell was removed and replaced with the micelle solution (1.0x10⁵ DPM/well). The apical chambers were then treated with either 12.5 μ L of 4 μ M LY335979 (100nM final concentration) or 12.5 μ L of DMSO (2.5% final concentration) as a vehicle control. The plates were returned to the incubator for the duration of the incubation (2h or 4h). All media was removed and the polycarbonate membrane was excised from the Transwell. The cells were washed twice with ice cold PBS. The cells were lysed in 250 μ L of distilled water using cell scrapers. A 200 μ L aliquot of the lysate and the polycarbonate membrane were transferred to a 16x100mm borosilicate test tube. The lipids were extracted according to Folch's protocol(320). Briefly, the lipids were extracted in 3.8mL of 2:1 (v/v) chloroform:methanol. The tubes were centrifuged to pellet the membrane and the supernatant was transferred to a new test tube. The organic solvent was washed with 0.8mL of 0.73% NaCl_(aq) and the phases separated by centrifugation (1000g for 5min at 4°C). The upper, aqueous, layer was discarded. The interface was washed once with 0.5mL of pure upper phase (48:3:49 v/v/v 0.58%NaCl_(aq):chloroform:methanol) without disrupting the interface; the wash was discarded. The remaining liquid was made monophasic through the drop wise

addition of methanol and then evaporated to dryness under N₂. The lipid film was reconstituted in 100µL of chloroform, 60µL was spotted onto a silica coated polyester TLC plate and 20µL was transferred to a scintillation vial for analysis. The plate was developed with a 9:1 (v/v) Hexanes: Ethyl Acetate mobile phase, dried and exposed to a phosphor storage screen for 24h (protected from light). The screen was visualized using Dr. Hafeli's Cyclone PhosphorImager. The densitometry was performed using Labworks software version 3 from UVP (Upland, CA). Esterification was determined by comparing the radioactivity in unesterified cholesterol vs. cholesteryl ester peaks, normalized to the total activity in the lane.

2.4.6 Cholesterol synthesis

The synthesis experiments were conducted on Caco-2 cells five days post-transfection to allow for formation of tight junctions and differentiation of the cells based on the results of section 2.4.4 . On day 4 post-transfection, a subset of cells were treated with 100nM LY335979 (a third generation P-glycoprotein inhibitor) or 2.5% DMSO (as a vehicle control). On day five, each well was treated with 5.0x10⁵ DPM of [¹⁴C]-acetate (in 10µL ethanol) for 4h in a 37°C humidified incubator with a 5% CO₂ atmosphere. After the incubation, the media was removed, the polycarbonate membrane excised from the Transwell and the lipids isolated and separated by TLC analysis as described above. The relative cholesterol synthesis rates were determined by quantifying the incorporation of ¹⁴C into cholesterol.

2.5 Data analysis

All data sets were analyzed for statistical significance by parametric methods using SigmaStat (version 3.5). If the data set did not meet the assumptions required of parametric methods (i.e. they were not normally distributed or had unequal variance) they were ln-transformed, or in one occasion transformed using a square root transform. For every data set in this thesis, these transforms were sufficient for the use of parametric methods for statistical testing.

For all statistical testing the following general hypothesis statements were used:

$$H_0: \mu_1 = \mu_2$$

$$H_1: \mu_1 \neq \mu_2$$

An alpha value of 0.05 was selected *a priori* as the threshold at which the null hypothesis can be rejected for all tests. The selection of statistical method used was determined by the data. When comparisons were made between two groups then unpaired two-tailed t-tests were used. If there were several groups to compare, for example four dietary groups, a one-way Analysis of Variance (ANOVA) was selected. If the groups were part of two separate factors, for example diet and genotype, then a two-way ANOVA was run. If the ANOVA revealed that the difference in means of the main groups was greater than could be expected by chance ($p\text{-value} < \alpha$), then Tukey post *hoc* tests were run to determine which groups were statistically significant.

Chapter 3: Cholesterol phenotype of the *Abcb1a*^{-/-}/*1b*^{-/-} knockout

mouse

In our efforts to characterize the cholesterol phenotype of the *Abcb1a*^{-/-}/*1b*^{-/-} mouse, our initial aim was to quantify changes to cholesterol absorption, based on the *in vitro* finding that Pgp inhibition affects cholesterol transport through enterocytes as described in section 1.5.3. Three *in vivo* studies are described in this chapter:

1. A pilot study that followed the experimental design published by Luker *et al.* designed to probe the contribution of Pgp to cholesterol absorption after the mice ate diets containing elevated fat and/or cholesterol for 12 weeks. The fractional cholesterol absorption was determined using a plasma dual-isotope method. The n-number was variable due to the success rate of the administration.
 2. A plasma dual-isotope cholesterol absorption study using methodology proposed by Wang and Carey (315) after 12-weeks on a high fat, high cholesterol diet (45%kcal from fat and 0.20% w/w cholesterol), n=5 per time point. This study was required due to the variability observed in the pilot study.
 3. A fecal dual-isotope cholesterol absorption study on mice fed test diets containing elevated fat and/or cholesterol for 8 weeks, n=10 per diet. This study was deemed to have more physiological relevance than the previous two studies.
- Consequently, the serum and tissue samples collected from these mice were utilized for all subsequent analyses.

Although the fractional cholesterol absorption and circulating lipids are reported for study #1 and study #2, no statistical testing was performed due to the inherent limitations of both studies, discussed later in this chapter.

3.1 Results

We used three different methods to probe alterations to cholesterol absorption, as described in section 2.1.4. The data collected in a pilot study (Study #1) based on the protocol published by Luker *et al.* (229) is shown in Figure 3-1. After revising the methodology based on the publication by Wang and Carey(315), we repeated the plasma dual isotope cholesterol absorption assay using mice fed the HFHC diet for 12 weeks (Study #2). The results of this study are shown in Figure 3-2. Finally, the fecal dual-isotope cholesterol absorption assay results obtained for mice fed each of the four test diets for 8 weeks are shown in Figure 3-3. This method is more physiologically relevant and reduced the number of mice required for a complete assessment of the effect of *Abcb1a* and *Abcb1b* deletion after chronic exposure to the range of test diets(315). The mice were genotyped upon arrival to confirm deletion of *Abcb1a/1b* in the knockout mice. In addition to assessing the magnitude of cholesterol absorption, we quantified the circulating cholesterol levels in the pilot study (Table 3-1), the plasma dual isotope study (Table 3-2), and the fecal dual isotope study (Table 3-3).

High cholesterol diets reduced the magnitude of cholesterol absorption (Figure 3-3) and the HFHC diet increased serum cholesterol concentrations (Table 3-3). Both data sets were analyzed by two-way ANOVA and although diet was a statistically

significant factor for both fractional cholesterol absorption and circulating cholesterol levels ($p < 0.001$), genotype was not ($p > 0.2$). Qualitative FPLC analysis of lipoprotein cholesterol revealed that KO mice fed either high fat or high cholesterol had increased cholesterol in very-low density lipoproteins (VLDL) when compared with the WT mice. In KO mice, this change was accompanied by decreased high-density lipoprotein (HDL) cholesterol (Figure 3-4). Both diet and genotype affected cholesterol accumulation in the liver ($p < 0.001$ for diet, $p = 0.009$ for genotype). The two-way ANOVA revealed a statistically significant interaction between diet and genotype, indicating that the effect of diet on cholesterol accumulation depends on genotype, and vice versa making it impossible to determine the contribution of each factor to the changes in cholesterol accumulation. Due to the limitations of the plasma dual isotope methods, the data collected in these studies were not subjected to statistical testing.

Table 3-1: Plasma cholesterol in the pilot study mice.

Plasma was isolated from mice after 12 weeks on the test diets and analyzed by cholesterol oxidase-based assays. The mean total plasma cholesterol \pm one SD is listed; n-number as shown. Statistical testing was not performed on this data set.

Genotype	Diet	Total cholesterol (mg/dL)	SD	n
Wild Type FVB	NFNC	133.6	\pm 18.8	3
	HFNC	161.2	\pm 15.1	4
	HFHC	198.4	\pm 16.2	7
<i>Abcb1a</i> ^{-/-} / <i>1b</i> ^{-/-} KO	NFNC	137.7	\pm 9.0	3
	HFNC	143.8	\pm 31.2	4
	HFHC	187.0	\pm 15.7	7

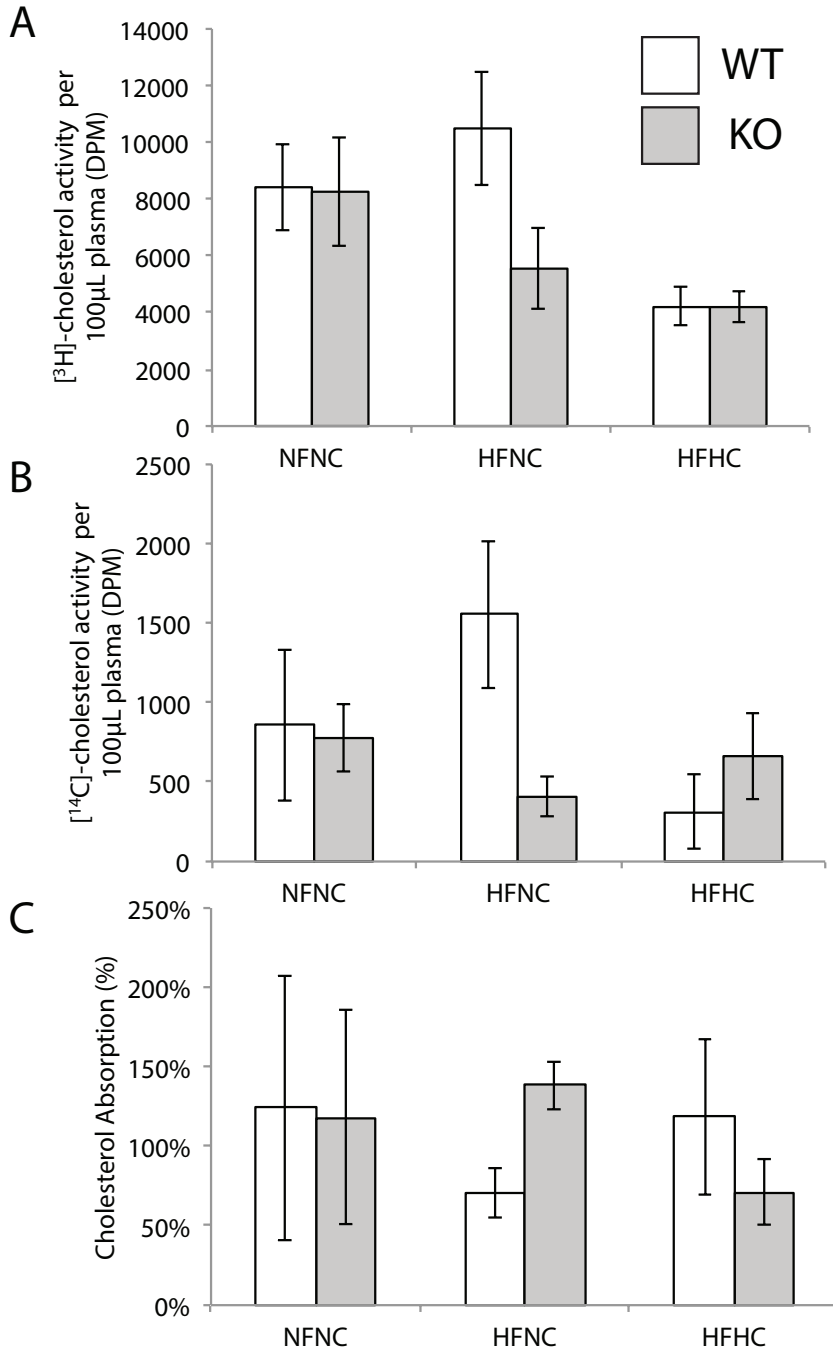


Figure 3-1: Cholesterol absorption calculated from the pilot study (Study #1). After 12 weeks on either the NFNC diet (n=3), the HFNC diet (n=4), or the HFHC diet (n=7), each mouse was administered 1μCi of [³H]-cholesterol in an oral gavage and 0.1μCi of [¹⁴C]-cholesterol as an intravenous bolus. (A) Plasma levels of PO-administered [³H]-cholesterol in 100μL of plasma. (B) Cholesterol absorption was calculated from Equation 1 using 100μL of plasma. For each graph, the mean values for the wild type (WT: hollow bars) and *Abcb1a^{-/-}/1b^{-/-}* (KO: grey bars) mice are shown ± SD. No statistical testing was performed on these data sets.

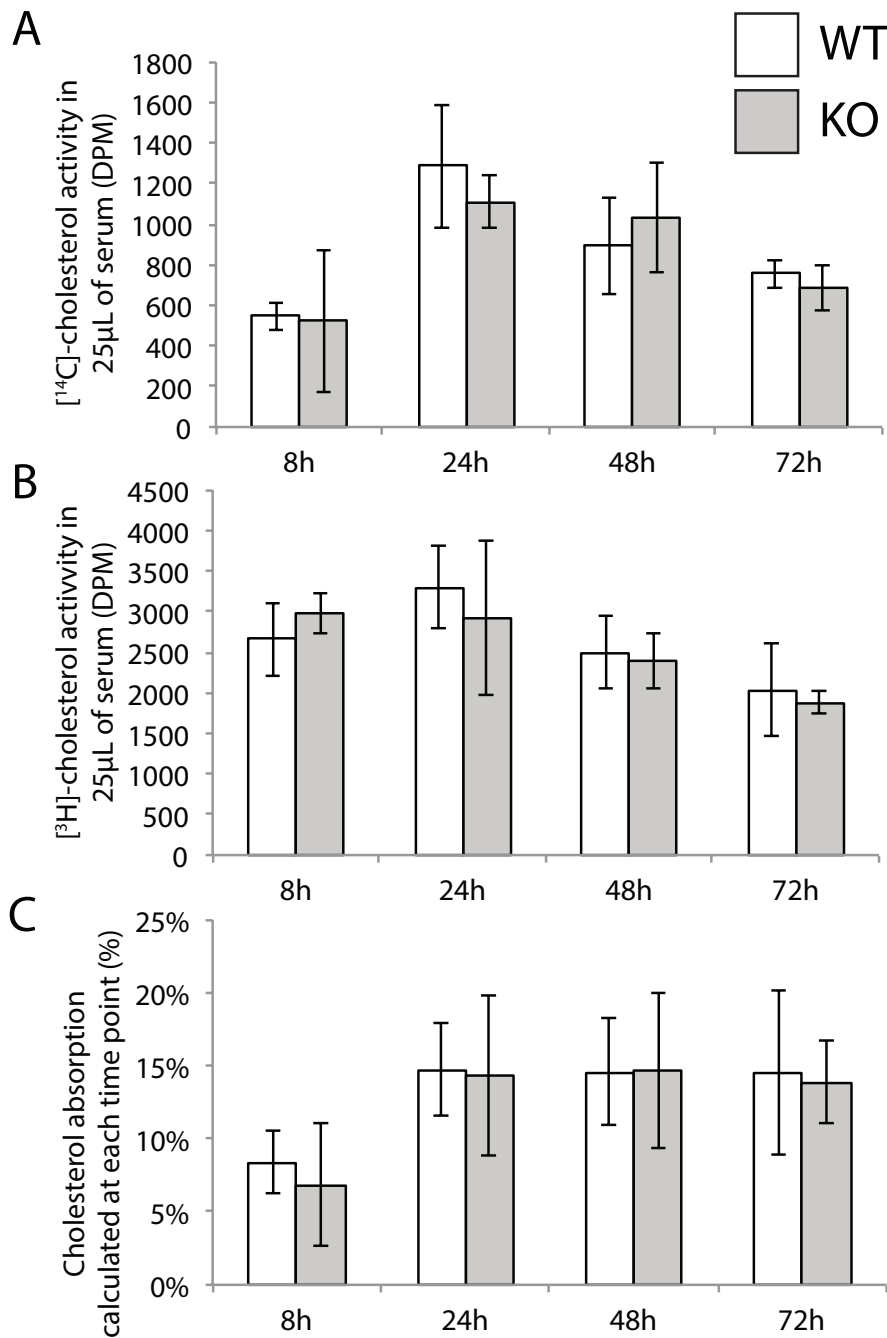


Figure 3-2: Plasma dual isotope cholesterol absorption assay (Study #2). (A) Activity of the PO-administered [^{14}C]-cholesterol in 25 μL of serum. (B) Activity of the IV-administered [^3H]-cholesterol in 25 μL of serum. (C) Cholesterol absorption as determined by Equation 1 based on a PO dose of 1 μCi of [^{14}C]-cholesterol and an IV dose of 2.5 μCi of [^3H]-cholesterol. The mean values for wild type FVB mice (WT: hollow bars) and *Abcb1a^{-/-}/1b^{-/-}* (KO: grey bars) are shown \pm SD; n=3-5.

Table 3-2: Plasma cholesterol levels after 12 weeks on the HFHC diet (Study#2). Mean plasma levels of total cholesterol and unesterified cholesterol are reported below for mice administered the HFHC diet for 12 weeks but not subjected to the cholesterol absorption assay.

Genotype	Diet	n	Total plasma cholesterol (mg/dL)			Unesterified plasma cholesterol (mg/dL)		
			Mean	±	SD	Mean	±	SD
Wild type	HFHC	8	227.1	±	26.6	55.6	±	19.5
<i>Abcb1a^{-/-}/1b^{-/-}</i> KO	HFHC	7	236.3	±	15.4	59.8	±	14.0

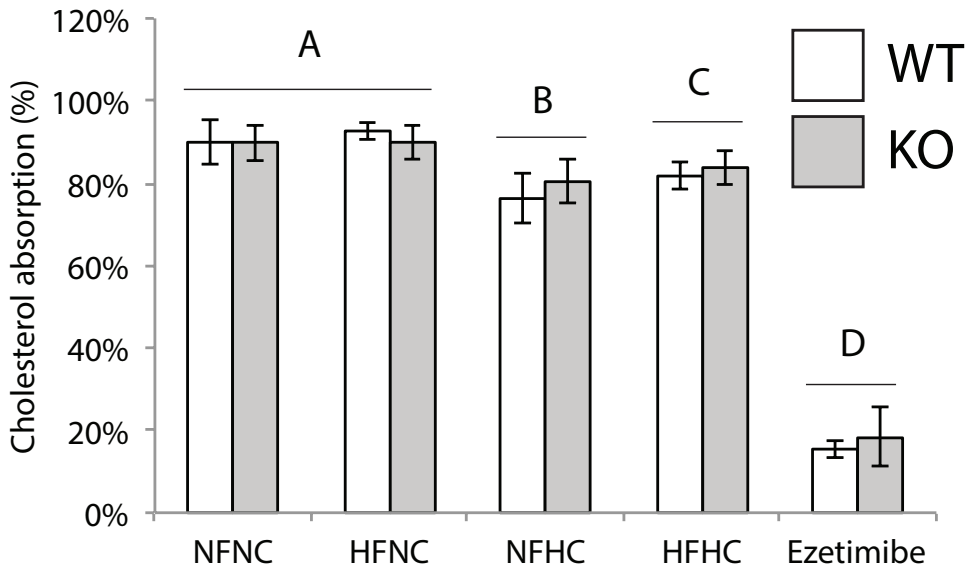


Figure 3-3: Effect of diet and P-glycoprotein deletion on fractional cholesterol absorption.

The results of the fecal dual isotope cholesterol assay are displayed for the wild type (WT: hollow bars) and *Abcb1a^{-/-}/1b^{-/-}* (KO: grey bars) mice after 8 weeks on the test diets. Mice were administered a single dose of cholesterol mixed with β -sitostanol (non-absorbed dosing control) and fecal matter was collected for 96h. The ezetimibe group was given a single 10mg/kg dose 60min prior to the administration of cholesterol. The mean cholesterol absorption values, calculated using Equation 2 are shown \pm SD; n=8-10. There are no statistically significant differences between WT and KO mice within a dietary group. The NFHC, HFHC, and ezetimibe treatment groups were statistically different from all other experimental groups ($p < 0.05$ by two-way ANOVA).

Table 3-3: Effect of diet and deletion of P-glycoprotein on serum cholesterol parameters after nine weeks on the test diets. Serum was collected and analyzed for total and unesterified cholesterol content using cholesterol oxidase-based assays.

Genotype	Diet	n	Total serum cholesterol (mg/dL)			Unesterified serum cholesterol (mg/dL)		
			mean	±	SD	mean	±	SD
Wild Type	NFNC	8	164.0	±	48.0	44.2	±	44.2
	HFNC	8	150.1	±	30.6	59.0	±	59.0
	NFHC	7	188.4	±	28.0	53.9	±	53.9
	HFHC	7	#216.3	±	34.8	#79.5	±	79.5
<i>Abcb1a^{-/-}/1b^{-/-}</i> KO	NFNC	8	144.8	±	33.9	48.8	±	21.8
	HFNC	8	165.5	±	33.0	50.4	±	22.2
	NFHC	8	177.4	±	42.9	52.8	±	9.1
	HFHC	8	#209.3	±	38.5	#79.9	±	21.9

#p<0.05 relative to the NFNC diet by two-way ANOVA with Tukey *post-hoc* tests; n=7-8

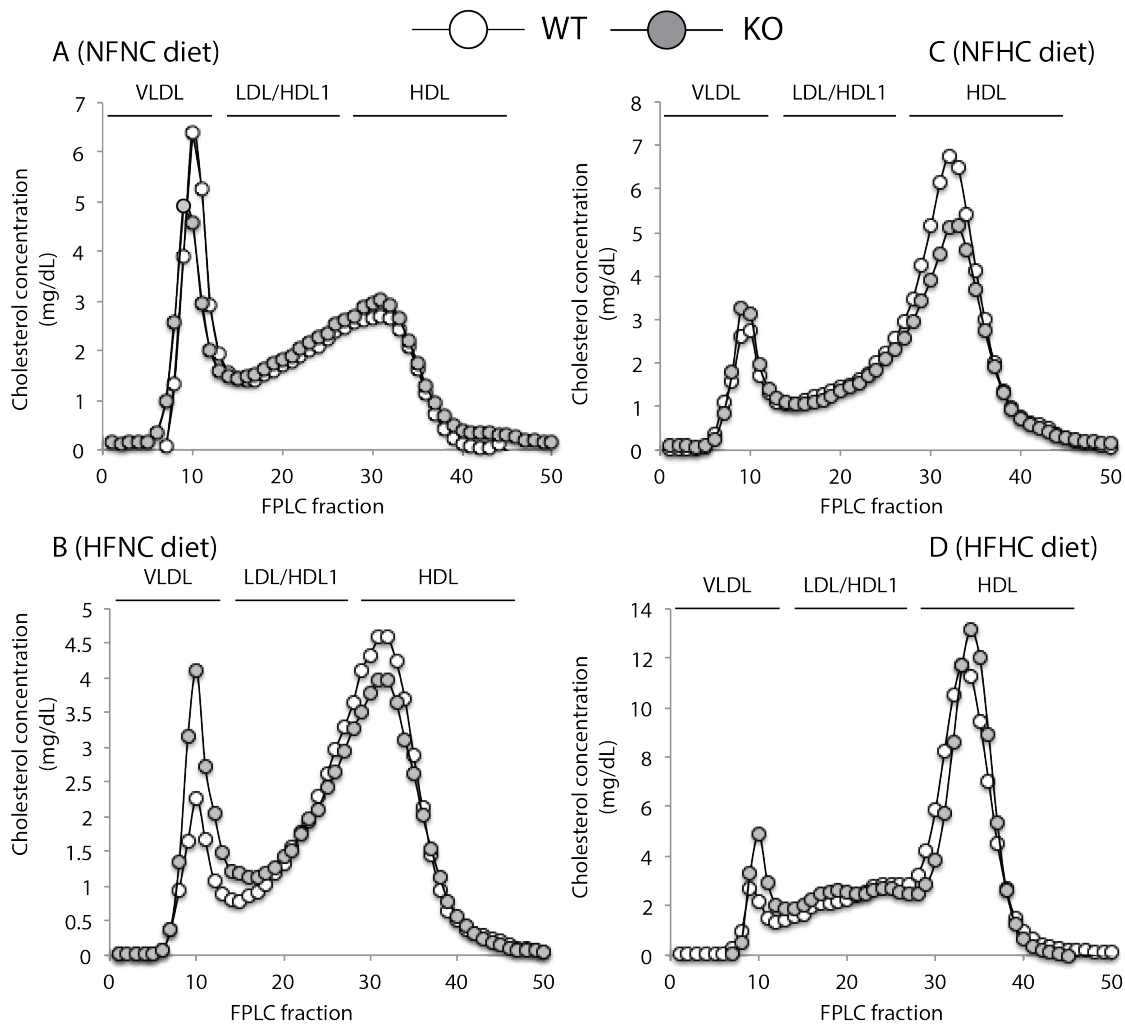


Figure 3-4: Effects of P-glycoprotein deletion on lipoprotein cholesterol. Equal volumes of pooled serum were separated by fast protein liquid chromatography (FPLC). Each panel contains the total cholesterol concentration obtained from wild-type (WT – hollow markers) or *Abcb1a^{-/-}/1b^{-/-}* knockout mice (KO – grey markers) administered the following test diets: (A) NFNC (25% kcal fat + 0.02% w/w cholesterol), (B) HFNC (45% kcal fat + 0.02% w/w cholesterol), (C) NFHC (25% kcal fat + 0.20% w/w cholesterol), (D) HFHC (45% kcal fat + 0.20% w/w cholesterol); pools consisted of equal volume aliquots from 6-10 mice. The cholesterol was distributed into Very Low-Density Lipoproteins (VLDL), Low-Density Lipoproteins (LDL) / sub fraction 1 of High Density Lipoproteins (HDL1), or HDL.

Table 3-4: Accumulation of cholesterol in the livers of wild type and knockout mice. The cholesterol content in total lipid extracts obtained from liver samples was measured using cholesterol oxidase-based assays. The mean total cholesterol content per gram of liver is shown along with the ratio of unesterified cholesterol to total cholesterol.

Group	n	Hepatic cholesterol content (mg/g)	Ratio of free to total cholesterol
		mean ± SD	mean ± SD
WT-NFNC	9	7.10 ± 1.06	0.86 ± 0.04
WT-HFNC	10	7.24 ± 0.75	0.85 ± 0.04
WT-NFHC	10	#13.40 ± 2.58	#0.73 ± 0.07
WT-HFHC	10	#9.31 ± 1.29	#0.78 ± 0.04
KO-NFNC	10	6.96 ± 1.39	0.87 ± 0.05
KO-HFNC	9	6.49 ± 1.09	0.89 ± 0.02
KO-NFHC	10	*#10.84 ± 1.63	#0.72 ± 0.06
KO-HFHC	10	#9.20 ± 1.04	#0.74 ± 0.06

The data were analyzed by a two-way ANOVA; n-number as shown. Diet contributes to both total cholesterol as well as the ratio ($p < 0.001$). Genotype contributes to the total hepatic cholesterol ($p = 0.009$) but not to the esterification ratio ($p = 0.976$), there is a statistically significant interaction between diet and genotype for the total cholesterol accumulation ($p = 0.032$). # $p < 0.05$ dietary group differs from NFNC, * $p < 0.05$ KO differs from WT.

Discussion

This chapter summarizes the characterization of the cholesterol phenotype of the *Abcb1a*^{-/-}/*1b*^{-/-} mouse after chronic exposure to a range of atherogenic diets. When the *Abcb1a*^{-/-} and the *Abcb1a*^{-/-}*1b*^{-/-} mice were first described by Schinkel *et al.* the authors were surprised at the lack of an obvious phenotype change(184). The authors speculated that by using these mutant mice the endogenous role of P-glycoprotein would be elucidated(321, 322). In fact, the authors found that the mutant mice have altered pharmacokinetics of a range of drugs and acute sensitivity to a derivative of a naturally occurring insecticide, ivermectin, caused by increased CNS exposure. These findings support the hypothesis that Pgp evolved as a xenobiotic defense mechanism(172, 173, 175, 187). Based on the *in vitro* studies summarized in 1.5.3, our

initial focus was to characterize any alterations to the cholesterol phenotype in *Abcb1a^{-/-}/1b^{-/-}* knockout mice relative to wild type. Consistent with previous studies, the deletion of Pgp did not cause an obvious change in the cholesterol phenotype. The knockout mice had unchanged circulating cholesterol (Table 3-3), cholesterol absorption (Figure 3-3), and only small changes to the lipoprotein cholesterol profile (Figure 3-4). This is complimentary to what is known about human polymorphisms of *ABCB1* and cholesterol homeostasis. While subtle differences in lipoprotein profiles have been attributed to the C3435T and A76T polymorphisms in the *ABCB1* gene(323), the impact of these polymorphisms does not compare with the effects of mutations that cause Tangier Disease (*ABCA1*) (95-97), Niemann Pick type C disease(*NPC1* and *NPC2*) (324, 325), Sitosterolemia (*ABCG5* and *ABCG8*) (6, 326) or Familial Hypercholesterolemia (*LDLR*) (16, 17).

Initially, we focused our efforts on establishing a model to probe the gastrointestinal absorption of cholesterol. The most provocative *in vitro* studies linking cholesterol trafficking with Pgp showed that inhibition of Pgp interrupted the flux of cholesterol into the cell. We hypothesized that Pgp knockout mice would have perturbed cholesterol absorption, especially after consuming cholesterol-rich diets. After 8 weeks of feeding, the fecal dual isotope method was employed for the determination of the fractional cholesterol absorption as summarized in Figure 3-3. Increased cholesterol in the NFHC and HFHC diets reduced the fractional cholesterol absorption but increased fat alone (HFNC diet) did not. A recent publication indicated that a “high-fat no-cholesterol diet” reduced the expression of cholesterol transporters in mice, resulting in a 31% reduction in fractional cholesterol

absorption(327). This is contrasted by a small crossover clinical trial in which the fractional cholesterol absorption of healthy men administered a “low-fat low-cholesterol diet” (24% kcal fat, 2.6mg/kg/d cholesterol) was similar to when they were administered a high-fat low cholesterol diet (39%kcal from fat, 4.1mg/kg/d cholesterol) but was higher than when they ate a low-fat high-cholesterol diet (30%kcal from fat, 11.4mg/kg/d cholesterol) (328). The data collected in our study are more closely aligned with the clinical trial results than with the murine study.

Diet, but not deletion of *Pgp* affected circulating cholesterol, as shown in Table 3-3. After 9 weeks on the Western-pattern HFHC diet, mice had increased total cholesterol, as expected. It is surprising that the mice on the NFHC diet did not have statistically significant increases to total circulating cholesterol. Unfortunately, these analyses provide only a gross overview of the circulating lipids and do not provide insight into the changes to lipoproteins linked to diet and genotype effects. With assistance from the Harvard Digestive Diseases Center, pooled serum was analyzed qualitatively by FPLC (Figure 3-4). Knockout mice fed the NFHC and HFHC diets had more cholesterol associated with larger lipoproteins (VLDL and LDL) (fractions 8-20) than the diet-matched wild type mice. The changes to HDL cholesterol were not as consistent: when challenged with either fat or cholesterol, knockout mice had a reduction in HDL-cholesterol but this trend did not hold when the mice were fed the HFHC diet. The results of this study give qualitative evidence that circulating cholesterol balance is affected by deletion of *Abcb1a/1b* but more quantitative measurements are needed to confirm this observation. Future studies should be

designed to quantify the changes to lipoprotein profile and test whether the changes have an effect on atherosclerotic plaque formation.

The liver is the primary organ for the regulation of whole body cholesterol homeostasis. When the cholesterol content of the liver was analyzed (Table 3-4), both diet and genotype affected the accumulation of cholesterol. As expected, diets containing elevated cholesterol raised the hepatic cholesterol content, accompanied by a shift to the esterified, storage form of cholesterol. Although there was a trend for the Pgp knockout animals to have decreased cholesterol content, there were no changes to cholesterol esterification. On the surface, this finding may contradict the assertion made by Luker *et al.* that Pgp affects hepatic cholesterol esterification(229). However, the data that form the basis for their conclusion were derived from orally administered cholesterol at 6h post-administration. No differences in esterification were noted between wild type and knockout mice when cholesterol was administered intravenously, nor at time points >6h when cholesterol was given orally(229). Our data, in combination with the data published by Luker *et al.* suggest that the effect of Pgp on hepatic cholesterol storage is minor, and that differences may only be seen using a more acute experimental design.

There are several limitations to the studies described in this chapter. All the methods used to probe cholesterol absorption are indirect measurements. The only method for directly assessing the magnitude of cholesterol absorption is to cannulate the mesenteric lymph duct and quantify the precise amount of a dose of cholesterol that reaches the lymphatic system(315, 329). This approach was not feasible as it requires a great deal of surgical skill and the mice need to be under a general

anesthetic for the duration of the experiment which impacts gastrointestinal motility(330, 331). The first studies performed in this thesis made use of the plasma dual isotope cholesterol absorption assay. We selected this approach to facilitate comparisons between our results and the work published by Luker *et al.* (229) Unfortunately, once we began analyzing the pilot study data, we realized that the amount of radiolabeled cholesterol given intravenously was insufficient for quantification at 72h post-administration. The problems associated with this are clearly demonstrated in Figure 3-1. Relative to the wild type mice, the Pgp knockout mice appeared to have reduced cholesterol absorption when fed the HFHC diet and increased cholesterol absorption when fed the HFNC diet (Figure 3-1C). If the analysis were limited to the orally administered, ³H-cholesterol, the knockout mice have reduced cholesterol absorption after consuming the HFNC diet and unchanged cholesterol absorption when fed the HFHC diet (Figure 3-1A). This apparent contradiction is caused by the low levels of intravenously administered cholesterol recovered in the plasma Figure 3-1B which is used as the denominator in the calculation (Equation 1).

In order to improve the method, the second study made use of a protocol published by Wang *et al.* (315) in which ¹⁴C-cholesterol was given orally and the activity of the IV dose (³H) is 20-fold higher than used in the Luker method. The data obtained by this method was more consistent (Figure 3-2), but the physiological relevance of using the plasma dual isotope method is questionable. Intravenously administered cholesterol (in a colloidal dispersion such as Intralipid), is rapidly cleared from the bloodstream by K upffer cells in the liver and is gradually released back to the

bloodstream, with a maximal concentration 24h post-administration(315, 332, 333).

The plasma dual isotope absorption assay is based on the pharmacokinetic determination of bioavailability; however, for a correct estimation the intravenous dose is assumed 100% bioavailable – this is not the case for cholesterol. Because of these limitations, we conducted our large-scale study using the fecal dual isotope cholesterol absorption assay. This assay is physiologically relevant and allowed us to correct for small differences in dosing volume by measuring the excretion of the non-absorbed β -sitostanol.

3.1.1 Conclusions

The *Abcb1a*^{-/-}/*1b*^{-/-} mice did not have an obvious change to their cholesterol phenotype compared to wild type FVB littermate controls. With knockout mice, it is important to examine the known regulatory pathways surrounding the phenotype under investigation, as compensatory shifts in regulation may be sufficient to maintain homeostasis. The precise changes to these regulatory networks may allow the investigator to elucidate the function of the deleted protein. This concept is developed in the following chapter.

Chapter 4: The effect of diet and P-glycoprotein deletion on cholesterol regulatory networks

Despite feeding mice diets rich in cholesterol and fat we did not observe any cholesterol phenotype differences between the wild type and *Abcb1a*^{-/-}/*1b*^{-/-} mice (Chapter 3). We speculated that if Pgp is a cholesterol transporter, cholesterol homeostasis in the knockout mice might be maintained through altered activation of two key pathways that regulate intracellular cholesterol, SREBP-2 and LXR. If Pgp is an efflux transporter of cholesterol, then deletion of *Abcb1a* and *Abcb1b* should increase intracellular cholesterol levels resulting in decreased SREBP-2 activation and increased LXR activation. In order to probe the state of each of these pathways, we used RT-qPCR to measure the expression of genes activated by these transcription factors.

4.1 Results

The expression of *Abcb1a* in the jejunum of the wild type mice was increased in response to dietary cholesterol but not fat, as shown in Figure 4-1. Addition of cholesterol alone to the diet induced expression of *Abcb1a* by 3.2-fold over the basal diet, and 4.9-fold when the mice were on the Western-style HFHC diet ($p < 0.001$; one-way ANOVA). In contrast, hepatic *Abcb1a* responded to both fat and cholesterol (Figure 4-2). Dietary fat alone induced *Abcb1a* expression by 3.2-fold over the basal diet and was further increased by dietary cholesterol ($p < 0.001$ vs. NFNC by one-way ANOVA).

High levels of dietary cholesterol (NFHC and HFHC diets) increased the expression of the efflux transporters *Abcg5*, *Abcg8* and *Abca1* in the jejunum of both

wild type and *Abcb1a*^{-/-}/*1b*^{-/-} mice (Table 4-1 and Table 4-2; p<0.05; one way ANOVA). Conversely, neither increased dietary fat nor cholesterol had a consistent effect on the expression of SREBP-2 target genes, *Ldlr*, *Hmgcr*, *Npc111* and *Scarb1* (Table 4-1 and Table 4-2).

As observed with the jejunum data, cholesterol feeding induced the LXR-target genes *Abcg5*, *Abcg8*, and *Cyp7a1* in the livers of both wild type and knockout mice (Table 4-3 and Table 4-4; p<0.05 by one-way ANOVA). The relationship between dietary conditions and the expression of FXR target genes was not consistent in these studies. Neither *Abcb11* nor *Abcb4* have alterations to their expression of the same magnitude seen with the LXR-target genes. In wild type mice, *Abcb11* expression was unchanged in all dietary conditions but *Abcb4* expression was modestly increased by dietary fat or cholesterol (Table 4-3; p<0.05 by one-way ANOVA). The pattern of dietary effects on the FXR pathway was similar in the knockout mouse livers (Table 4-4).

Deletion of *Pgp* affected both the SREBP-2 and LXR pathways. In the jejunum, knockout mice administered the NFNC diet had decreased expression of *Ldlr*, *Hmgcr*, and *Npc111* (p<0.05 vs. WT by t-test). This was not accompanied by changes to the expression of LXR target genes (Figure 4-3; p>0.05). Total accumulation of cholesterol was unaffected by *Pgp* deletion (3.9mg cholesterol/g tissue in wild type vs. 3.8mg/g in knockout jejunum for mice fed the NFNC diet; p>0.05).

In the liver, the expression of LXR-target genes *Abcg5* and *Cyp7a1* were increased in *Pgp* knockout mice relative to wild type littermates. There were no changes to the expression of FXR target genes *Abcb4* or *Abcb11* (Table 4-3 and Table

4-4), or SREBP-2 target genes *Hmgcr*, *Ldlr*, or *Scarb1* when administered the NFNC diet (Figure 4-4). There were no consistent changes to LXR, SREBP-2 or FXR target genes attributable to *Abcb1a/Abcb1b* deletion in the other dietary groups.

Table 4-1: Summary of changes to the transcriptional networks in the jejunum of wild type FVB mice induced by dietary conditions.

Measuring the expression of *Ldlr*, *Npc111*, *Hmgcr* and *Scarb1* genes by RT-qPCR assessed the activation of SREBP-2. The expression of *Abca1*, *Abcg5* and *Abcg8* (by RT-qPCR) determined the activation of LXR. The mean ΔCt value of the NFNC dietary group was set as the reference to which all samples were compared using the $\Delta\Delta\text{Ct}$ methodology. The mean relative expression and SD is shown to indicate the variability of the response to dietary stimulus.

LXR target gene	0.02% cholesterol		0.02% cholesterol		0.20% cholesterol		0.20% cholesterol	
	25% kcal fat		45% kcal fat		25% kcal fat		45% kcal fat	
	mean	SD	mean	SD	mean	SD	mean	SD
<i>Abca1</i>	1.00	± 0.33	0.98	± 0.48	*2.39	± 0.54	*2.94	± 0.69
<i>Abcg5</i>	1.00	± 0.30	*0.59	± 0.10	*1.78	± 0.40	*2.54	± 1.05
<i>Abcg8</i>	1.00	± 0.37	*0.46	± 0.14	*2.29	± 0.58	*2.74	± 0.95

SREBP-2 target gene	0.02% cholesterol		0.02% cholesterol		0.20% cholesterol		0.20% cholesterol	
	25% kcal fat		45% kcal fat		25% kcal fat		45% kcal fat	
	mean	SD	mean	SD	mean	SD	mean	SD
<i>Ldlr</i>	1.00	± 0.39	1.31	± 0.35	0.85	± 0.28	*1.38	± 0.23
<i>Npc111</i>	1.00	± 0.55	0.73	± 0.37	1.06	± 0.30	1.12	± 0.30
<i>Hmgcr</i>	1.00	± 0.46	1.09	± 0.30	0.78	± 0.22	*2.18	± 0.57
<i>Scarb1</i>	1.00	± 0.54	0.50	± 0.38	0.93	± 0.71	1.30	± 0.57

* p<0.05 vs. WT-NFNC by one-way ANOVA and Tukey *post-hoc* tests; n=9-10.

Table 4-2: Summary of changes to transcriptional networks in the jejunum of *Abcb1a^{-/-}/1b^{-/-}* mice induced by dietary conditions.

Measuring the expression of *Ldlr*, *Npc1l1*, *Hmgcr* and *Scarb1* genes by RT-qPCR assessed the activation of SREBP-2. The activation of LXR was determined by measuring the expression of *Abca1*, *Abcg5* and *Abcg8* by RT-qPCR. The mean Δ Ct value of the WT-NFNC dietary group was set as the reference to which all samples were compared using the $\Delta\Delta$ Ct methodology. The mean relative expression and SD is shown to indicate the variability of the response to dietary stimulus.

LXR target gene	0.02% cholesterol		0.02% cholesterol		0.20% cholesterol		0.20% cholesterol	
	25% kcal fat		45% kcal fat		25% kcal fat		45% kcal fat	
	mean	SD	mean	SD	mean	SD	mean	SD
<i>Abca1</i>	0.69	± 0.25	1.15	± 0.46	*3.32	± 1.53	*2.65	± 1.38
<i>Abcg5</i>	0.78	± 0.35	0.91	± 0.35	*2.09	± 0.63	*2.84	± 1.60
<i>Abcg8</i>	0.86	± 0.43	1.02	± 0.38	*2.28	± 0.81	*2.48	± 1.43

SREBP-2 target gene	0.02% cholesterol		0.02% cholesterol		0.20% cholesterol		0.20% cholesterol	
	25% kcal fat		45% kcal fat		25% kcal fat		45% kcal fat	
	mean	SD	mean	SD	mean	SD	mean	SD
<i>Ldlr</i>	0.54	± 0.15	*1.45	± 0.42	*0.71	± 0.26	*1.06	± 0.17
<i>Npc1l1</i>	0.34	± 0.19	*1.00	± 0.52	*1.27	± 0.98	*1.19	± 0.75
<i>Hmgcr</i>	0.55	± 0.31	*1.53	± 0.45	0.91	± 0.46	*1.60	± 0.61
<i>Scarb1</i>	0.66	± 0.58	0.70	± 0.29	*1.14	± 0.52	0.99	± 0.43

* $p < 0.05$ vs. KO-NFNC by one-way ANOVA and Tukey *post-hoc* tests; n=9-10.

Table 4-3: Summary of the changes to transcriptional networks in the livers of wild type FVB mice induced by dietary conditions

Measuring the expression of *Abcb11* and *Abcb4* by RT-qPCR assessed the activation of FXR. The activation of LXR was determined by measuring the expression of *Abca1*, *Abcg5* and *Abcg8* using RT-qPCR. The mean ΔC_t value of the NFNC dietary group was the reference to which all samples were compared using the $\Delta\Delta C_t$ methodology. The mean relative expression is shown \pm SD.

LXR target gene	0.02% cholesterol		0.02% cholesterol		0.20% cholesterol		0.20% cholesterol	
	25% kcal fat		45% kcal fat		25% kcal fat		45% kcal fat	
	mean	SD	mean	SD	mean	SD	mean	SD
<i>Abcg5</i>	1.00	\pm 0.40	1.10	\pm 0.29	*3.51	\pm 0.89	*2.54	\pm 0.65
<i>Abcg8</i>	1.00	\pm 0.34	*1.47	\pm 0.40	*3.04	\pm 0.68	*3.14	\pm 0.76
<i>Cyp7a1</i>	1.00	\pm 0.66	*6.83	\pm 4.47	*8.52	\pm 3.24	*7.44	\pm 3.82

FXR target gene	0.02% cholesterol		0.02% cholesterol		0.20% cholesterol		0.20% cholesterol	
	25% kcal fat		45% kcal fat		25% kcal fat		45% kcal fat	
	mean	SD	mean	SD	mean	SD	mean	SD
<i>Abcb4</i>	1.00	\pm 0.23	*1.68	\pm 0.35	*1.39	\pm 0.24	*1.65	\pm 0.28
<i>Abcb11</i>	1.00	\pm 0.29	1.06	\pm 0.36	0.95	\pm 0.21	1.00	\pm 0.22

* $p < 0.05$ vs. WT-NFNC by one-way ANOVA and Tukey post-hoc tests; n=9-10 after ln transform of data.

Table 4-4: Summary of the changes to transcriptional networks in the livers of *Abcb1a^{-/-}/1b^{-/-}* mice induced by dietary conditions.

Measuring the expression of *Abcb11* and *Abcb4* by RT-qPCR assessed the activation of FXR; measuring expression of *Abca1*, *Abcg5* and *Abcg8* using RT-qPCR determined the activation of LXR. The mean Δ Ct value of the WT-NFNC dietary group was the reference to which all samples were compared using the $\Delta\Delta$ Ct methodology. The mean relative expression is shown \pm SD.

LXR target gene	0.02% cholesterol		0.02% cholesterol		0.20% cholesterol		0.20% cholesterol	
	25% kcal fat		45% kcal fat		25% kcal fat		45% kcal fat	
	mean	SD	mean	SD	mean	SD	mean	SD
<i>Abcg5</i>	1.48	\pm 0.60	0.98	\pm 0.21	*3.34	\pm 0.75	*2.54	\pm 0.50
<i>Abcg8</i>	1.31	\pm 0.51	1.33	\pm 0.35	*3.07	\pm 0.68	*3.04	\pm 0.59
<i>Cyp7a1</i>	2.38	\pm 1.06	5.14	\pm 2.51	*6.44	\pm 2.66	*9.10	\pm 6.02

FXR target gene	0.02% cholesterol		0.02% cholesterol		0.20% cholesterol		0.20% cholesterol	
	25% kcal fat		45% kcal fat		25% kcal fat		45% kcal fat	
	mean	SD	mean	SD	mean	SD	mean	SD
<i>Abcb4</i>	0.90	\pm 0.27	*1.88	\pm 0.44	*1.58	\pm 0.32	1.12	\pm 0.24
<i>Abcb11</i>	0.76	\pm 0.23	*1.41	\pm 0.49	0.65	\pm 0.17	*1.14	\pm 0.35

*p<0.05 vs. KO-NFNC by one-way ANOVA and Tukey post-hoc tests; n=9-10.

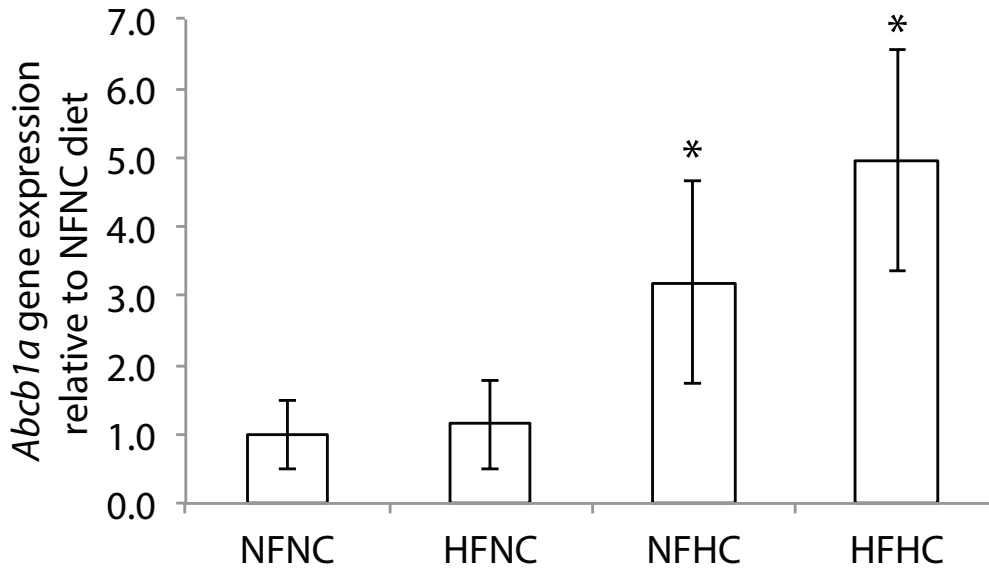


Figure 4-1: Effects of diet on the expression of *Abcb1a* in the jejunum. The expression of *Abcb1a*, the isoform expressed in enterocytes, was measured in jejunum samples isolated from mice on each of the four diets. The mean ΔCt of the NFNC dietary group was the reference to which all samples were compared using the $\Delta\Delta Ct$ methodology relative to *Actb*. The mean relative expression is shown \pm SD; n=9-10. *p<0.05 vs. NFNC by one-way ANOVA and Tukey post-hoc tests

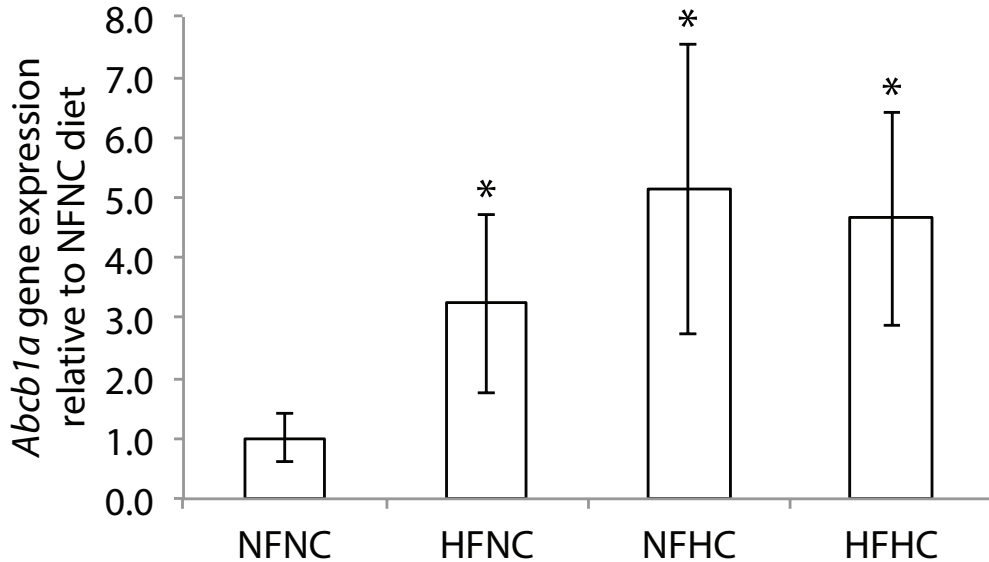


Figure 4-2: Effects of diet on the expression of *Abcb1a* in the liver. The expression of *Abcb1a*, the isoform expressed in hepatocytes, was measured in liver samples isolated from mice on each of the four diets. The mean ΔCt of the NFNC dietary group was the reference to which all samples were compared using the $\Delta\Delta Ct$ methodology relative to *Actb*. The mean relative expression is shown \pm SD; n=9-10. *p<0.05 vs. NFNC by one-way ANOVA and Tukey post-hoc tests

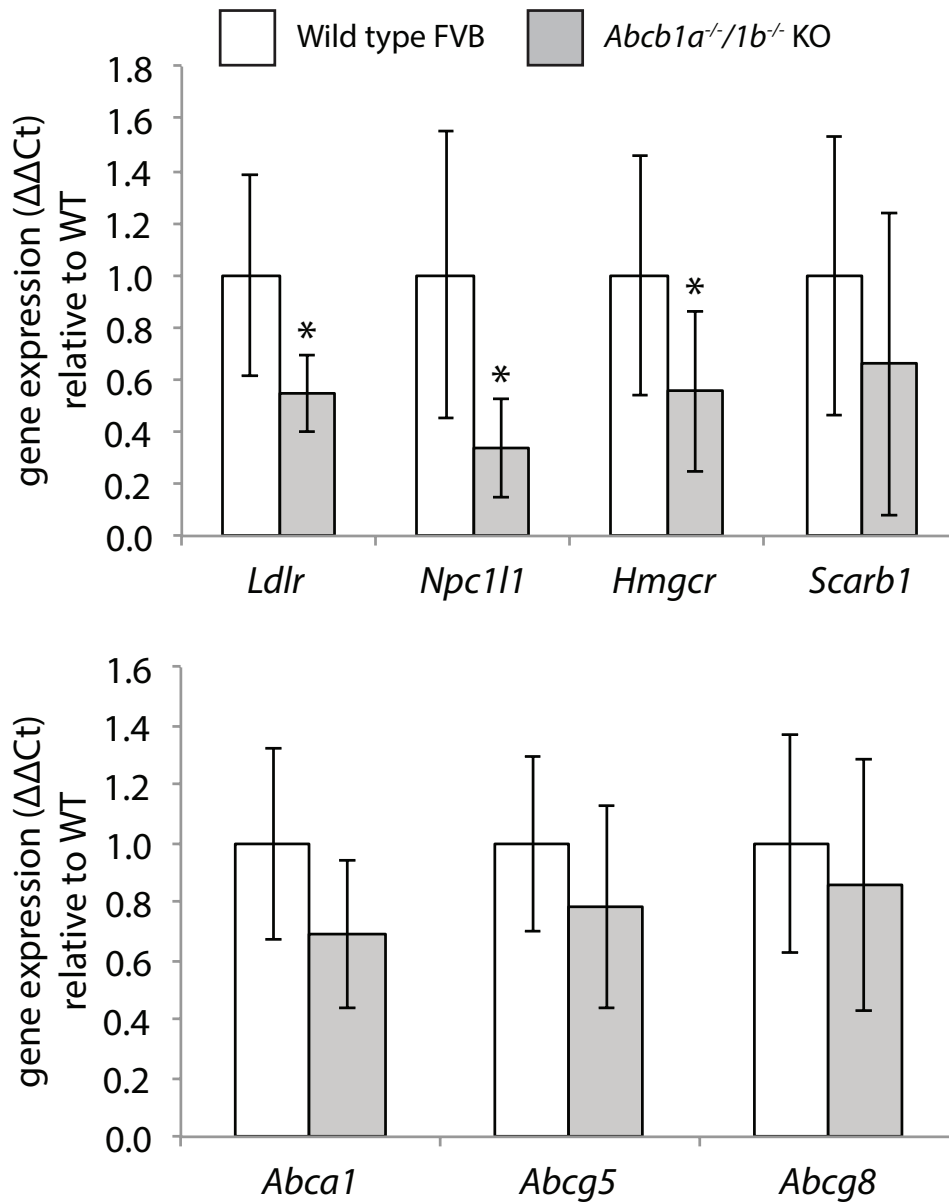


Figure 4-3: Effect of *Abcb1a/1b* deletion on SREBP-2 and LXR activation in the jejunum. (A) Relative to WT mice, *Abcb1a*^{-/-}/*1b*^{-/-} KO mice have reduced expression of genes under the transcriptional control of SREBP-2 after administration of the NFNC diet. (B) WT and KO mice do not show alterations to the expression of genes under transcriptional control of LXR. Mean values shown \pm SD; n=9-10. *p<0.05 vs. WT by unpaired t-test

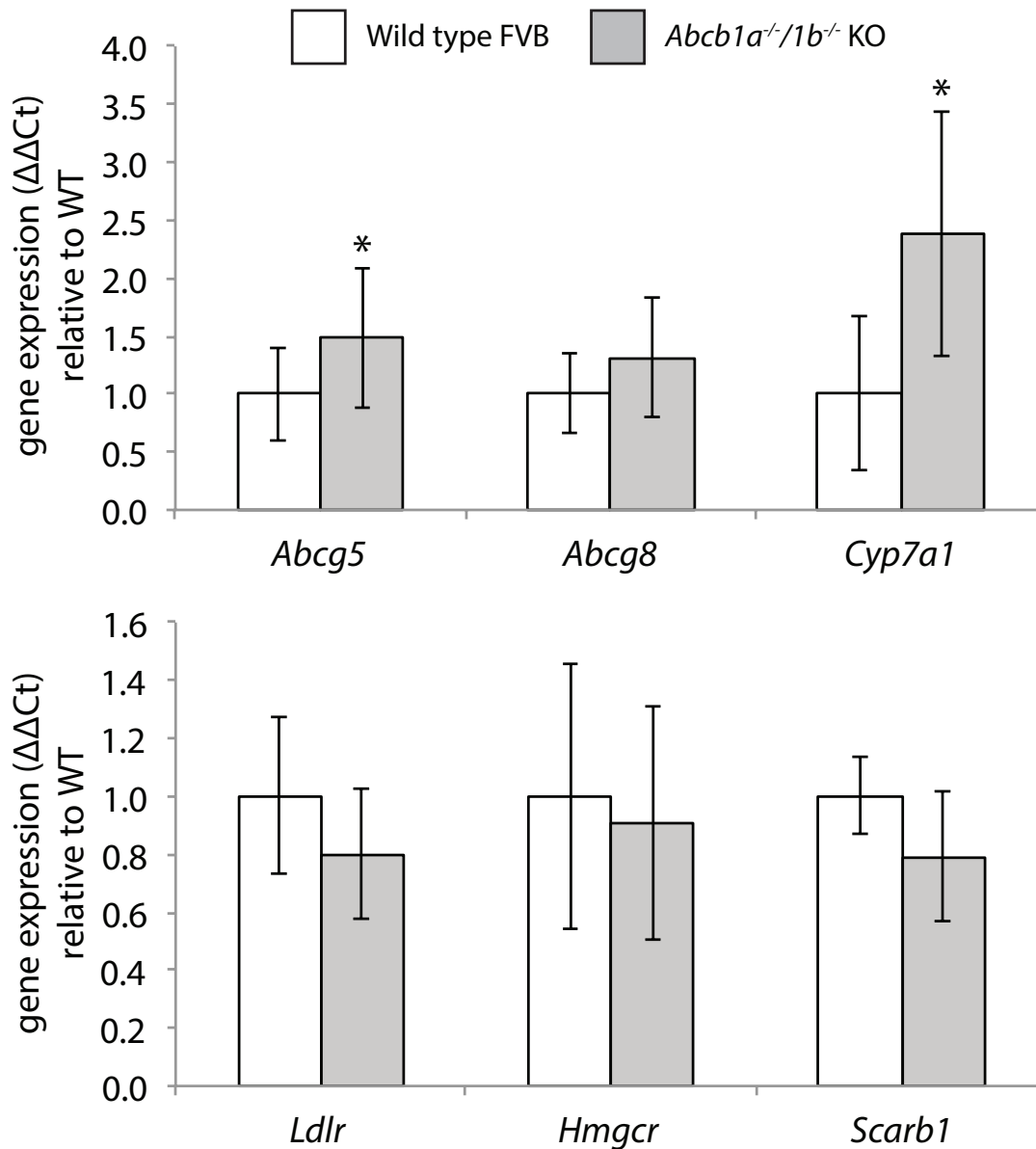


Figure 4-4: Effect of *Abcb1a/1b* deletion on SREBP-2 and LXR activation in the liver. (A) KO mice have increased expression of genes under the transcriptional control of LXR after chronic administration of the NFNC diet; similar results were seen with the HFHC diet. (B) Knockout mice do not show changed hepatic expression of SREBP-2 target genes as they did in the jejunum samples. Mean values shown \pm SD; n=9-10. *p<0.05 vs. WT by unpaired t-test

Table 4-5: Accumulation of cholesterol in the jejunum.

Lipids were extracted from a sample of jejunum using the Folch method(320) and analyzed for cholesterol content using the Amplex Red cholesterol assay. The mean cholesterol content per gram of tissue is shown \pm SD; n=9.

	n	Total cholesterol (mg/g)		Unesterified Cholesterol		Ratio (unesterified:total)	
		mean	SD	mean	SD	mean	SD
WT	9	3.88	\pm 1.16	3.56	\pm 1.06	0.93	\pm 0.026
<i>Abcb1a</i> ^{-/-} / <i>1b</i> ^{-/-} knockout	9	3.76	\pm 0.79	3.46	\pm 0.75	0.92	\pm 0.022

4.2 Discussion

Knockout mice are widely used to study the role proteins play in physiological processes; however, compensatory mechanisms can be activated in knockout mice obscuring the role of the protein. As discussed in Chapter 3, we hypothesized that P-glycoprotein functions as a cholesterol transporter but we did not observe any changes in cholesterol phenotype in the *Abcb1a*^{-/-}/*1b*^{-/-} mice. By examining both the LXR and SREBP-2 cholesterol regulatory networks in the jejunum and liver, we hoped to determine whether Pgp had an effect on murine cholesterol homeostasis. Two key pieces of data in this chapter indicate that cholesterol homeostasis is perturbed in the *Abcb1a*^{-/-}/*1b*^{-/-} mouse: (1) reduced activation of the sterol sensing pathway (SREBP-2) in the intestines of knockout mice relative to wild type mice, and (2) increased LXR activation in the livers of knockout mice relative to wild type. The nature of alterations to these pathways suggests that the Pgp knockout mice lack a cholesterol efflux mechanism.

If cholesterol is a substrate for Pgp mediated efflux, then removal of the protein should increase intracellular cholesterol levels. Our data do not indicate that the cholesterol content of jejunum from knockout mice was significantly different from wild type mice (Table 4-5). However, total tissue cholesterol content cannot identify alterations to cholesterol trafficking. The activation of the SREBP-2 transcription factor can act as a probe to determine whether intracellular cholesterol levels are affected by deletion of Pgp. Small increases to the cholesterol content of the endoplasmic reticulum deactivate SREBP-2(232, 233), providing us with a sensitive measure for alterations to the intracellular pool of cholesterol. The results presented in Figure 4-3 indicate that SREBP-2 activity was decreased in the jejunum of Pgp knockout mice, suggesting that intracellular cholesterol levels were increased relative to wild type. There were minimal dietary effects to SREBP-2 activation in both wild type and knockout mice challenged by high cholesterol. SREBP-2 is a transcription factor that is activated by low levels of cholesterol in order to increase cellular cholesterol content(232, 233, 279). The stimulus of a ten-fold increase in dietary cholesterol in the intestinal lumen (for the NFHC and HFHC diets, relative to the NFNC diet) likely deactivated SREBP-2, regardless of a knockout effect.

All known cholesterol efflux mechanisms are activated transcriptionally(247, 248, 254, 334) or post- translationally(335, 336) through the nuclear receptor LXR. We probed the contributions of both diet and Pgp deletion to the expression of LXR target genes in the liver and jejunum. As predicted, when mice were fed diets with elevated cholesterol (NFHC and HFHC) they had increased expression of LXR target genes (*Abcg5*, *Abcg8*, *Abca1*, and *Cyp7a1*) in the jejunum and in the liver (Table 4-1,

Table 4-2, Table 4-3, and Table 4-4). In Figure 4-4 we report that LXR target genes were up regulated in the livers of knockout mice relative to their wild type counterparts. LXR is activated in response to oxysterols, intracellular metabolites of cholesterol(237, 240, 247). Despite increased LXR activation, total accumulation of cholesterol in the livers was unchanged in the Pgp knockout mice (Table 3-4). Unfortunately, we were unable to characterize hepatic oxysterol content. We suggest that further studies should be initiated to determine if the increased LXR activation in the knockout mouse liver was caused by increased oxysterols.

The expression of *Abcb1a* in WT mice was induced in response to increased dietary cholesterol (Figure 4-1 and Figure 4-2), though it is not currently thought to be an LXR target gene(337). The *in vitro* induction of *ABCB1* expression is linked to three nuclear receptors, the pregnane X receptor (PXR), the constitutive androstane receptor, and the vitamin D receptor(338-340). To date, *in vivo* data is only available for PXR; a nuclear receptor that regulates the expression of drug metabolizing enzymes and efflux transporters. There are a number of cholesterol metabolites among the identified PXR ligands, including lithocholic acid, 24(S), 25-epoxycholesterol and a number of naturally occurring steroids(341, 342). While it is possible that the increased dietary cholesterol raised the levels of PXR ligands, *Abcb1a* may also be a LXR target. The promoter region for human *ABCB1* contains three DR4 sequence motifs (AGGTTAxxxxAGGTTA) (343), associated with LXR binding(252). By comparison, PXR usually binds to inverted repeat 6 or direct repeat 3 motifs, though some PXR genes do contain DR4 motifs in their promoter regions(248, 343-345). The reported presence of DR4 motifs in the promoter for human *ABCB1* combined with our finding that

murine *Abcb1a* expression was increased in response to cholesterol feeding suggests that *Abcb1a* may be a target of LXR, though more work is needed to test this idea before any conclusions can be drawn.

There are several limitations to this set of studies. Unfortunately, we failed to include a low cholesterol diet (0.002% w/w cholesterol) in the experimental design, which may have allowed us to probe the activation of SREBP-2 in Pgp knockout mice further. By measuring the expression of SREBP-2 target genes, we only have an indirect measurement of the activity of the transcription factor. We attempted to confirm our findings by examining cleavage of SREBP-2 to its active form(232, 233, 346) but there was insufficient jejunum remaining after the lipid extractions and RT-qPCR analyses to conduct the experiment. When examining tissue cholesterol, we were limited to quantifying the total cholesterol content, rather than specifically measuring the intracellular membrane cholesterol content. This is usually estimated by indirect methods such as esterification rates(347) or the oxidation of cell surface cholesterol(348). Recently, a new protocol was published in which endoplasmic reticulum cholesterol content is measured directly (232), which can perhaps be used in future studies. The biggest limitation to this set of studies is the lack of direct evidence that Pgp functions as a cholesterol efflux transporter. Future, *ex vivo*, cholesterol binding studies comparing brush border membranes isolated from the jejunum of *Abcb1a*^{-/-}/*1b*^{-/-} mice to membranes isolated from *Abcg5*^{-/-}/*g8*^{-/-} mice may provide direct evidence that Pgp is a cholesterol efflux transporter.

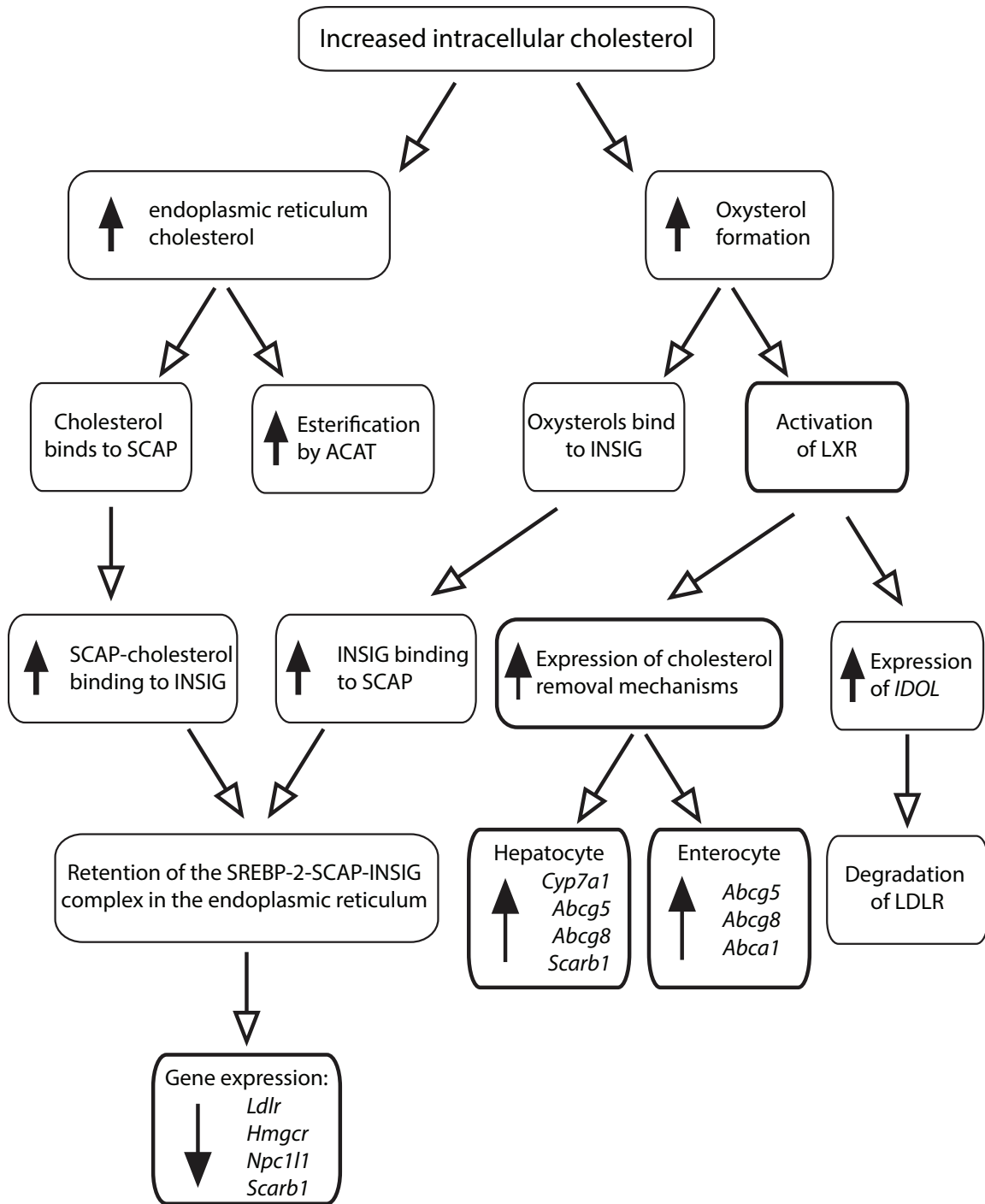


Figure 4-5: Intracellular responses to increased cholesterol. This schematic outlines several key alterations to the cholesterol regulatory mechanisms activated by increased intracellular cholesterol in the mouse. The processes that are measured in this chapter are outlined with a thicker border.

In summary, Pgp is located on the canalicular membrane of hepatocytes, where it effluxes substrates into bile(181, 349). Based on this subcellular location and well-established role in the efflux of drugs, we postulated that it may account for some of the ABCG5/G8-independent cholesterol flux from the liver(8, 150). The data in this chapter demonstrate that *Abcb1a^{-/-}/1b^{-/-}* mice had perturbed cholesterol regulatory pathways relative to wild type mice but we were unable to measure cholesterol efflux directly using our experimental design. The observation that *Abcb1a^{-/-}/1b^{-/-}* mice had reduced expression of genes regulated by the SREBP-2 transcription factor in the jejunum and increased expression of genes regulated by the LXR transcription factor in the liver suggests that these mice lack a cholesterol efflux mechanism, providing interesting preliminary evidence to support future cholesterol efflux studies.

Chapter 5: P-glycoprotein and the efflux of bile acids

Victor Ling has published substantial *in vivo* evidence that bile acid efflux is maintained in mice lacking the well-established bile acid export pump, BSEP(10, 207). Furthermore, Pgp is required to prevent cholestasis in BSEP knockout mice, suggesting that Pgp can function as a bile acid efflux transporter when the normal bile acid efflux mechanism is absent(12). In this chapter we describe our efforts to characterize the contributions of Pgp to bile acid homeostasis after chronic feeding of diets enriched in fat and cholesterol in mice that lack *Abcb1a/1b* but that express *Abcb11*. Our experimental design included a 60min ligation of the common bile duct to allow the gallbladder to fill. We quantified the bile acid, phospholipid, and cholesterol content of the gallbladders to determine if diet and/or Pgp deletion affected bile composition.

5.1 Results

Both wild type FVB and *Abcb1a^{-/-}/1b^{-/-}* knockout mice fed the NFNC diet had equal molar ratios of bile salt, cholesterol and phospholipid in gallbladders (Figure 5-1). The molar composition of cholesterol, phospholipids and bile acids was perturbed in Pgp knockout mice relative to wild type mice after being fed the HFNC, NFHC, or HFHC diets. Deletion of Pgp did not affect the gallbladder concentration of phospholipid for mice fed any of the test diets ($p=0.142$, $p=0.212$, $p=0.095$, $p=0.465$ in the NFNC, HFNC, NFHC, and HFHC groups respectively (Figure 5-2). Consequently, bile acid efflux was normalized to phospholipid to account for inter-individual variability in flow rate. As shown in Figure 5-3, the *Abcb1a^{-/-}/1b^{-/-}* mice had a 30-50% reduction in

bile acid efflux capacity relative to wild type mice when fed cholesterol or fat-rich diets (p=0.001, p=0.03, p=0.011 by two-tailed unpaired t-test for the HFNC, NFHC, and HFHC groups respectively). We assessed the specific molar composition of taumuricholic acid (TMC), tauroursodeoxycholic acid (TUDC), glyoursodeoxycholic acid (GUDC), taurocholic acid (TC), taurochenodeoxycholic acid (TCDC), taurodeoxycholic acid (TDC) in the gallbladders to determine if Pgp demonstrated specificity for a particular type of bile acid. The molar composition of bile acids was not affected by Pgp deletion (Figure 5-4). A bioinformatics screen revealed that 48% of the amino acid sequences of murine BSEP and Pgp (the amino acid sequence encoded by the isoform of the gene expressed in the liver: *Abcb1a*) are identical (Table 5-1). Additionally, the two proteins share 66.3% similarity over the entire amino acid sequence as determined by the BLOSUM62 substitution matrix(350). In contrast, when Pgp was compared with other multidrug resistance associated proteins, there was <22% identity and <41% similarity between the amino acid sequences. This homology pattern was closely mirrored for the human orthologs of the proteins (Table 5-2). There are two exceptions to this observation: the protein expressed by the *Abcb5* gene, and the phospholipid transporter protein, ABCB4. These two proteins had >51% and >73% sequence conservation with Pgp respectively in both humans and mice.

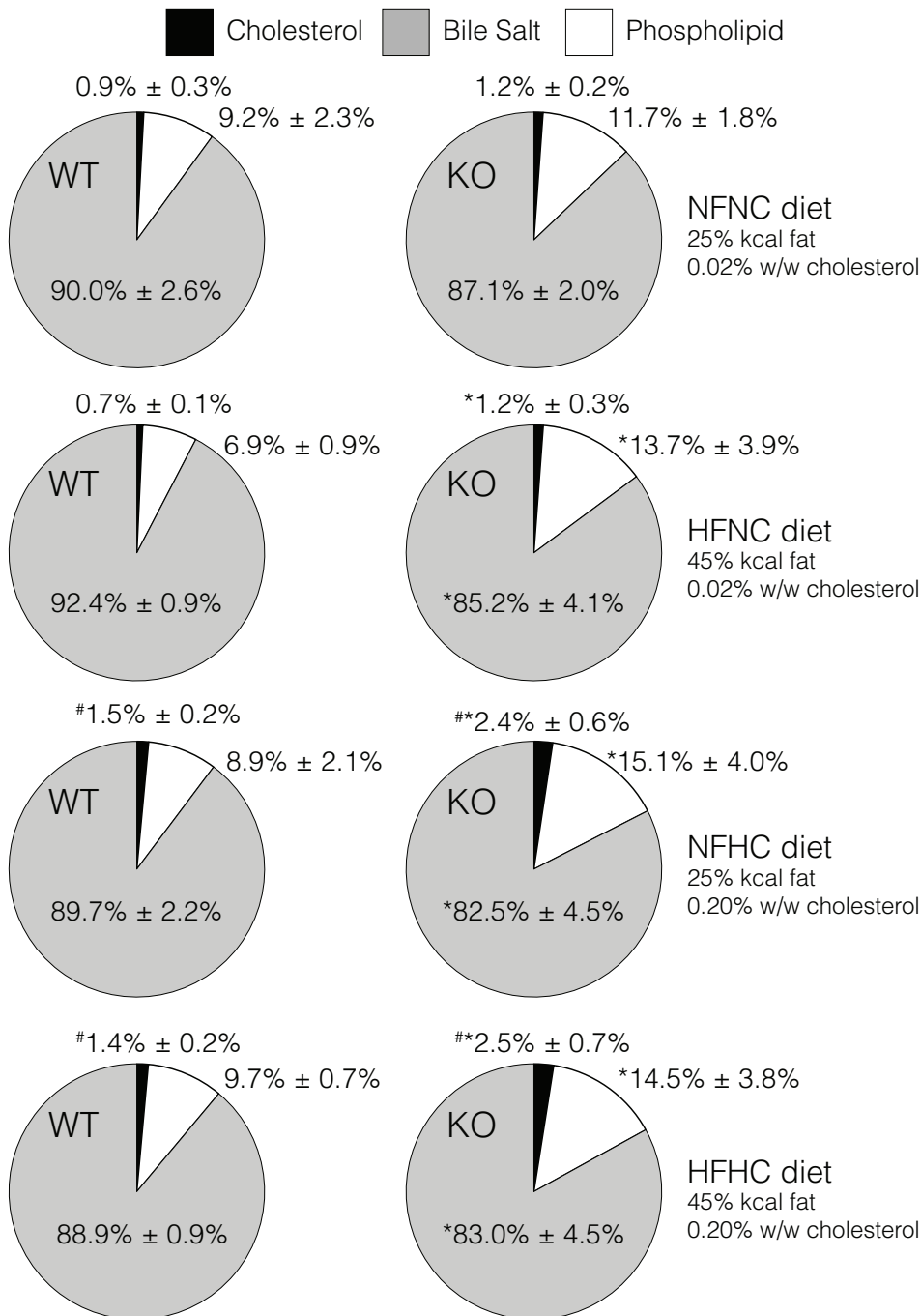


Figure 5-1: Effects of *Abcb1a/1b* deletion and diet on the molar composition of bile constituents.

The mean molar percentage of cholesterol, phospholipid, and bile salts in gallbladder bile is shown \pm SD for each of the four diets tested. NFNC: 25%kcal fat and 0.02% (w/w) cholesterol. HFNC: 45%kcal fat and 0.02% (w/w) cholesterol. NFHC: 25%kcal fat and 0.20% (w/w) cholesterol. HFHC: 45%kcal fat and 0.20% (w/w) cholesterol. * $p < 0.05$ vs. WT on the same diet by two-way ANOVA with Tukey *post-hoc* tests; # $p < 0.05$ vs. NFNC by two-way ANOVA with Tukey *post hoc* tests; n=5 for all groups except KO-HFNC where n=4.

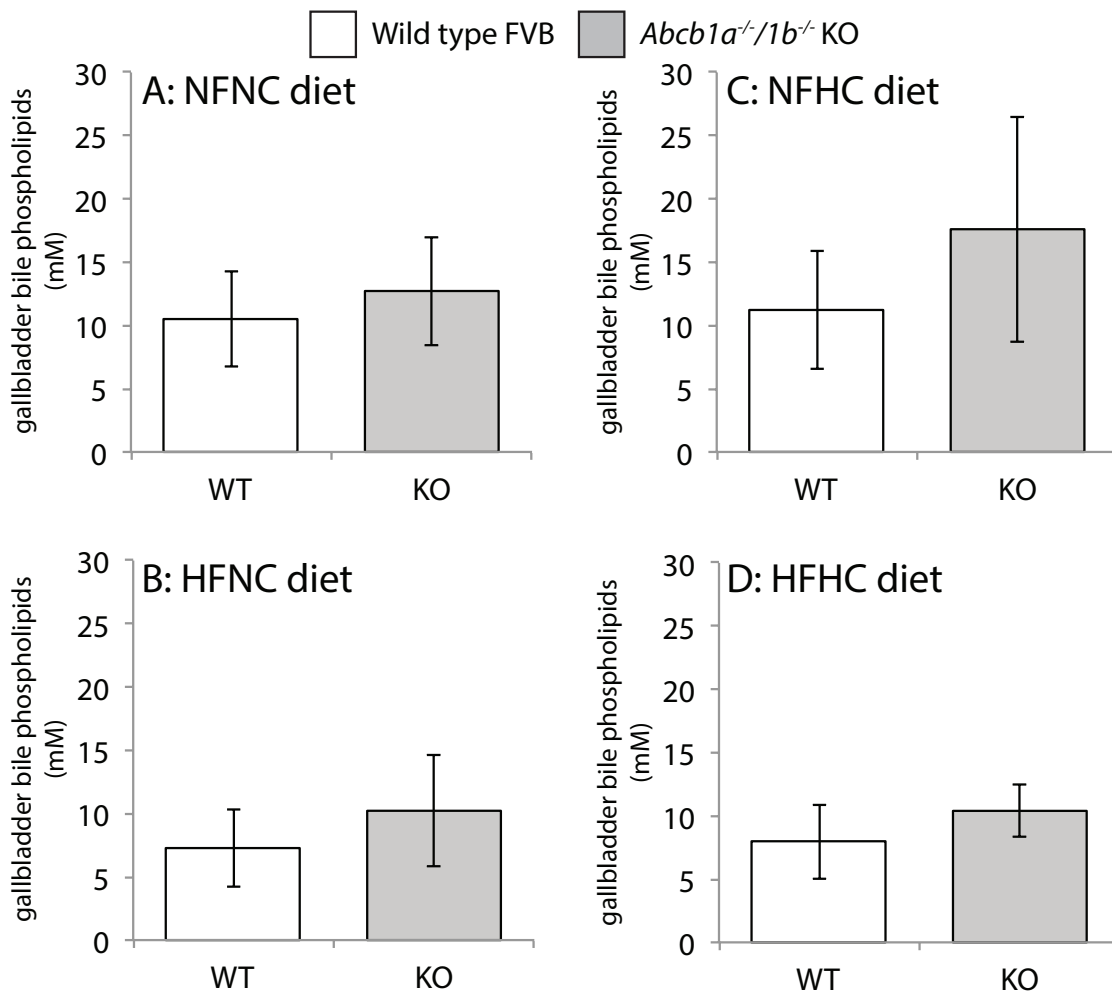


Figure 5-2: Effect of *Abcb1a/1b* deletion on gallbladder bile phospholipid content. The phospholipid content of gallbladder bile is shown after ligation of the common bile duct for 60min. **(A)** NFNC diet, 25%kcal fat and 0.02% (w/w) cholesterol; **(B)** HFNC diet, 45%kcal fat and 0.02% (w/w) cholesterol; **(C)** NFHC diet, 25%kcal fat and 0.20% (w/w) cholesterol; **(D)** HFHC diet, 45%kcal fat and 0.20% (w/w) cholesterol. Mean values are shown \pm SD. There were no statistically significant differences between FVB wild type (WT) and *Abcb1a*^{-/-}/*1b*^{-/-} (KO) mice in any dietary group by unpaired t-test; n=6-9.

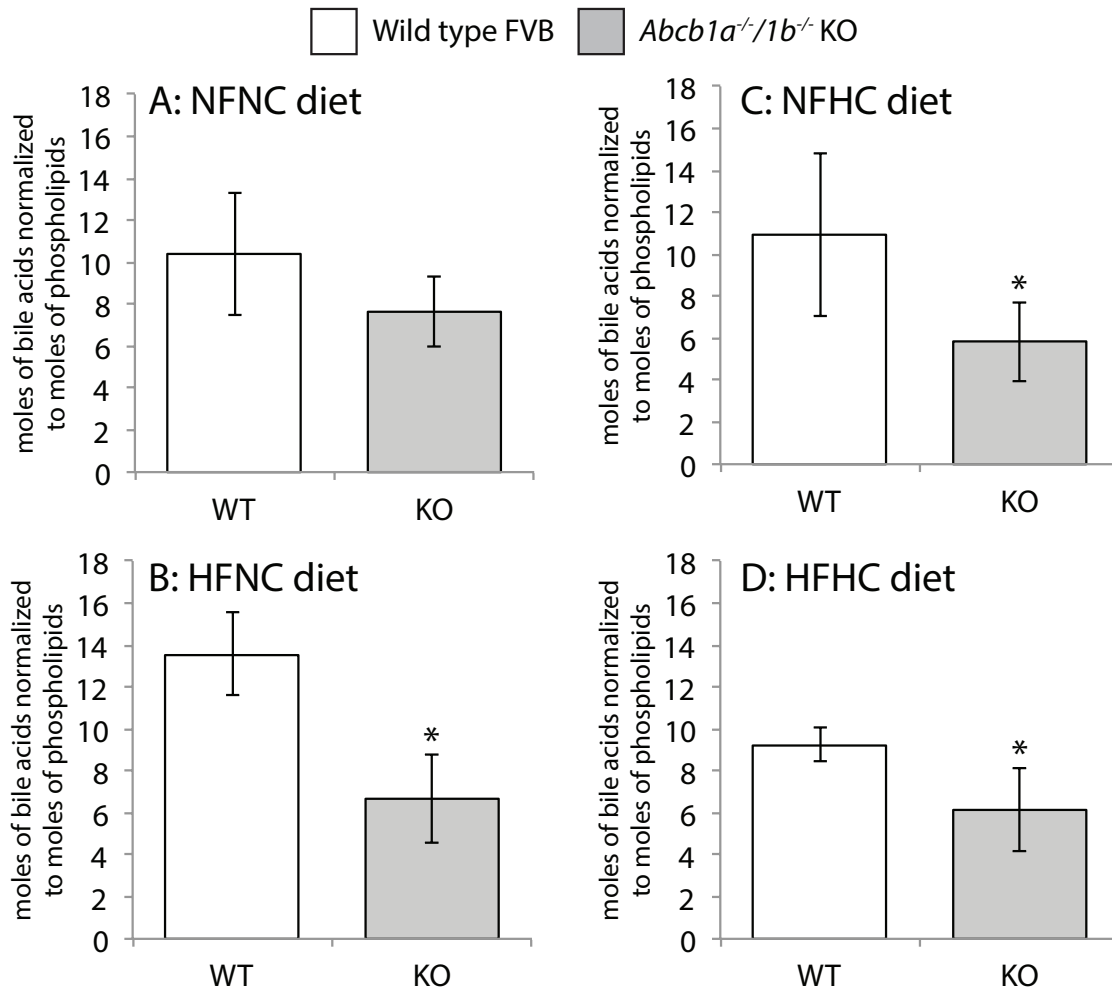


Figure 5-3: Effect of *Abcb1a/1b* deletion on bile acid efflux to the gallbladder. The molar ratio of bile acids to phospholipids was calculated for each mouse for which there was a complete data set. The mean ratio of the moles of bile acid acids to moles of phospholipid are shown \pm SD for wild type FVB mice (WT: hollow bars) and *Abcb1a^{-/-}/1b^{-/-}* knockout mice (KO: grey bars); **(A)** NFNC diet, 25%kcal fat and 0.02% (w/w) cholesterol; **(B)** HFNC diet, 45%kcal fat and 0.02% (w/w) cholesterol; **(C)** NFHC diet, 25%kcal fat and 0.20% (w/w) cholesterol; **(D)** HFHC diet, 45%kcal fat and 0.20% (w/w) cholesterol. * $p < 0.05$ vs. wild type by two-tailed unpaired t-test; $n=5$, except for HFNC knockout mice where $n=4$.

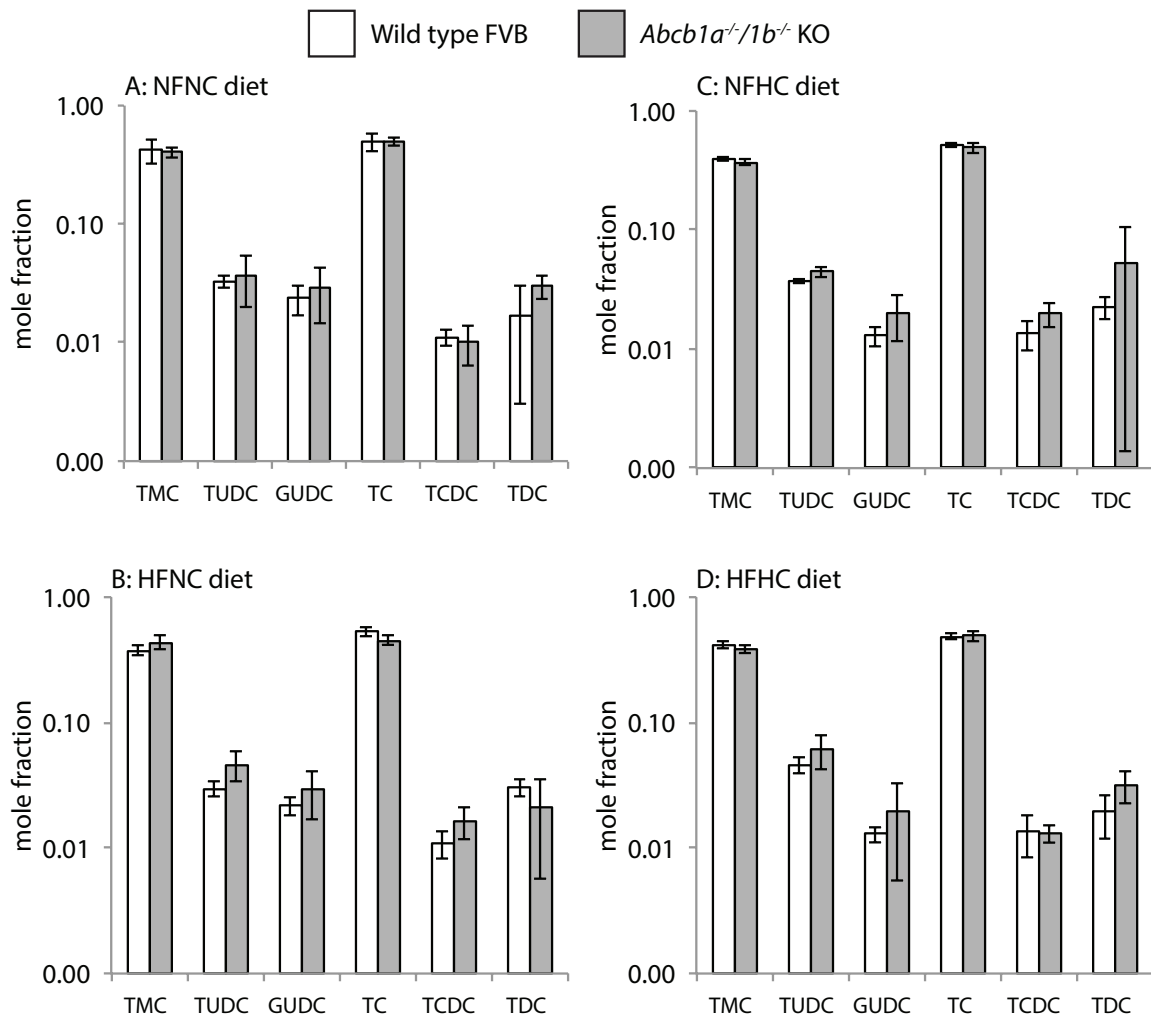


Figure 5-4: Effects of *Abcb1a/1b* deletion on the molar composition of the bile acid pool.

Individual bile acid species in the gallbladder were quantified by HPLC and the mean mole fractions of the individual bile acid species are shown on a log scale \pm SD for Wild Type FVB mice (hollow bars) and P-glycoprotein knockout mice (*Abcb1a*^{-/-}/*1b*^{-/-}; grey bars); n=5, except for HFNC knockout mice where n=4. TMC: Tauromuricholic acid, TUDC: Tauroursodeoxycholic acid, GUDC: Glycoursodeoxycholic acid, TC: Taurocholic acid, TCDC: Taurochenodeoxycholic acid, TDC: taurodeoxycholic acid. **(A)** NFNC diet, 25%kcal fat and 0.02% (w/w) cholesterol; **(B)** HFNC diet, 45%kcal fat and 0.02% (w/w) cholesterol; **(C)** NFHC diet, 25%kcal fat and 0.20% (w/w) cholesterol; **(D)** HFHC diet, 45%kcal fat and 0.20% (w/w) cholesterol.

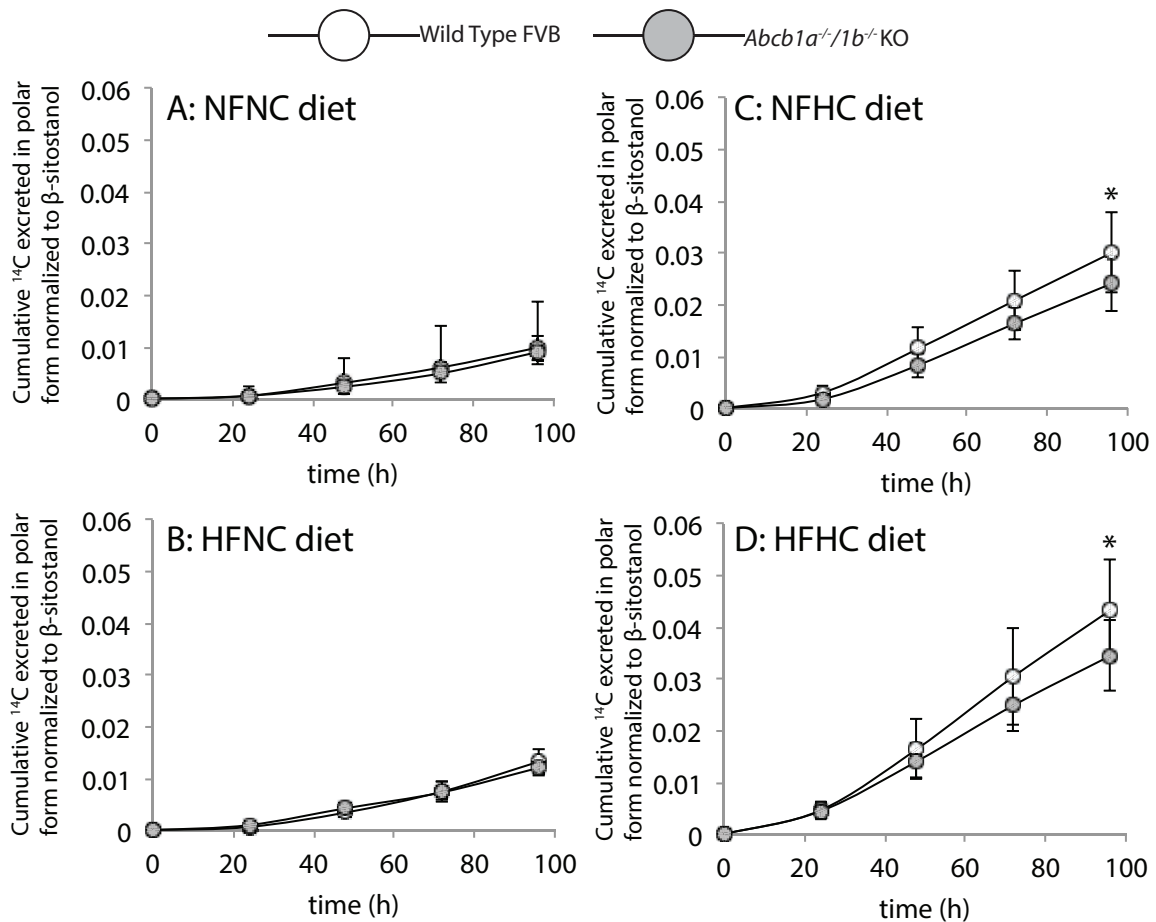


Figure 5-5: Cumulative fecal excretion of polar ^{14}C derived from $[^{14}\text{C}]$ -cholesterol. After administration of ^{14}C -cholesterol, a fraction of the dose becomes incorporated into a polar, "saponifiable" molecule. The fecal extract is separated into polar and hydrophobic fractions through a 60min saponification reaction. After removing the neutral sterols, the ^{14}C carried in polar molecules was quantified by scintillation counting and expressed as the cumulative excretion normalized to the dosing control (β -sitostanol). The data set collected at each time point was analyzed by two-way ANOVA (Diet and Genotype as the two factors) with Tukey post-hoc testing; Diet was a significant factor at all time points ($p < 0.001$). * $p < 0.005$ WT vs. KO at the indicated time point; $n = 8-10$.

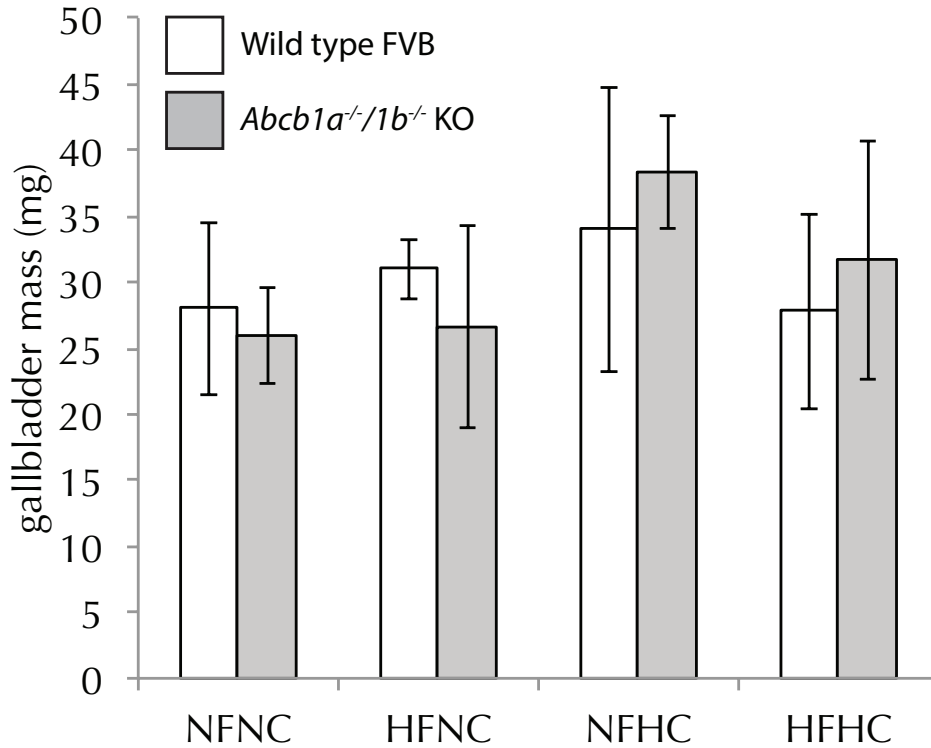


Figure 5-6: Mass of gallbladders after a 60min ligation of the common bile duct. The mass of the gallbladders was determined prior to freezing in liquid nitrogen. There were no differences between wild type (hollow bars) and *Abcb1a*^{-/-}/*1b*^{-/-} knockout mice (shaded bars) by two-way ANOVA. Mean values \pm SD; n=6-9.

Table 5-1: Assessment of global homology between the amino acid sequence of murine P-glycoprotein (ABCB1A: *Mus musculus*) and members of the ABC transporter superfamily associated with drug resistance.

All comparisons were conducted using a Needleman-Wunch algorithm for global pairwise sequence alignment (European Bioinformatics Institute: <http://www.ebi.ac.uk/>)

Gene Symbol	Gene ID	NCBI Accession	Common Name	Chromosome(18)	Amino Acids	Identity	Similar	Gaps
Abcb1a	18671	NP_035206.2		Chr 5 3.43cM	1276			
Abcb1b	18669	NP_035205.1		Chr 5 3.43cM	1276	83.9%	92.1%	0.5%
<i>Tap1</i>	21354	NP_038711.2	ABCB2	Chr 17 17.98cM	724	14.5%	23.0%	58.0%
<i>Tap2</i>	21355	NP_035660.3	ABCB3	Chr 17 17.98cM	702	13.1%	22.1%	61.0%
Abcb4	18670	NP_032856.2	MDR3	Chr 5 3.43cM	1276	73.2%	84.7%	2.8%
Abcb5	77706	NP_084237.1		Chr 12 63.48cM	1255	51.6%	71.3%	3.5%
<i>Abcb6</i>	74104	NP_076221.1		Chr 1 38.62cM	842	13.4%	20.3%	62.7%
<i>Abcb7</i>	11306	NP_033722.1		Chr X 46.58 cM	752	13.8%	22.0%	58.0%
<i>Abcb8</i>	74610	NP_083296.2		Chr 5 11.57cM	717	15.9%	24.8%	58.1%
<i>Abcb9</i>	56325	NP_063928.2		Chr 5 63.36cM	762	14.6%	23.6%	57.7%
<i>Abcb10</i>	56199	NP_062425.1		Chr 8 72.31cM	715	17.1%	25.9%	57.7%
Abcb11	27413	NP_066302.2	BSEP	Chr 2 39.69cM	1321	48.0%	66.3%	5.3%
<i>Abcc1</i>	17250	NP_032602.1	MRP1	Chr 16 9.75cM	1528	18.9%	33.6%	34.2%
<i>Abcc2</i>	12780	NP_038834.2	MRP2	Chr 19 36.57cM	1543	18.6%	34.7%	33.6%
<i>Abcc3</i>	76408	NP_083876.3	MRP3	Chr 11 58.9cM	1522	17.4%	34.9%	29.4%
<i>Abcc4</i>	239273	NP_001028508.2	MRP4	Chr 14 62.24cM	1325	21.7%	40.8%	22.9%
<i>Abcc5</i>	27416	NP_038818.2	MRP5	Chr 16 12.41cM	1436	21.0%	37.6%	27.3%
<i>Abcc6</i>	27421	NP_061265.2	MRP6	Chr 7 29.64cM	1498	19.2%	34.3%	35.2%
<i>Abcc10</i>	224814	NP_660122.1	MRP7	Chr 17 22.9cM	1460	19.9%	34.8%	32.4%
<i>Abcg2</i>	26357	NP_036050.1	BCRP	Chr 6 27.82cM	657	11.2%	18.3%	62.9%

Table 5-2: Assessment of global homology between the amino acid sequence of human P-glycoprotein (ABCB1: *Homo sapiens*) and members of the ABC transporter superfamily associated with drug resistance.

All comparisons were conducted using a Needleman-Wunch algorithm for global pairwise sequence alignment (European Bioinformatics Institute: <http://www.ebi.ac.uk/>)

Gene Symbol	Gene ID	Accession	Common Name	Location	Amino Acids	Identity	Similar	Gaps
<i>ABCB1</i>	5243	NP_000918.2	MDR1	7q21.12	1280	n/a	n/a	n/a
<i>TAP1</i>	6890	NP_038711.2	ABCB2	6p21.3	724	13.4%	21.1%	61.2%
<i>TAP2</i>	6891	NP_000535.3	ABCB3	6p21.3	703	13.6%	23.1%	60.2%
<i>ABCB4</i>	5244	NP_000434.1	MDR2	7q21.1	1279	75.7%	86.4%	1.8%
<i>ABCB5</i>	340273	NP_001157413.1		7p21.1	1257	54.6%	74.5%	2.4%
<i>ABCB6</i>	10058	NP_005680.1	MTABC3	2q36	842	13.8%	21.0%	61.5%
<i>ABCB7</i>	22	NP_004290.2	ABC7	Xq13.3	753	13.6%	22.7%	57.7%
<i>ABCB8</i>	11194	NP_009119.2	MABC1	7q36	718	18.0%	26.0%	55.8%
<i>ABCB9</i>	23457	NP_062571.1		12q24	766	13.7%	24.0%	58.5%
<i>ABCB10</i>	23456	NP_036221.2	MTABC2	1q42.13	738	16.0%	24.0%	59.5%
<i>ABCB11</i>	8647	NP_003733.2	BSEP	2q24	1321	50.0%	68.6%	4.1%
<i>ABCC1</i>	4363	NP_004987.2	MRP1	16p13.1	1531	19.3%	34.8%	31.2%
<i>ABCC2</i>	1244	NP_000383.1	MRP2	10q24	1545	20.4%	35.3%	32.5%
<i>ABCC3</i>	8714	NP_003777.2	MRP3	17q22	1527	18.2%	34.0%	32.7%
<i>ABCC4</i>	10257	NP_005836.2	MRP4	13q32	1325	22.2%	40.1%	24.2%
<i>ABCC5</i>	10057	NP_005679.2	MRP5	3q27	1437	21.5%	36.9%	27.3%
<i>ABCC6</i>	368	NP_001162.4	MRP6	16p13.1	1505	19.7%	34.5%	33.6%
<i>ABCC10</i>	89845	NP_001185863.1	MRP7	6p21.1	1492	19.4%	34.1%	36.4%
<i>ABCG2</i>	9429	NP_004818.2	BCRP	4q22	655	13.6%	23.2%	57.1%

5.2 Discussion

Studies published by Victor Ling's group showed that Pgp might support BSEP in murine bile acid efflux(11, 12, 207). Conservation of amino acid sequence is linked with common ancestry of proteins and is often associated with conserved function. We used global pairwise sequence homology assessments to test whether there is substantial homology between two proteins by comparing the two sequences over the entire protein. As shown in Table 5-1 and Table 5-2, the amino acid sequence of Pgp in humans and mice is most conserved with three other transporters, the bile salt export pump (encoded by *ABCB11*), the phospholipid efflux protein (encoded by *ABCB4*) and the protein encoded by *ABCB5*. Human *ABCB5* has no known physiological function and is being studied for chemoresistance in several malignancies(351-353). A recent phylogeny analysis of the ATP binding region revealed that these four transporters are closely related to one another, suggesting a common ancestor(354). It is interesting to note that mouse studies have demonstrated that both BSEP(10) and *ABCB4*(197) are key physiologic regulators of bile formation. The data presented in this chapter suggest that Pgp may also contribute to bile homeostasis.

Although the *in silico* data presented in Table 5-1 and Table 5-2 are suggestive, *in vivo* studies are required to test whether function is conserved. Our experimental model involved ligation of the common bile duct for 60min after several groups demonstrated that deletion of Pgp does not affect the rate of bile flow(12, 184, 355). The data in Figure 5-1 show differences in the bile composition of Pgp knockout mice

relative to diet-matched wild type mice when they were fed diets containing high levels of fat and/or cholesterol. The mole fraction of bile acids was decreased with subsequent gains in the mole percentage of phospholipid and cholesterol. These data may explain the increased fecal cholesterol (mole fraction) in Pgp knockout mice in a previous study(230). Subsequent analysis of the bile revealed that the phospholipid efflux was unaffected by Pgp deletion (Figure 5-2) despite clear evidence that purified Pgp acts as a phospholipid flippase *in vitro*(356). Consequently, the efflux of bile acids was normalized to the phospholipid efflux for each mouse to account for any inter-individual variability in flow rate(355). This clearly demonstrated the reduced capacity of Pgp knockout mice to efflux bile acids when challenged with physiologically relevant levels of dietary fat, cholesterol or both (Figure 5-3).

Victor Ling's group have clearly shown that Pgp is required to maintain bile acid flow in the absence of BSEP(12). Our data build on the findings of Ling *et al.* to demonstrate a role for Pgp in bile acid removal in the presence of BSEP. Additionally, these data demonstrated the contribution of Pgp to bile acid flux without the cholestatic stress of high levels of cholic acid added to the diet(12). Prior studies established that BSEP preferentially effluxes hydrophobic bile acids. To determine if Pgp has a similar preference for a class of bile acids, the analysis of the gallbladder bile included quantification of six common murine bile acids, comprising a range of hydrophilic and hydrophobic types. Although Pgp knockout mice had reduced total moles of bile acids in the gallbladder, the molar composition of specific bile acids was not significantly different from wild type mice (Figure 5-4). These data suggest that Pgp, unlike BSEP, effluxed the six bile salts in a non-specific manner. The lack of

specificity demonstrated by Pgp is desirable for a low-affinity secondary efflux mechanism that supports BSEP. Based on this finding we postulate that murine bile acid homeostasis is regulated through a dual-transporter system comprised of Pgp and BSEP.

Based on human inherited diseases and mouse knockout studies, we know that BSEP is the primary bile salt efflux mechanism. We propose that BSEP is supported by Pgp when the system is stressed. The dual transporter bile acid efflux system is likely regulated transcriptionally: the expression of both *Abcb11* and *Abcb1a* is regulated by nuclear receptors that respond differently to bile acids. An accumulation of bile acids activates FXR (300, 301), which acts by positive regulation of genes involved in bile acid removal (including *Abcb11*) and by inducing the expression of *NR0B2* (the gene encoding SHP). SHP represses the transcription of several factors required for *Cyp7a1* expression, thereby reducing synthesis of more bile acids (See Figure 1-8) (302, 303). Due to the substrate specificity of BSEP, hydrophobic bile acids such as chenodeoxycholic acid (CDC) will only accumulate in the liver when the activity of BSEP is unable to maintain homeostasis. A toxic metabolite of CDC called lithocholic acid is a ligand for the Steroid X Receptor (SXR) and its murine ortholog, PXR; these nuclear receptors activate a detoxification response(341, 342), including the induction of *Abcb1a/1b* expression. The PXR gene (*Nr1i2*) itself is up-regulated by FXR(357), suggesting that PXR levels are increased prior to the accumulation of toxic secondary bile acids such as lithocholic acid.

Although the data presented in this chapter support the hypothesis that bile acids are a class of endogenous substrates for P-glycoprotein, there are some

limitations to the work. The experimental model used was ligation of the common bile duct followed by quantitative analysis of the bile. The validity of this technique is predicated by the unchanged bile flow rates demonstrated by other groups(12, 184, 355). The flow rates reported in the literature were determined in mice administered normal chow diets, and the authors did not note alterations to bile acid efflux. Similarly in our data, changes in bile composition between wild type and knockout mice were only seen after consumption of high fat or high cholesterol diets. While we have not directly measured the flow rates between wild type and knockout mice, we did not see any differences in gallbladder mass between the two genotypes after the 60min ligation (Figure 5-6).

An additional limitation to the model is the inherent differences between murine and human bile physiology. One of the primary differences between humans and mice is the nature of bile flow. Bile components are derived from two bile flows, termed bile acid-dependent and bile acid-independent. Bile flow in humans (and dogs) is driven by bile acid dependent flow, whereas the bile flow in rodents is predominantly bile acid-independent(329). This observation may provide an alternate hypothesis to the dual-transporter model to explain why mutations in *ABCB11* cause type II progressive familial intrahepatic cholestasis(204), lethal in humans(329), and yet *Abcb11*^{-/-} mice do not display any obvious pathologies(10). In addition to bile flow differences, mice have a more hydrophilic bile acid composition than humans, owing to the preferential conjugation with taurine instead of glycine and the prevalence of muricholic acid. The limitations discussed must be considered when determining what conclusions are appropriately drawn from these data. Although the data

presented in this chapter support the hypothesis that Pgp functions as a bile acid transporter *in vivo* we must exercise caution before extrapolating this finding to human physiology.

Our findings identified an endogenous role for P-glycoprotein in the efflux of bile acids in mice. We postulate that this finding may have relevance to studying both cholestatic liver disease and reverse cholesterol transport. Figure 5-5 includes some very preliminary data showing that the Pgp knockout mice had a reduction in the removal of polar forms of orally administered ¹⁴C-labeled cholesterol. Unfortunately, we could not determine the molecular identity of the molecule being excreted but these data support further studies examining the flux of cholesterol from the body in Pgp knockout mice. There are very few studies published to date examining the impact of canalicular bile transporters on the reverse cholesterol transport pathway, despite a great deal of research on the early stages of the pathway. Our data provide initial evidence that Pgp functions as a bile acid efflux mechanism in mice; however, as murine bile acid physiology differs from human, further studies are required to determine whether the dual transporter system of BSEP and P-glycoprotein has relevance in human bile acid homeostasis.

Chapter 6: Transient knockdown of *ABCB1* in Caco-2 cells

The rationale for investigating the *in vivo* role of Pgp in cholesterol homeostasis is based on the *in vitro* observations that non-specific Pgp inhibitors inhibit cholesterol trafficking. Although the role of Pgp in cholesterol trafficking *in vitro* has been reported by five groups using eight different cell lines(221-227, 358), the majority of these studies have relied on chemical inhibitors as part of their experimental design. Unfortunately, most of the small molecule inhibitors of Pgp are non-specific (refer to section 1.5.1 page 41) making it challenging to unequivocally characterize the role of Pgp. Consequently, targeting the expression of *ABCB1* may provide a more specific experimental system. In this chapter we present a model for transient down-regulation of *ABCB1* in Caco-2 cells and use this model to determine whether there is an association between Pgp levels and cholesterol trafficking in a cell culture model of enterocytes.

6.1 Results

After a series of experiments determining the optimal conditions to transfect the Caco-2 cells, we were able to conduct siRNA dosage experiments, using three different *ABCB1*-targetting siRNA constructs summarized in Figure 6-1, Figure 6-2, and Figure 6-3. The dose response experiments revealed that a single dose of 100nM HSS182278 or 200nM HSS107919 reduced *ABCB1* mRNA by >70% relative to untreated cells at five days post-transfection. The silencing was inconsistent when HSS107918 is used. In order for the experimental model to be valid, the transfected Caco-2 cells must form confluent monolayers and differentiate into enterocyte-like cells while

ABCB1 remains silenced. The cells formed tight junctions within 4 days of seeding the transfectants on semi-permeable polycarbonate membranes, determined both by TEER values $>250\Omega\cdot\text{cm}^2$ (359) and by immunofluorescence microscopy for ZO-1 cellular localization as shown in Figure 6-4. Differentiation of Caco-2 cells was demonstrated by the presence of sucrase-isomaltase protein detected by Western blot within five days of plating the transfectants (Figure 6-7 and Figure 6-8). Both HSS182278 and HSS107919 siRNA constructs suppressed Pgp protein levels up to six days post-transfection, as shown in Figure 6-5 and Figure 6-6.

Preliminary cholesterol uptake and trafficking data are presented in Figure 6-9. There were no statistically significant differences between silenced Caco-2 cells, untreated Caco-2 cells or cells treated with the third generation Pgp inhibitor, LY335979. In contrast, silencing *ABCB1* appeared to increase cholesterol synthesis relative to negative control siRNA transfectants ($p < 0.05$ by unpaired t-test). This finding was not consistent with cells treated with LY335979 (Figure 6-10).

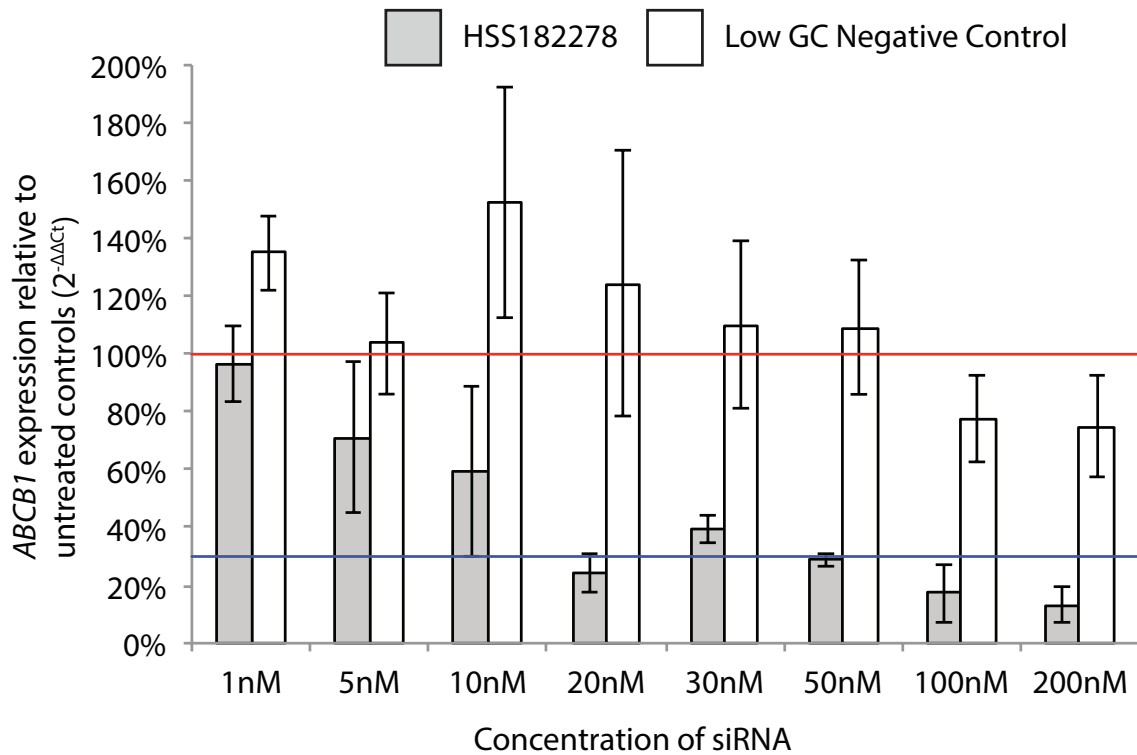


Figure 6-1: Dose response of the *ABCB1*-targeting siRNA construct HSS182278. The expression of *ABCB1* was determined by RT-qPCR for cells treated with HSS182278, a GC-matched negative control, and an untreated control. The mean expression ($\Delta\Delta C_t$ versus the untreated control cells) at day 5 post-transfection is shown \pm SD for 2-3 independent experiments.

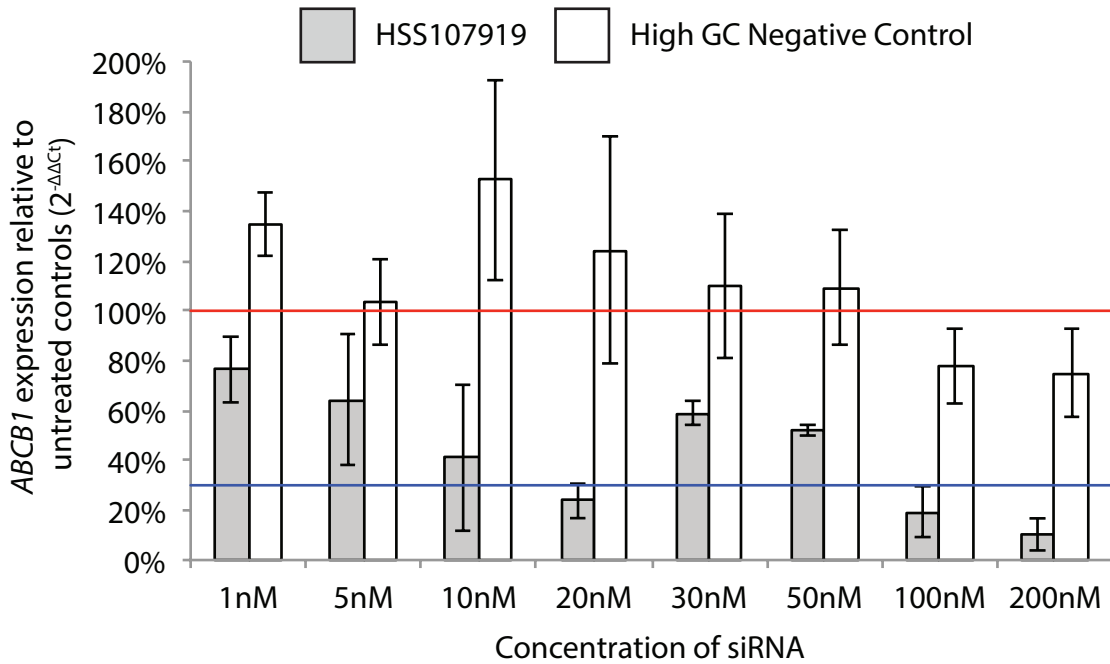


Figure 6-2: Dose response of the *ABCB1*-targetting siRNA construct HSS107919. The expression of *ABCB1* was determined by RT-qPCR for cells treated with HSS107919, a GC-matched negative control, and an untreated control. The mean expression ($\Delta\Delta C_t$ versus the untreated control cells) at day 5 post-transfection is shown \pm SD for 2-3 independent experiments.

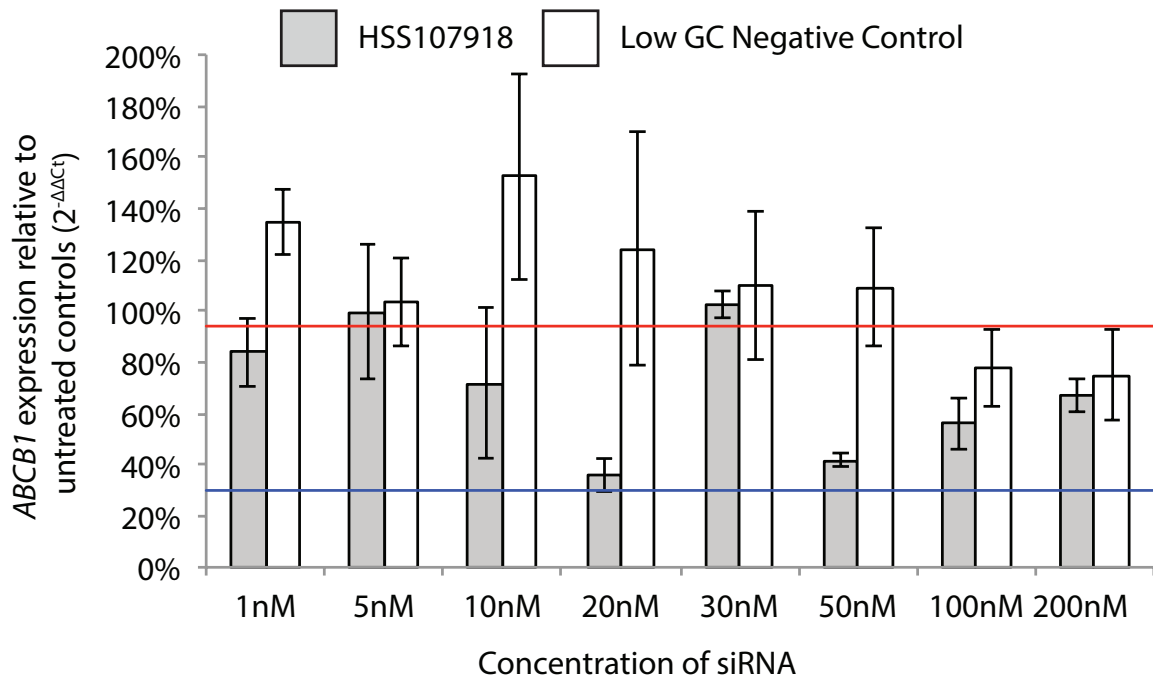


Figure 6-3: Dose response of the *ABCB1*-targeting siRNA construct HSS107918. The expression of *ABCB1* was determined by RT-qPCR for cells treated with HSS107918, a GC-matched negative control, and an untreated control. The mean expression ($\Delta\Delta C_t$ versus the untreated control cells) at day 5 post-transfection is shown \pm SD for 2-3 independent experiments.

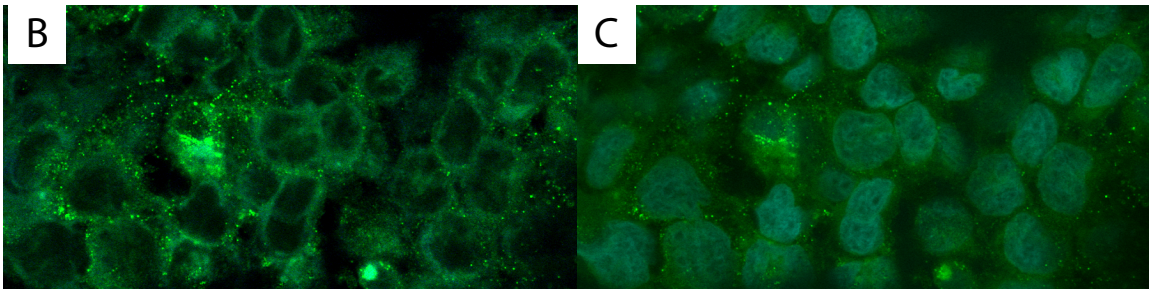
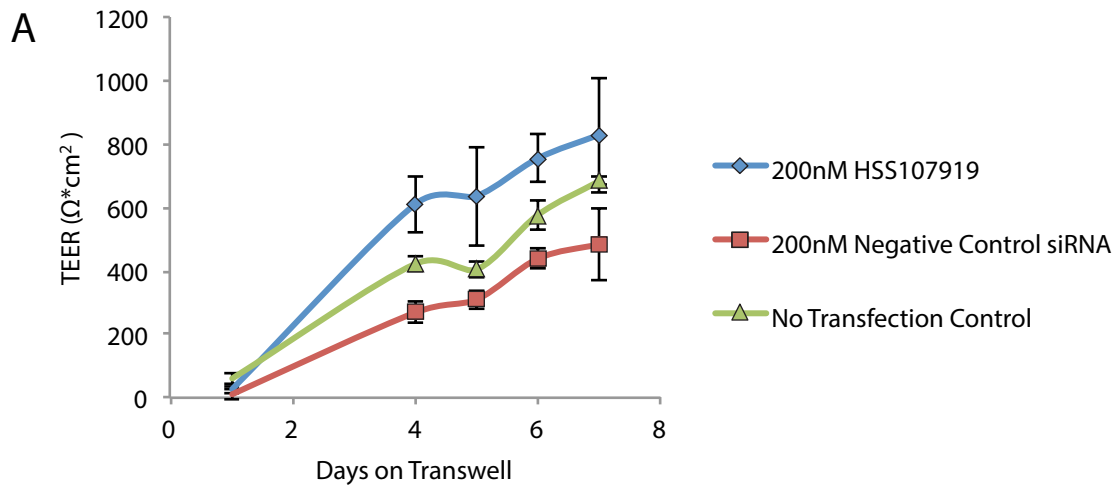


Figure 6-4: Representative figure showing formation of a confluent Caco-2 monolayer with tight junctions within 4 days growth on a polycarbonate membrane. (A) Transepithelial Electrical Resistance values ($\Omega \cdot \text{cm}^2$) as a measure for the formation of tight junctions. (B) Immunofluorescence staining of Tight Junction Protein-1 (ZO-1, in green) of a Caco-2 monolayer treated with the negative control siRNA for 4 hours followed by 92h in normal cell culture media at 60x magnification showing the proper formation of tight junctions around each cell and (C) 60x magnification of the same strip showing the DAPI-stained (blue) nuclei and ZO-1 in green showing the location of the tight junctions around each columnar cell.

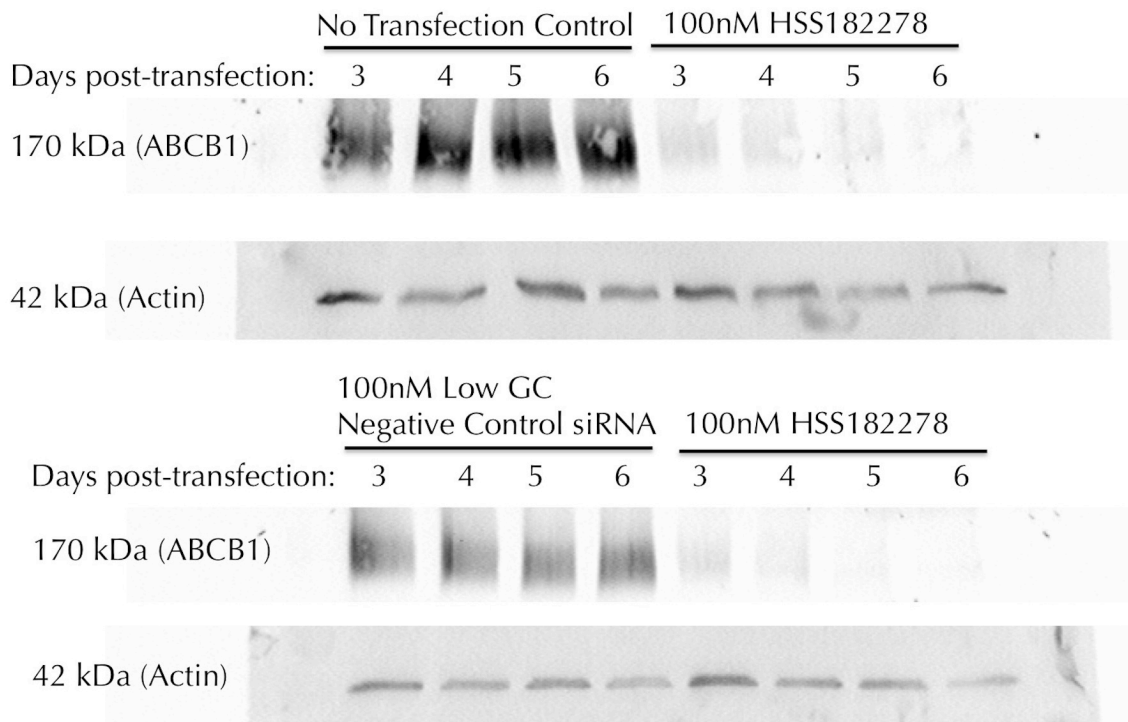


Figure 6-5: Time dependent silencing of Pgp using the HSS182278 siRNA construct. The Pgp level in Caco-2 cells treated with HSS182278, a GC-matched control siRNA, or media alone was determined using Western blot at day 3, 4, 5, and 6 post-transfection. The loading consistency was determined by measuring β -actin.

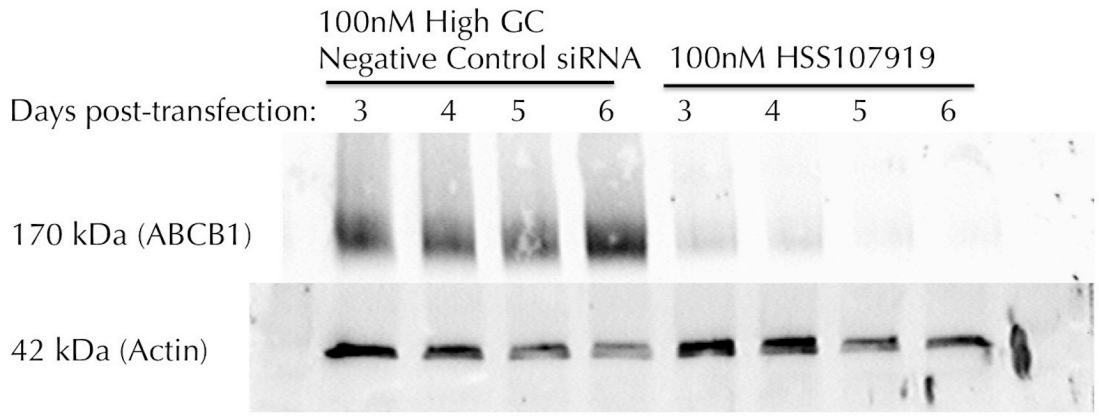
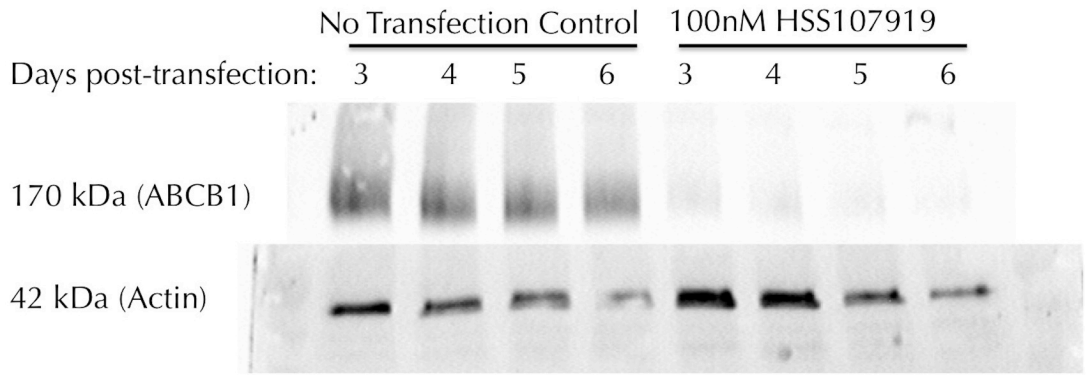


Figure 6-6: Time dependent silencing of Pgp using the HSS107919 siRNA construct. The Pgp level in Caco-2 cells treated with HSS107919, a GC-matched control siRNA, or media alone was determined using Western blot at day 3, 4, 5, and 6 post-transfection. The loading consistency was determined by measuring β -actin.

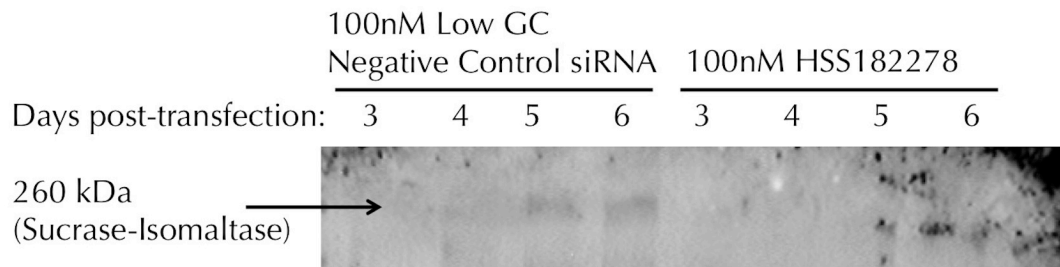
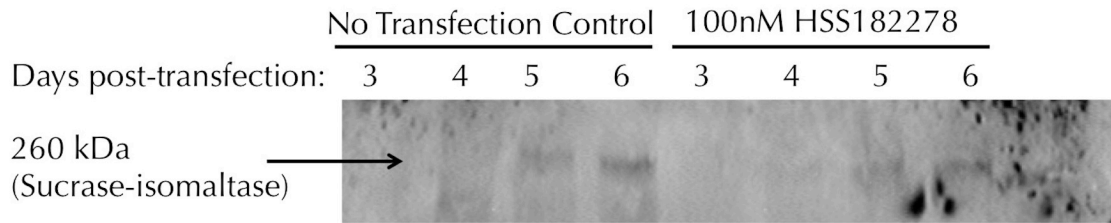


Figure 6-7: Detection of sucrase-isomaltase in Caco-2 cells treated with the HSS182278 siRNA construct.

Sucrase-Isomaltase, a marker for brush border formation, in Caco-2 cells treated with HSS182278, GC-matched control siRNA, or media alone was determined using Western blot at day 3, 4, 5, and 6 post-transfection. The membranes used in Figure 6-5 were stripped and re-probed for sucrase-isomaltase.

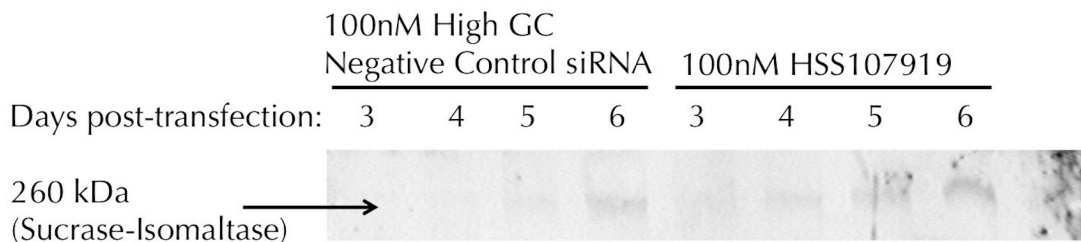
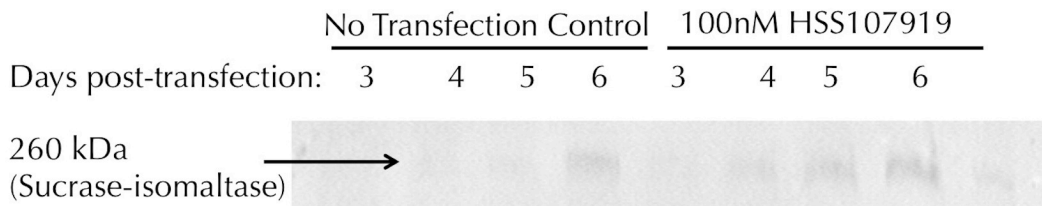


Figure 6-8: Detection of sucrase-isomaltase in Caco-2 cells treated with the HSS107919 siRNA construct.

Sucrase-Isomaltase, a marker for brush border formation, in Caco-2 cells treated with HSS182278, GC-matched control siRNA, or media alone was determined using Western blot at day 3, 4, 5, and 6 post-transfection. The membranes used in Figure 6-6 were stripped and re-probed for sucrase-isomaltase.

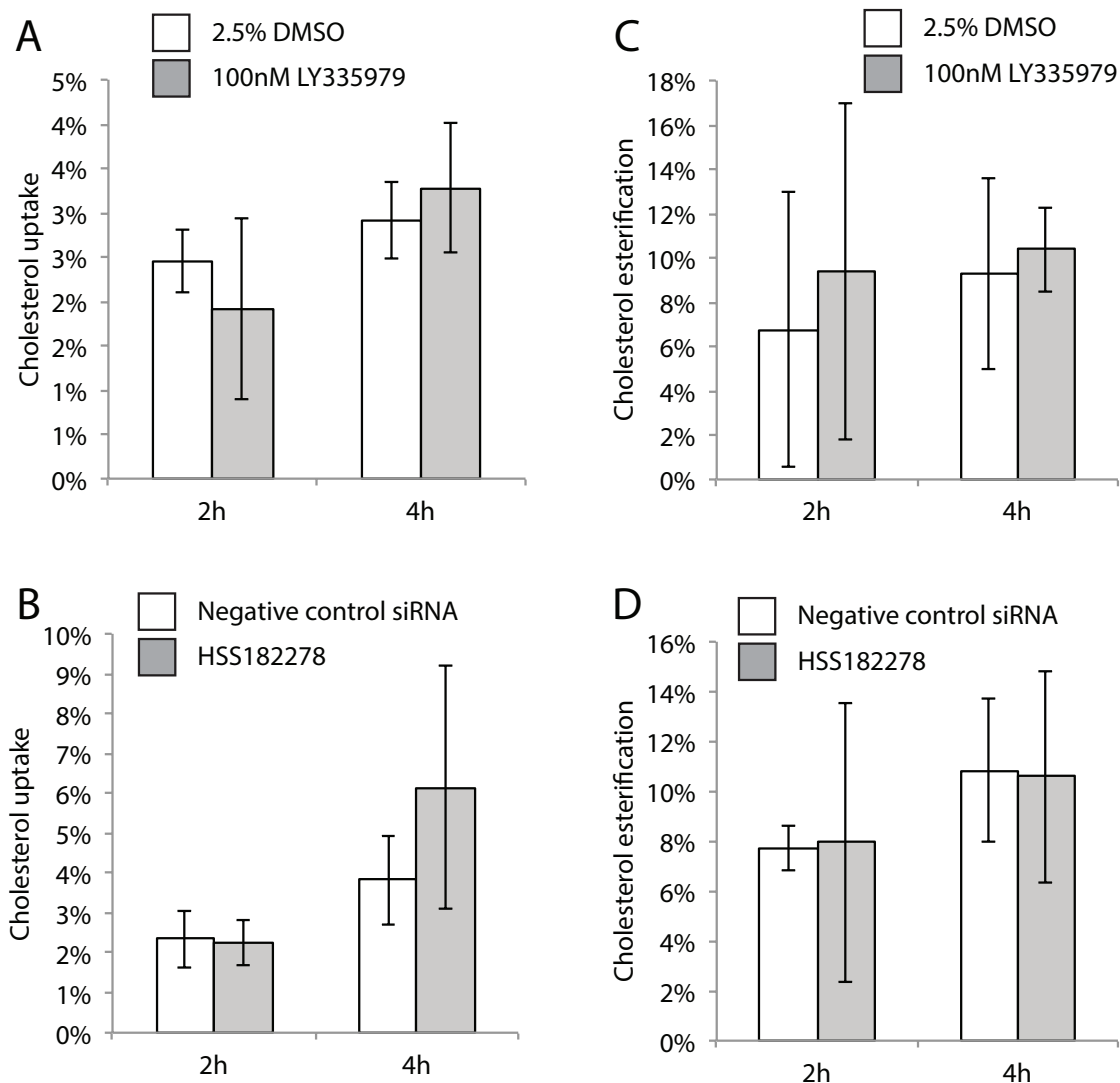


Figure 6-9: Cholesterol uptake and esterification in silenced Caco-2 cells. Caco-2 cells were either pre-treated with an *ABCB1* targeting siRNA construct (HSS182278), a GC-matched negative control, or media negative control. On day 4 post-transfection, the cells were treated with media (siRNA-treated cells), 2.5% DMSO, or 100nM LY335979 in DMSO. On day 5-post transfection, the cells were treated with radiolabeled cholesterol in bile acid micelles to determine the uptake (A and B) and esterification (C and D) of exogenous cholesterol after 2h or 4h incubation. The mean values \pm SD are shown; taken from n=3 independent experiments.

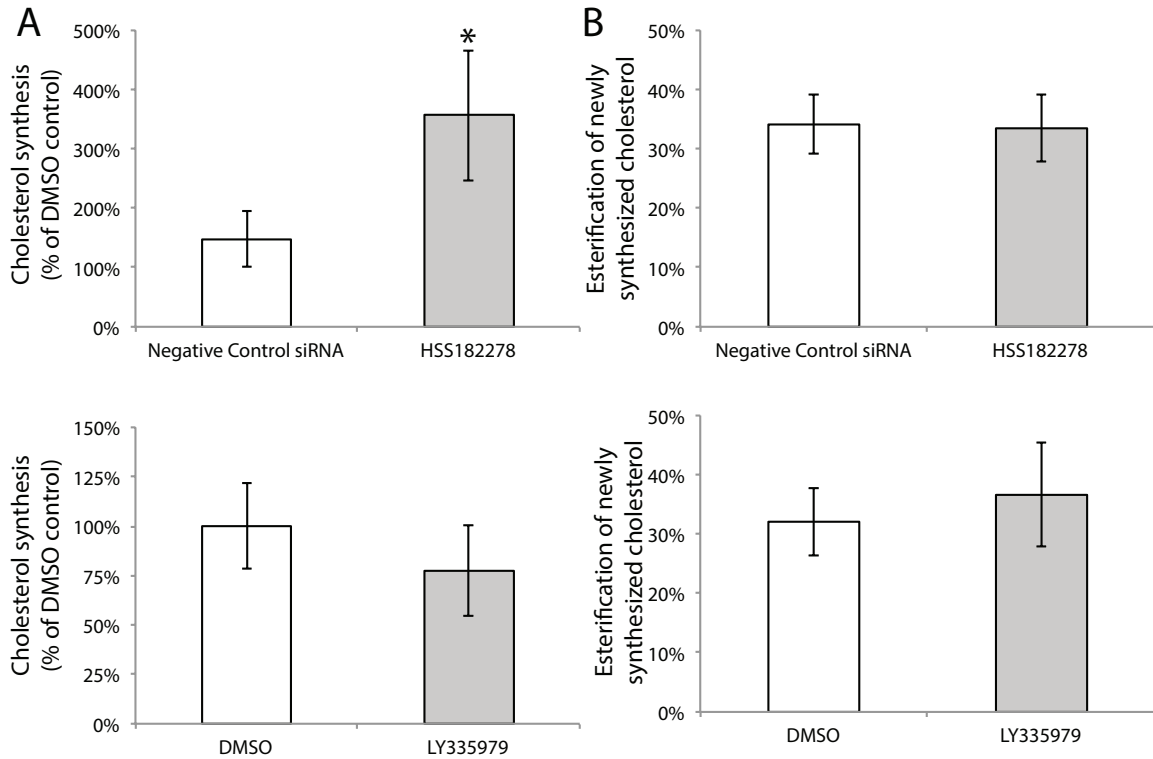


Figure 6-10: Cholesterol synthesis and esterification in silenced Caco-2 cells. Caco-2 cells were either pre-treated with an *ABCB1* targeting siRNA construct (HSS182278), a GC-matched negative control, or media negative control. On day 4 post-transfection, the cells were treated with media (siRNA-treated cells), 2.5% DMSO, or 100nM LY335979 in DMSO. On day 5-post transfection, the cells were administered ¹⁴C-acetate for 4h to determine the (A) synthesis and (B) esterification of endogenous cholesterol. The mean values \pm SD are shown; taken from n=3 independent experiments. *p<0.05 vs. Negative Control siRNA by two-tailed unpaired t-test.

6.2 Discussion

Investigations into the purported role of P-glycoprotein in cholesterol trafficking originate with cell culture studies(358), the results of which implicated Pgp in either in the uptake and internalization of cholesterol(223-226) or the efflux(227) and biosynthesis of cholesterol(221, 222). The literature surrounding Pgp and cholesterol is fraught with contradictions, as summarized in two recent papers(213,

214). Some of the confusion may stem from the differing experimental designs used to test the association between cholesterol and Pgp. While many of the investigators used non-specific chemical inhibitors in loss-of-function experiments(221-224, 358), some used Pgp overexpression in gain-of-function type experiments(225-227). Each method is subject to off-target effects. The small molecule inhibitors used are not specific to Pgp. The use of drug resistance as a selection method for Pgp overexpressing cell lines does not distinguish between cell lines that have multiple adaptive responses that confer the multidrug resistance phenotype. This leads to confounding factors when interpreting data(227, 360). In this chapter we presented the initial characterization of an *ABCB1*-specific siRNA-mediated knockdown of Caco-2 cells as a specific loss-of-function model for assessing Pgp function.

Caco-2 cells are a well-established model for the absorptive cells of the digestive tract, enterocytes, because of their ability to differentiate to a polarized monolayer with ordered microvilli and brush border enzymes on the apical face(361-364). Unfortunately, while these characteristics make the cells a good model of enterocytes, they make effective transfections challenging. Undifferentiated Caco-2 cells can be transfected but under normal culture conditions, the cells require 14-21 days for full differentiation(365), which exceeds the effective duration of silencing for siRNA in other cell lines with doubling times of 30h(366, 367), comparable to Caco-2(368, 369). In order to overcome these hurdles, we transfected the cells while in suspension, then seeded them at high density onto polycarbonate membranes to reduce the time needed for differentiation. This approach is based on a protocol by Clayburgh *et al.*(359, 370) As this protocol differs from the established method for

growing differentiated Caco-2 cells, the focus of this chapter on the characterization of the knockdown cells.

After extensive optimization experiments, two siRNA constructs, HSS182278 and HSS107919, reduced *ABCB1* expression to <30% consistently after 5 days growth on polycarbonate membranes (Figure 6-1 and Figure 6-2). The Caco-2 cells grown as described achieved confluence rapidly and formed tight junctions by day 4 post-transfection, as determined by transepithelial electrical resistance monitoring and by immunostaining for Zonula occludens-1 (ZO-1), a key protein involved in maintenance of tight junctions(371, 372). The highest expression of *ZO-1* mRNA occurs in undifferentiated Caco-2 cells and ZO-1 protein is detected prior to confluence. Consequently, RT-qPCR and Western blot techniques cannot be used to determine tight junction formation; however, the specific localization of ZO-1 at cell-cell contact points only occurs upon formation of a monolayer(373). Using our transfection protocol, tight junctions form after treatment with each siRNA construct. For brevity only a single representative figure was included (Figure 6-4). The formation of a brush border in the transfected and non-transfected cells was demonstrated by Western blot analysis for sucrase-isomaltase(374) (Figure 6-7 and Figure 6-8), a brush border enzyme that is only expressed upon full differentiation of Caco-2 cells(362, 375).

The success of this model depends on the reduction not only of *ABCB1* mRNA but also of Pgp protein levels and, ultimately, activity. In Figure 6-5 and Figure 6-6 we demonstrate that 72h-96h of growth was required for Pgp turnover using these culture conditions and cell line, consistent with Pgp turnover (half life of 5-17h) reported in other cell lines(376-378). By 4 days of culture Pgp protein was nearly

undetectable and remained low for at least an additional 48h (Figure 6-5 and Figure 6-6). Another graduate student in Dr. Wasan's laboratory, Jo-Ann Osei-Twum, is studying Pgp function. At the time this thesis is being written, the transfected cells have a reduced Pgp activity as measured by the retention of a fluorescent Pgp substrate, rhodamine 123, relative to untransfected Caco-2 cells (unpublished data by Jo-Ann Osei-Twum). Future studies by Jo-Ann will include the determination of trans-cellular flux of Pgp substrates using this cell model.

After characterization of the Caco-2 knockdown cells, the model was used to test whether or not knockdown of Pgp replicated the cholesterol trafficking phenotype observed when Caco-2 cells were treated with Pgp inhibitors(223-225). If Pgp is an efflux transporter of cholesterol, deletion or inhibition of the protein should increase the intracellular cholesterol levels, leading to increased esterification. Conversely, if Pgp facilitates trafficking and internalization of cholesterol then deletion of Pgp would decrease cholesterol esterification. Using our model, neither silencing Pgp nor chemical inhibition with the third-generation inhibitor LY335979 (Zosuquidar: Lilly) had any effect on the uptake of cholesterol from cholesterol/monoolein/taurocholate micelles (Figure 6-9A), consistent with the literature. In contrast with published reports, neither treatment affected esterification of the cholesterol taken up by the cells (Figure 6-9B). The inter-experiment variability in esterification made it difficult to determine if there were no changes in esterification due to experimental error or because Pgp does not have a role in the internalization of cholesterol. Consequently, future studies are needed before definitive conclusions can be drawn using this model.

Likewise, the cholesterol synthesis experiments had high levels of inter-experiment variability, making analysis of the three experiments challenging. Despite the variability, cholesterol synthesis was increased in cells silenced with HSS18278 relative to the GC-matched control, as measured by incorporation of ^{14}C -acetate into cholesterol (Figure 6-10A $p < 0.05$ by unpaired t-test). Interestingly, the lysates from cells treated with HSS182278 had 3-fold more ^{14}C activity than lysates from any other treatment group (data not shown, $p < 0.001$; $n = 6$ replicates spread over 3 experiments). Pgp inhibition decreased cholesterol synthesis in all previous cell culture experiments, regardless of cell type, suggesting that there may have been a confounding factor in the cells treated with HSS182278 leading to increased cholesterol synthesis. Future experiments using the HSS107919 construct should test whether the cholesterol synthesis data is a product of the HSS182278 construct or silencing *ABCB1*. Inhibition of Pgp with LY335979 did not reduce cholesterol synthesis (Figure 6-10B), as it did in previous studies(225). Based on the trend towards decreased synthesis, additional experimentation may discriminate between the untreated and treated cells. Neither treatment affected the esterification of newly synthesized cholesterol (Figure 6-10C/D), although the cells may not have been incubated with ^{14}C -acetate long enough for differences in cholesterol esterification to be observed.

Our goal in using siRNA to specifically silence the expression *ABCB1* was to create an experimental system lacking the confounders present in previous cell culture studies. Unfortunately, high inter-experiment variability prevented us from drawing any conclusions from these studies. As discussed above, Pgp may be an efflux

transporter, an influx mechanism, or not involved in cholesterol trafficking. The numbers of independent studies linking Pgp with cellular cholesterol homeostasis suggest that it is not the latter. Perhaps future studies using siRNA or chemical inhibitors with improved specificity will be able to determine the precise role of Pgp in intracellular cholesterol homeostasis.

Chapter 7: Conclusions and future directions

7.1 Summary of key findings

- The data presented and discussed in Chapter 3: demonstrated that cholesterol homeostasis was maintained in the *Abcb1a^{-/-}/1b^{-/-}* mice. These studies did not provide evidence to support the hypothesis that cholesterol absorption was affected by deletion of Pgp, even after administration of atherogenic diets.
- When probing the intracellular cholesterol regulatory pathways in Chapter 4 several key findings were made:
 - Chronic feeding of cholesterol, but not fat resulted in a sustained activation of LXR, both in the jejunum and in the liver. This observation confirms that our experimental design and methodology successfully detected perturbations to the regulatory pathways.
 - Relative to FVB wild type mice, *Abcb1a^{-/-}/1b^{-/-}* knockout mice administered the NFNC diet had reduced SREBP-2 activity in the jejunum and increased LXR activity in the liver. The pattern of these changes suggests that the knockout mice lacked a cholesterol efflux mechanism.
 - Consumption of high cholesterol diets induced the expression of *Abcb1a* in the jejunum and in the liver of wild type mice. The response to dietary cholesterol suggests a role for Pgp in maintaining cholesterol homeostasis under conditions of excess cholesterol.
- The *Abcb1a^{-/-}1b^{-/-}* knockout mice had a reduced capacity to efflux bile acids compared to the wild type mouse after chronic feeding of diets rich in fat and/or

cholesterol. This finding supports the hypothesis that Pgp, along with BSEP, is required for normal bile acid efflux after physiologically relevant dietary stress. Furthermore, deletion of Pgp did not affect the composition of bile acids in the gallbladder, signifying that it did not have specificity for a particular class of bile acid.

- We successfully silenced the *ABCB1* gene in Caco-2 cells using siRNA such that the cells formed a confluent differentiated monolayer. This provides a model for future students to probe the interactions between Pgp and established cholesterol trafficking proteins in a more controlled environment than possible with *in vivo* studies.

7.2 Summary of unanswered questions

The research presented in this thesis was driven by three specific research questions: does P-glycoprotein have an endogenous role in cholesterol absorption, cholesterol efflux, and bile acid homeostasis. As summarized above, the data presented in this thesis do not support the hypothesis that Pgp contributes to the gastrointestinal absorption of cholesterol. However, we noted perturbations to SREBP-2 and LXR cholesterol regulatory pathways in the *Abcb1a^{-/-}/1b^{-/-}* knockout mice consistent with a role for Pgp in cholesterol efflux. Unfortunately, we were not able to directly test the cholesterol efflux capacity of Pgp. Future studies using different experimental models are required to test this hypothesis.

The data presented in Figure 5-3 demonstrate that BSEP can maintain bile acid homeostasis when mice are fed a normal chow diet; however, it appears that P-glycoprotein is required in addition to BSEP to maintain bile acid efflux to the gallbladder after chronic consumption of cholesterol and fat. There are a number of provocative research questions raised by this finding. We have shown that Pgp deletion affects the accumulation of bile acids in the gallbladder but we did not probe whether there are changes to the bile acid pool in the knockout mice. Additionally, if Pgp is an efflux mechanism for bile acids, it could be an uncharacterized feedback mechanism to limit the reabsorption of bile acids from the gastrointestinal tract. Pgp levels are lowest in the duodenum, rising in the jejunum and peaking in the distal ileum and colon. Other groups have demonstrated that *ABCB1* is induced by PXR, which responds to accumulations of toxic bile acids. This knowledge, combined with our finding that intestinal *Abcb1a* increased in response to dietary cholesterol gives provocative preliminary evidence to suggest a role for Pgp in maintaining the enterohepatic circulation of bile acids. Chronic feeding of cholesterol has only a small effect on circulating cholesterol levels due to feedback mechanisms including suppression of biosynthesis and a reduction in cholesterol absorption. If Pgp limits the reabsorption of bile acids in the distal ileum, this could be an uncharacterized feedback mechanism that increases catabolism of cholesterol in the liver, affecting the whole body cholesterol pool. This hypothesis could be tested using intestine-specific Pgp knockout animals.

An additional question that has not been addressed in the biomedical literature is the contribution of canalicular bile acid transporters on reverse cholesterol

transport. The contributions of macrophage transporters have been thoroughly quantified using a method first proposed by Rader *et al.* (379) outlined in Chapter 1. Although the discovery that ABCG5/ABCG8 are responsible for sterol efflux from the liver was made a decade ago, only a single paper has been published in which the contributions of this transporter to the macrophage to feces RCT pathway were characterized(380). There are no papers published testing if *Abcb11*^{-/-} mice have decreased macrophage-to-feces RCT, nor are there papers examining the importance of bile acid synthesis to this pathway. Determining the contributions of hepatic transport and catabolism of cholesterol to the macrophage to feces RCT pathway remain important unanswered questions in the field of cardiovascular health.

7.3 Future studies

The results presented in this thesis suggest two avenues for future studies: investigation of P-glycoprotein in cholesterol and bile salt transport. As discussed above, we have not been able to directly characterize Pgp as a cholesterol efflux transporter. This is perhaps because of the compensatory mechanisms that maintain homeostasis in complex biological systems. In order to determine if Pgp is functioning as a cholesterol transporter, a series of mechanistic *in vitro* studies are warranted. The data presented in Chapter 6 supports the idea that *ABCB1* can be effectively silenced in Caco-2 cells. This cell culture model presents a potential starting point for future studies. Cholesterol efflux studies using mixed micelles as acceptors in *ABCB1* silenced cells need to be compared with studies in *ABCG5* or *ABCG8* silenced cells. Silencing either of the hemi-transporter genes is sufficient as the expression of both is required

for transport of the protein from the endoplasmic reticulum, after translation of the mRNA(381). Additionally, *in vitro* cholesterol uptake and efflux studies using vesicles prepared from brush border membranes isolated from *Abcb1a^{-/-}/1b^{-/-}* mice and from *Abcg5^{-/-}/g8^{-/-}* mice would provide kinetics data comparing the relative affinity and efficacy of cholesterol transport between a putative cholesterol transporter and a well established one.

The role of Pgp in macrophage cholesterol efflux has not been characterized. Current research suggests that cholesterol efflux from macrophages is accomplished by one of four mechanisms: ABCA1-mediated, ABCG1-mediated, SCARB1-mediated and aqueous diffusion. Studies using macrophages isolated from knockout mice clearly demonstrated that ABCA1 and ABCG1 combined contribute approximately 50% of the cholesterol efflux when serum or HDL is used as an acceptor(101), underscoring the importance of looking for additional efflux mechanisms. Two sets of studies are proposed to test the putative contributions of Pgp to macrophage cholesterol efflux. 1. *In vitro* studies using siRNA-mediated silencing of *ABCB1* in monocytes. 2. Isolation of macrophages from *Abcb1a^{-/-}/1b^{-/-}* mice for *ex vivo* cholesterol efflux studies. If the cell-based studies reveal a role for Pgp in macrophage cholesterol efflux, the logical next step involves characterizing the role of Pgp in the initiation and regression of atherosclerosis *in vivo*.

There are a tremendous number of studies required for the full characterization of Pgp as a bile acid transporter. The impact of Pgp on the flow of bile acids should be the first study undertaken. Our data relied on the observation that deletion of *Abcb1a/1b* had no effect on bile flow rates, published by other groups.

None of these groups characterized bile flow in mice after chronic feeding of high fat/high cholesterol diets, such as were necessary to for Pgp-dependent changes to gallbladder bile acid content described in Chapter 5. These studies should be accompanied by an assessment of the bile acid pool size, accomplished by estimating the bile acids in the ileum, circulation, liver, and gallbladder in mice not subjected to gallbladder cannulation.

Studying whether or not Pgp acts as a barrier to bile acid uptake in the distal ileum, especially after chronic consumption of a high cholesterol diet, could provide evidence for an additional negative feedback mechanism that increases hepatic cholesterol catabolism. Because Pgp is found both in the liver and in the ileum, a targeted loss of ileum Pgp function is required. If a non-absorbed Pgp inhibitor were available, this would be a relatively easy experiment to conduct; however, it is likely that a targeted deletion of *ABCB1* is required. This set of experiments should include an evaluation of the enterohepatic circulation of bile acids as well as catabolism of cholesterol into new bile acids in the liver.

The final set of studies I propose based on outcomes of this thesis are the macrophage to feces RCT studies to determine the contribution of hepatic canalicular transporters, discussed in section 7.2. These studies would follow radiolabeled cholesterol carried by lipid-loaded macrophages obtained from wild type mice (or cell culture) after injection into mice lacking *Bsep* or *Abcb1a/1b*. Although this experimental model was designed to probe the contribution of macrophage transporters, the model has been expanded to examine the role of three steps in hepatic cholesterol trafficking on RCT: the effect of SCARB1-mediated uptake(143), the

contribution of ABCG5/G8(380), and the role of cholesteryl ester hydrolase(382). I propose that this model be adapted to probe the contributions of canalicular bile acid transporters to RCT. These studies have the potential to identify new targets in the RCT pathway that can be exploited for atherosclerotic plaque reduction.

References

1. Seal, R. L., S. M. Gordon, M. J. Lush, M. W. Wright, and E. A. Bruford. 2011. genenames.org: the HGNC resources in 2011. *Nucleic Acids Res.* **39**: D514–9.
2. Eppig, J. T., J. A. Blake, C. J. Bult, J. A. Kadin, J. E. Richardson, Mouse Genome Database Group. 2012. The Mouse Genome Database (MGD): comprehensive resource for genetics and genomics of the laboratory mouse. *Nucleic Acids Res.* **40**: D881–6.
3. Benson, D. A., I. Karsch-Mizrachi, K. Clark, D. J. Lipman, J. Ostell, and E. W. Sayers. 2012. GenBank. *Nucleic Acids Res.* **40**: D48–53.
4. Claudel, T., G. Zollner, M. Wagner, and M. Trauner. 2011. Role of nuclear receptors for bile acid metabolism, bile secretion, cholestasis, and gallstone disease. *Biochim. Biophys. Acta.* **1812**: 867–878.
5. Dietschy, J. M., S. D. Turley, and D. K. Spady. 1993. Role of liver in the maintenance of cholesterol and low density lipoprotein homeostasis in different animal species, including humans. *J. Lipid Res.* **34**: 1637–1659.
6. Berge, K. E., H. Tian, G. A. Graf, L. Yu, N. V. Grishin, J. Schultz, P. Kwiterovich, B. Shan, R. Barnes, and H. H. Hobbs. 2000. Accumulation of dietary cholesterol in sitosterolemia caused by mutations in adjacent ABC transporters. *Science.* **290**: 1771–1775.
7. Yu, L., R. E. Hammer, J. Li-Hawkins, K. Von Bergmann, D. Lutjohann, J. C. Cohen, and H. H. Hobbs. 2002. Disruption of Abcg5 and Abcg8 in mice reveals their crucial role in biliary cholesterol secretion. *Proc. Natl. Acad. Sci. U.S.A.* **99**: 16237–16242.
8. Plösch, T., J. N. van der Veen, R. Havinga, N. C. A. Huijkman, V. W. Bloks, and F. Kuipers. 2006. Abcg5/Abcg8-independent pathways contribute to hepatobiliary cholesterol secretion in mice. *Am. J. Physiol. Gastrointest. Liver Physiol.* **291**: G414–23.
9. Geuken, E., D. S. Visser, H. G. D. Leuvenink, K. P. de Jong, P. M. J. G. Peeters, M. J. H. Slooff, F. Kuipers, and R. J. Porte. 2005. Hepatic expression of ABC transporters G5 and G8 does not correlate with biliary cholesterol secretion in liver transplant patients. *Hepatology.* **42**: 1166–1174.
10. Wang, R., M. Salem, I. M. Yousef, B. Tuchweber, P. Lam, S. J. Childs, C. D. Helgason, C. Ackerley, M. J. Phillips, and V. Ling. 2001. Targeted inactivation of sister of P-glycoprotein gene (spgp) in mice results in nonprogressive but persistent intrahepatic cholestasis. *Proc. Natl. Acad. Sci. U.S.A.* **98**: 2011–2016.
11. Lam, P., R. Wang, and V. Ling. 2005. Bile acid transport in sister of P-glycoprotein

- (ABCB11) knockout mice. *Biochemistry*. **44**: 12598–12605.
12. Wang, R., H.-L. Chen, L. Liu, J. A. Sheps, M. J. Phillips, and V. Ling. 2009. Compensatory role of P-glycoproteins in knockout mice lacking the bile salt export pump. *Hepatology*. **50**: 948–956.
 13. Yusuf, S., S. Hawken, S. Ounpuu, T. Dans, A. Avezum, F. Lanas, M. McQueen, A. Budaj, P. Pais, J. Varigos, L. Lisheng, and INTERHEART Study Investigators. 2004. Effect of potentially modifiable risk factors associated with myocardial infarction in 52 countries (the INTERHEART study): case-control study. *Lancet*. **364**: 937–952.
 14. Keys, A. 1970. Coronary heart disease in seven countries. Summary. *Circulation*. **41**: 1186–95.
 15. Verschuren, W. M., D. R. Jacobs, B. P. Bloemberg, D. Kromhout, A. Menotti, C. Aravanis, H. Blackburn, R. Buzina, A. S. Dontas, and F. Fidanza. 1995. Serum total cholesterol and long-term coronary heart disease mortality in different cultures. Twenty-five-year follow-up of the seven countries study. *JAMA*. **274**: 131–136.
 16. Goldstein, J. L., H. H. Hobbs, and M. S. Brown. *In* Scriver's Online Metabolic and Molecular Bases of Inherited Disease (Valle, D., Beaudet, A. L., Vogelstein, B., Ballabio, A., Antonarakis, S. E., and Kinzler, K. W., eds.). pp. 1–122., McGraw-Hill.
 17. Brown, M. S., and J. L. Goldstein. 1986. A receptor-mediated pathway for cholesterol homeostasis. *Science*. **232**: 34–47.
 18. Breslow, J. L. 1996. Mouse models of atherosclerosis. *Science*. **272**: 685–688.
 19. Zadelaar, S., R. Kleemann, L. Verschuren, J. de Vries-Van der Weij, J. van der Hoorn, H. M. Princen, and T. Kooistra. 2007. Mouse models for atherosclerosis and pharmaceutical modifiers. *Arterioscler. Thromb. Vasc. Biol.* **27**: 1706–1721.
 20. Baigent, C., A. Keech, P. M. Kearney, L. Blackwell, G. Buck, C. Pollicino, A. Kirby, T. Sourjina, R. Peto, R. Collins, R. Simes, Cholesterol Treatment Trialists' (CTT) Collaborators. 2005. Efficacy and safety of cholesterol-lowering treatment: prospective meta-analysis of data from 90,056 participants in 14 randomised trials of statins. *Lancet*. **366**: 1267–1278.
 21. World Health Organization. 2008. Global Burden of Disease. World Health Organization Press, Geneva.
 22. Fuster, V., B. B. Kelly, and R. Vedanthan. 2011. Global cardiovascular health: urgent need for an intersectoral approach. *J. Am. Coll. Cardiol.* **58**: 1208–1210.
 23. Canada, P. H. A. O. 2009. Tracking Heart Disease and Stroke in Canada. (Canada, P. H. A. O., Canadian Institute for Health Information, Network, C. S., Heart and Stroke Foundation of Canada, and Canada, S., eds.). Public Health Agency of Canada,

Ottawa.

24. Libby, P., P. M. Ridker, and G. K. Hansson. 2011. Progress and challenges in translating the biology of atherosclerosis. *Nature*. **473**: 317–325.
25. Moore, K. J., and I. Tabas. 2011. Macrophages in the pathogenesis of atherosclerosis. *Cell*. **145**: 341–355.
26. Castelli, W. P., R. J. Garrison, P. W. Wilson, R. D. Abbott, S. Kalousdian, and W. B. Kannel. 1986. Incidence of coronary heart disease and lipoprotein cholesterol levels. The Framingham Study. *JAMA*. **256**: 2835–2838.
27. Stampfer, M. J., R. M. Krauss, J. Ma, P. J. Blanche, L. G. Holl, F. M. Sacks, and C. H. Hennekens. 1996. A prospective study of triglyceride level, low-density lipoprotein particle diameter, and risk of myocardial infarction. *JAMA*. **276**: 882–888.
28. National Cholesterol Education Program (NCEP) Expert Panel on Detection, Evaluation, and Treatment of High Blood Cholesterol in Adults (Adult Treatment Panel III). 2002. Third Report of the National Cholesterol Education Program (NCEP) Expert Panel on Detection, Evaluation, and Treatment of High Blood Cholesterol in Adults (Adult Treatment Panel III) final report. *Circulation*. **106**: 3143–3421.
29. Genest, J., R. McPherson, J. Frohlich, T. Anderson, N. Campbell, A. Carpentier, P. Couture, R. Dufour, G. Fodor, G. A. Francis, S. Grover, M. Gupta, R. A. Hegele, D. C. Lau, L. Leiter, G. F. Lewis, E. Lonn, G. B. J. Mancini, D. Ng, G. J. Pearson, A. Sniderman, J. A. Stone, and E. Ur. 2009. 2009 Canadian Cardiovascular Society/Canadian guidelines for the diagnosis and treatment of dyslipidemia and prevention of cardiovascular disease in the adult - 2009 recommendations. *Can. J. Cardiol.* **25**: 567–579.
30. Chau, P., Y. Nakamura, C. J. Fielding, and P. E. Fielding. 2006. Mechanism of prebeta-HDL formation and activation. *Biochemistry*. **45**: 3981–3987.
31. Vance, J. E. 2002. *In Biochemistry of Lipids, Lipoproteins and Membranes, Volume 36, Fourth Edition (New Comprehensive Biochemistry)*. 4th Ed. pp. 505–526., Elsevier Science. [online] [http://dx.doi.org/10.1016/S0167-7306\(02\)36021-6](http://dx.doi.org/10.1016/S0167-7306(02)36021-6).
32. Wasan, K. M., D. R. Brocks, S. D. Lee, K. Sachs-Barrable, and S. J. Thornton. 2008. Impact of lipoproteins on the biological activity and disposition of hydrophobic drugs: implications for drug discovery. *Nat. Rev. Drug. Discov.* **7**: 84–99.
33. Jonas, A. 2002. *In Biochemistry of Lipids, Lipoproteins and Membranes, Volume 36, Fourth Edition (New Comprehensive Biochemistry)*. 4th Ed. pp. 483–504., Elsevier Science. [online] [http://dx.doi.org/10.1016/S0167-7306\(02\)36020-4](http://dx.doi.org/10.1016/S0167-7306(02)36020-4).
34. Fielding, P. E., and C. J. Fielding. 2002. *In Biochemistry of Lipids, Lipoproteins and*

Membranes, Volume 36, Fourth Edition (New Comprehensive Biochemistry). 4th Ed. pp. 527–552., Elsevier Science. [online] [http://dx.doi.org/10.1016/S0167-7306\(02\)36022-8](http://dx.doi.org/10.1016/S0167-7306(02)36022-8).

35. Havel, R. J., and J. P. Kane. *In* Scriver's Online Metabolic and Molecular Bases of Inherited Disease (Valle, D., Beaudet, A. L., Ballabio, A., Antonarakis, S. E., Kinzler, K. W., and Vogelstein, B., eds.). pp. 1–23., McGraw-Hill.
36. Powell, L. M., S. C. Wallis, R. J. Pease, Y. H. Edwards, T. J. Knott, and J. Scott. 1987. A novel form of tissue-specific RNA processing produces apolipoprotein-B48 in intestine. *Cell*. **50**: 831–840.
37. Morton, R. E., and D. B. Zilversmit. 1983. Inter-relationship of lipids transferred by the lipid-transfer protein isolated from human lipoprotein-deficient plasma. *J. Biol. Chem.* **258**: 11751–11757.
38. Tall, A. R. 1993. Plasma cholesteryl ester transfer protein. *J. Lipid Res.* **34**: 1255–1274.
39. Krauss, R. M., and D. J. Burke. 1982. Identification of multiple subclasses of plasma low density lipoproteins in normal humans. *J. Lipid Res.* **23**: 97–104.
40. Lamarche, B., A. Tchernof, S. Moorjani, B. Cantin, G. R. Dagenais, P. J. Lupien, and J. P. Després. 1997. Small, dense low-density lipoprotein particles as a predictor of the risk of ischemic heart disease in men. Prospective results from the Québec Cardiovascular Study. *Circulation*. **95**: 69–75.
41. Kuivenhoven, J. A., H. Pritchard, J. Hill, J. Frohlich, G. Assmann, and J. Kastelein. 1997. The molecular pathology of lecithin:cholesterol acyltransferase (LCAT) deficiency syndromes. *J. Lipid Res.* **38**: 191–205.
42. Fielding, P. E., and C. J. Fielding. 1980. A cholesteryl ester transfer complex in human plasma. *Proc. Natl. Acad. Sci. U.S.A.* **77**: 3327–3330.
43. Rader, D. J. 2006. Molecular regulation of HDL metabolism and function: implications for novel therapies. *J. Clin. Invest.* **116**: 3090–3100.
44. Tall, A. R., L. Yvan-Charvet, N. Terasaka, T. Pagler, and N. Wang. 2008. HDL, ABC transporters, and cholesterol efflux: implications for the treatment of atherosclerosis. *Cell Metab.* **7**: 365–375.
45. Krieger, M. 1999. Charting the fate of the “good cholesterol”: identification and characterization of the high-density lipoprotein receptor SR-BI. *Annu. Rev. Biochem.* **68**: 523–558.
46. Acton, S., A. Rigotti, K. T. Landschulz, S. Xu, H. H. Hobbs, and M. Krieger. 1996. Identification of scavenger receptor SR-BI as a high density lipoprotein receptor.

- Science*. **271**: 518–520.
47. Kozarsky, K. F., M. H. Donahee, A. Rigotti, S. N. Iqbal, E. R. Edelman, and M. Krieger. 1997. Overexpression of the HDL receptor SR-BI alters plasma HDL and bile cholesterol levels. *Nature*. **387**: 414–417.
 48. Stamler, J., D. Wentworth, and J. D. Neaton. 1986. Is relationship between serum cholesterol and risk of premature death from coronary heart disease continuous and graded? Findings in 356,222 primary screenees of the Multiple Risk Factor Intervention Trial (MRFIT). *JAMA*. **256**: 2823–2828.
 49. 1984. The Lipid Research Clinics Coronary Primary Prevention Trial results. I. Reduction in incidence of coronary heart disease. *JAMA*. **251**: 351–364.
 50. McQueen, M. J., S. Hawken, X. Wang, S. Ounpuu, A. Sniderman, J. Probstfield, K. Steyn, J. E. Sanderson, M. Hasani, E. Volkova, K. Kazmi, S. Yusuf, and INTERHEART Study Investigators. 2008. Lipids, lipoproteins, and apolipoproteins as risk markers of myocardial infarction in 52 countries (the INTERHEART study): a case-control study. *Lancet*. **372**: 224–233.
 51. Cholesterol Treatment Trialists' (CTT) Collaboration, C. Baigent, L. Blackwell, J. Emberson, L. E. Holland, C. Reith, N. Bhalra, R. Peto, E. H. Barnes, A. Keech, J. Simes, and R. Collins. 2010. Efficacy and safety of more intensive lowering of LDL cholesterol: a meta-analysis of data from 170,000 participants in 26 randomised trials. *Lancet*. **376**: 1670–1681.
 52. Scandinavian Simvastatin Survival Study Group. 1994. Randomised trial of cholesterol lowering in 4444 patients with coronary heart disease: the Scandinavian Simvastatin Survival Study (4S). *Lancet*. **344**: 1383–1389.
 53. Shepherd, J., S. M. Cobbe, I. Ford, C. G. Isles, A. R. Lorimer, P. W. MacFarlane, J. H. McKillop, and C. J. Packard. 1995. Prevention of coronary heart disease with pravastatin in men with hypercholesterolemia. West of Scotland Coronary Prevention Study Group. *N. Engl. J. Med.* **333**: 1301–1307.
 54. Sacks, F. M., M. A. Pfeffer, L. A. Moye, J. L. Rouleau, J. D. Rutherford, T. G. Cole, L. Brown, J. W. Warnica, J. M. Arnold, C. C. Wun, B. R. Davis, and E. Braunwald. 1996. The effect of pravastatin on coronary events after myocardial infarction in patients with average cholesterol levels. Cholesterol and Recurrent Events Trial investigators. *N. Engl. J. Med.* **335**: 1001–1009.
 55. Investigators, T. P. C. A. B. G. T. 1997. The effect of aggressive lowering of low-density lipoprotein cholesterol levels and low-dose anticoagulation on obstructive changes in saphenous-vein coronary-artery bypass grafts. The Post Coronary Artery Bypass Graft Trial Investigators. *N. Engl. J. Med.* **336**: 153–162.

56. Downs, J. R., M. Clearfield, S. Weis, E. Whitney, D. R. Shapiro, P. A. Beere, A. Langendorfer, E. A. Stein, and W. Kruyer. 1998. Primary prevention of acute coronary events with lovastatin in men and women with average cholesterol levels: results of AFCAPS/TexCAPS. Air Force/Texas Coronary Atherosclerosis Prevention Study. *JAMA*. **279**: 1615–1622.
57. 1998. Prevention of cardiovascular events and death with pravastatin in patients with coronary heart disease and a broad range of initial cholesterol levels. The Long-Term Intervention with Pravastatin in Ischaemic Disease (LIPID) Study Group. *N. Engl. J. Med.* **339**: 1349–1357.
58. Heart Protection Study Collaborative Group. 2002. MRC/BHF Heart Protection Study of cholesterol lowering with simvastatin in 20,536 high-risk individuals: a randomised placebo-controlled trial. *Lancet*. **360**: 7–22.
59. ALLHAT Officers and Coordinators for the ALLHAT Collaborative Research Group. The Antihypertensive and Lipid-Lowering Treatment to Prevent Heart Attack Trial. 2002. Major outcomes in moderately hypercholesterolemic, hypertensive patients randomized to pravastatin vs usual care: The Antihypertensive and Lipid-Lowering Treatment to Prevent Heart Attack Trial (ALLHAT-LLT). *JAMA*. **288**: 2998–3007.
60. Gardner, C. D., S. P. Fortmann, and R. M. Krauss. 1996. Association of small low-density lipoprotein particles with the incidence of coronary artery disease in men and women. *JAMA*. **276**: 875–881.
61. Kunjathoor, V. V., M. Febbraio, E. A. Podrez, K. J. Moore, L. Andersson, S. Koehn, J. S. Rhee, R. Silverstein, H. F. Hoff, and M. W. Freeman. 2002. Scavenger receptors class A-I/II and CD36 are the principal receptors responsible for the uptake of modified low density lipoprotein leading to lipid loading in macrophages. *J. Biol. Chem.* **277**: 49982–49988.
62. Endemann, G., L. W. Stanton, K. S. Madden, C. M. Bryant, R. T. White, and A. A. Protter. 1993. CD36 is a receptor for oxidized low density lipoprotein. *J. Biol. Chem.* **268**: 11811–11816.
63. Steinberg, D., and J. L. Witztum. 2010. Oxidized low-density lipoprotein and atherosclerosis. *Arterioscler. Thromb. Vasc. Biol.* **30**: 2311–2316.
64. Hansson, G. K. 2005. Inflammation, atherosclerosis, and coronary artery disease. *N. Engl. J. Med.* **352**: 1685–1695.
65. Serruys, P. W. J. C., P. de Feyter, C. Macaya, N. Kokott, J. Puel, M. Vrolix, A. Branzi, M. C. Bertolami, G. Jackson, B. Strauss, B. Meier, Lescol Intervention Prevention Study (LIPS) Investigators. 2002. Fluvastatin for prevention of cardiac events following successful first percutaneous coronary intervention: a randomized controlled trial. *JAMA*. **287**: 3215–3222.

66. European Association for Cardiovascular Prevention & Rehabilitation, Z. Reiner, A. L. Catapano, G. De Backer, I. Graham, M.-R. Taskinen, O. Wiklund, S. Agewall, E. Alegria, M. J. Chapman, P. Durrington, S. Erdine, J. Halcox, R. Hobbs, J. Kjekshus, P. P. Filardi, G. Riccardi, R. F. Storey, D. Wood, ESC Committee for Practice Guidelines (CPG) 2008-2010 and 2010-2012 Committees, J. Bax, A. Vahanian, A. Auricchio, H. Baumgartner, C. Ceconi, V. Dean, C. Deaton, R. Fagard, G. Filippatos, C. Funck-Brentano, D. Hasdai, R. Hobbs, A. Hoes, P. Kearney, J. Knuuti, P. Kolh, T. McDonagh, C. Moulin, D. Poldermans, B. A. Popescu, Z. Reiner, U. Sechtem, P. A. Sirnes, M. Tendera, A. Torbicki, P. Vardas, P. Widimsky, S. Windecker, C. Funck-Brentano, D. Poldermans, et al. 2011. ESC/EAS Guidelines for the management of dyslipidaemias: the Task Force for the management of dyslipidaemias of the European Society of Cardiology (ESC) and the European Atherosclerosis Society (EAS). *Eur. Heart J.* **32**: 1769–1818.
67. Libby, P. 2005. The forgotten majority: unfinished business in cardiovascular risk reduction. *J. Am. Coll. Cardiol.* **46**: 1225–1228.
68. Gordon, T., W. P. Castelli, M. C. Hjortland, W. B. Kannel, and T. R. Dawber. 1977. High density lipoprotein as a protective factor against coronary heart disease. The Framingham Study. *Am. J. Med.* **62**: 707–714.
69. Gordon, D. J., J. L. Probstfield, R. J. Garrison, J. D. Neaton, W. P. Castelli, J. D. Knoke, D. R. Jacobs, S. Bangdiwala, and H. A. Tyroler. 1989. High-density lipoprotein cholesterol and cardiovascular disease. Four prospective American studies. *Circulation.* **79**: 8–15.
70. Assmann, G., H. Schulte, A. von Eckardstein, and Y. Huang. 1996. High-density lipoprotein cholesterol as a predictor of coronary heart disease risk. The PROCAM experience and pathophysiological implications for reverse cholesterol transport. *Atherosclerosis.* **124 Suppl**: S11–20.
71. Turner, R. C., H. Millns, H. A. Neil, I. M. Stratton, S. E. Manley, D. R. Matthews, and R. R. Holman. 1998. Risk factors for coronary artery disease in non-insulin dependent diabetes mellitus: United Kingdom Prospective Diabetes Study (UKPDS: 23). *BMJ.* **316**: 823–828.
72. Wilson, P. W., R. B. D'Agostino, D. Levy, A. M. Belanger, H. Silbershatz, and W. B. Kannel. 1998. Prediction of coronary heart disease using risk factor categories. *Circulation.* **97**: 1837–1847.
73. Sharrett, A. R., C. M. Ballantyne, S. A. Coady, G. Heiss, P. D. Sorlie, D. Catellier, W. Patsch, Atherosclerosis Risk in Communities Study Group. 2001. Coronary heart disease prediction from lipoprotein cholesterol levels, triglycerides, lipoprotein(a), apolipoproteins A-I and B, and HDL density subfractions: The Atherosclerosis Risk in Communities (ARIC) Study. *Circulation.* **104**: 1108–1113.

74. Curb, J. D., R. D. Abbott, B. L. Rodriguez, K. Masaki, R. Chen, D. S. Sharp, and A. R. Tall. 2004. A prospective study of HDL-C and cholesteryl ester transfer protein gene mutations and the risk of coronary heart disease in the elderly. *J. Lipid Res.* **45**: 948–953.
75. Castelli, W. P., J. T. Doyle, T. Gordon, C. G. Hames, M. C. Hjortland, S. B. Hulley, A. Kagan, and W. J. Zukel. 1977. HDL cholesterol and other lipids in coronary heart disease. The cooperative lipoprotein phenotyping study. *Circulation.* **55**: 767–772.
76. Miller, G. J., and N. E. Miller. 1975. Plasma-high-density-lipoprotein concentration and development of ischaemic heart-disease. *Lancet.* **1**: 16–19.
77. Trigatti, B., H. Rayburn, M. Viñals, A. Braun, H. Miettinen, M. Penman, M. Hertz, M. Schrenzel, L. Amigo, A. Rigotti, and M. Krieger. 1999. Influence of the high density lipoprotein receptor SR-BI on reproductive and cardiovascular pathophysiology. *Proc. Natl. Acad. Sci. U.S.A.* **96**: 9322–9327.
78. Braun, A., B. L. Trigatti, M. J. Post, K. Sato, M. Simons, J. M. Edelberg, R. D. Rosenberg, M. Schrenzel, and M. Krieger. 2002. Loss of SR-BI expression leads to the early onset of occlusive atherosclerotic coronary artery disease, spontaneous myocardial infarctions, severe cardiac dysfunction, and premature death in apolipoprotein E-deficient mice. *Circ. Res.* **90**: 270–276.
79. Covey, S. D., M. Krieger, W. Wang, M. Penman, and B. L. Trigatti. 2003. Scavenger receptor class B type I-mediated protection against atherosclerosis in LDL receptor-negative mice involves its expression in bone marrow-derived cells. *Arterioscler. Thromb. Vasc. Biol.* **23**: 1589–1594.
80. Degoma, E. M., and D. J. Rader. 2011. Novel HDL-directed pharmacotherapeutic strategies. *Nat. Rev. Cardiol.* **8**: 266–277.
81. Natarajan, P., K. K. Ray, and C. P. Cannon. 2010. High-density lipoprotein and coronary heart disease: current and future therapies. *J. Am. Coll. Cardiol.* **55**: 1283–1299.
82. Cannon, C. P., S. Shah, H. M. Dansky, M. Davidson, E. A. Brinton, A. M. Gotto, M. Stepanavage, S. X. Liu, P. Gibbons, T. B. Ashraf, J. Zafarino, Y. Mitchel, P. Barter, Determining the Efficacy and Tolerability Investigators. 2010. Safety of anacetrapib in patients with or at high risk for coronary heart disease. *N. Engl. J. Med.* **363**: 2406–2415.
83. Tardif, J.-C., J. Grégoire, P. L. L'Allier, R. Ibrahim, J. Lespérance, T. M. Heinonen, S. Kouz, C. Berry, R. Basser, M.-A. Lavoie, M.-C. Guertin, J. Rodés-Cabau, Effect of rHDL on Atherosclerosis-Safety and Efficacy (ERASE) Investigators. 2007. Effects of reconstituted high-density lipoprotein infusions on coronary atherosclerosis: a randomized controlled trial. *JAMA.* **297**: 1675–1682.

84. Shaw, J. A., A. Bobik, A. Murphy, P. Kanellakis, P. Blombery, N. Mukhamedova, K. Woollard, S. Lyon, D. Sviridov, and A. M. Dart. 2008. Infusion of reconstituted high-density lipoprotein leads to acute changes in human atherosclerotic plaque. *Circ. Res.* **103**: 1084–1091.
85. Nissen, S. E., T. Tsunoda, E. M. Tuzcu, P. Schoenhagen, C. J. Cooper, M. Yasin, G. M. Eaton, M. A. Lauer, W. S. Sheldon, C. L. Grines, S. Halpern, T. Crowe, J. C. Blankenship, and R. Kerensky. 2003. Effect of recombinant ApoA-I Milano on coronary atherosclerosis in patients with acute coronary syndromes: a randomized controlled trial. *JAMA.* **290**: 2292–2300.
86. Nicholls, S. J., A. Gordon, J. Johansson, K. Wolski, C. M. Ballantyne, J. J. P. Kastelein, A. Taylor, M. Borgman, and S. E. Nissen. 2011. Efficacy and safety of a novel oral inducer of apolipoprotein a-I synthesis in statin-treated patients with stable coronary artery disease a randomized controlled trial. *J. Am. Coll. Cardiol.* **57**: 1111–1119.
87. Kendall, D. M., C. J. Rubin, P. Mohideen, J.-M. Ledezine, R. Belder, J. Gross, P. Norwood, M. O'Mahony, K. Sall, G. Sloan, A. Roberts, F. T. Fiedorek, and R. A. DeFronzo. 2006. Improvement of glycemic control, triglycerides, and HDL cholesterol levels with muraglitazar, a dual (alpha/gamma) peroxisome proliferator-activated receptor activator, in patients with type 2 diabetes inadequately controlled with metformin monotherapy: A double-blind, randomized, pioglitazone-comparative study. *Diabetes Care.* **29**: 1016–1023.
88. Henry, R. R., A. M. Lincoff, S. Mudaliar, M. Rabbia, C. Chognot, and M. Herz. 2009. Effect of the dual peroxisome proliferator-activated receptor-alpha/gamma agonist aleglitazar on risk of cardiovascular disease in patients with type 2 diabetes (SYNCHRONY): a phase II, randomised, dose-ranging study. *Lancet.* **374**: 126–135.
89. Glomset, J. A. 1968. The plasma lecithins:cholesterol acyltransferase reaction. *J. Lipid Res.* **9**: 155–167.
90. Rosenson, R. S., H. B. Brewer, W. S. Davidson, Z. A. Fayad, V. Fuster, J. Goldstein, M. Hellerstein, X.-C. Jiang, M. C. Phillips, D. J. Rader, A. T. Remaley, G. H. Rothblat, A. R. Tall, and L. Yvan-Charvet. 2012. Cholesterol efflux and atheroprotection: advancing the concept of reverse cholesterol transport. *Circulation.* **125**: 1905–1919.
91. Boadu, E., N. J. Bilbey, and G. A. Francis. 2008. Cellular cholesterol substrate pools for adenosine-triphosphate cassette transporter A1-dependent high-density lipoprotein formation. *Curr Opin Lipidol.* **19**: 270–276.
92. Hansson, G. K., and P. Libby. 2006. The immune response in atherosclerosis: a double-edged sword. *Nat. Rev. Immunol.* **6**: 508–519.
93. Rothblat, G. H., and M. C. Phillips. 2010. High-density lipoprotein heterogeneity and

- function in reverse cholesterol transport. *Curr Opin Lipidol.* **21**: 229–238.
94. Yancey, P. G., A. E. Bortnick, G. Kellner-Weibel, M. de La Llera-Moya, M. C. Phillips, and G. H. Rothblat. 2003. Importance of different pathways of cellular cholesterol efflux. *Arterioscler. Thromb. Vasc. Biol.* **23**: 712–719.
95. Rust, S., M. Rosier, H. Funke, J. Real, Z. Amoura, J. C. Piette, J. F. Deleuze, H. B. Brewer, N. Duverger, P. Denèfle, and G. Assmann. 1999. Tangier disease is caused by mutations in the gene encoding ATP-binding cassette transporter 1. *Nat. Genet.* **22**: 352–355.
96. Brooks-Wilson, A., M. Marcil, S. M. Clee, L. H. Zhang, K. Roomp, M. van Dam, L. Yu, C. Brewer, J. A. Collins, H. O. Molhuizen, O. Loubser, B. F. Ouellette, K. Fichter, K. J. Ashbourne-Excoffon, C. W. Sensen, S. Scherer, S. Mott, M. Denis, D. Martindale, J. Frohlich, K. Morgan, B. Koop, S. Pimstone, J. J. Kastelein, J. Genest, and M. R. Hayden. 1999. Mutations in ABC1 in Tangier disease and familial high-density lipoprotein deficiency. *Nat. Genet.* **22**: 336–345.
97. Bodzioch, M., E. Orsó, J. Klucken, T. Langmann, A. Böttcher, W. Diederich, W. Drobnik, S. Barlage, C. Büchler, M. Porsch-Ozcürümez, W. E. Kaminski, H. W. Hahmann, K. Oette, G. Rothe, C. Aslanidis, K. J. Lackner, and G. Schmitz. 1999. The gene encoding ATP-binding cassette transporter 1 is mutated in Tangier disease. *Nat. Genet.* **22**: 347–351.
98. Francis, G. A., R. H. Knopp, and J. F. Oram. 1995. Defective removal of cellular cholesterol and phospholipids by apolipoprotein A-I in Tangier Disease. *J. Clin. Invest.* **96**: 78–87.
99. Remaley, A. T., U. K. Schumacher, J. A. Stonik, B. D. Farsi, H. Nazih, and H. B. Brewer. 1997. Decreased reverse cholesterol transport from Tangier disease fibroblasts. Acceptor specificity and effect of brefeldin on lipid efflux. *Arterioscler. Thromb. Vasc. Biol.* **17**: 1813–1821.
100. Wang, X., H. L. Collins, M. Ranalletta, I. V. Fuki, J. T. Billheimer, G. H. Rothblat, A. R. Tall, and D. J. Rader. 2007. Macrophage ABCA1 and ABCG1, but not SR-BI, promote macrophage reverse cholesterol transport in vivo. *J. Clin. Invest.* **117**: 2216–2224.
101. Yvan-Charvet, L., M. Ranalletta, N. Wang, S. Han, N. Terasaka, R. Li, C. Welch, and A. R. Tall. 2007. Combined deficiency of ABCA1 and ABCG1 promotes foam cell accumulation and accelerates atherosclerosis in mice. *J. Clin. Invest.* **117**: 3900–3908.
102. Klucken, J., C. Büchler, E. Orsó, W. E. Kaminski, M. Porsch-Ozcürümez, G. Liebisch, M. Kapinsky, W. Diederich, W. Drobnik, M. Dean, R. Allikmets, and G. Schmitz. 2000. ABCG1 (ABC8), the human homolog of the *Drosophila* white gene, is a regulator of macrophage cholesterol and phospholipid transport. *Proc. Natl. Acad. Sci. U.S.A.* **97**:

817–822.

103. Kennedy, M. A., G. C. Barrera, K. Nakamura, A. Baldán, P. Tarr, M. C. Fishbein, J. Frank, O. L. Francone, and P. A. Edwards. 2005. ABCG1 has a critical role in mediating cholesterol efflux to HDL and preventing cellular lipid accumulation. *Cell Metab.* **1**: 121–131.
104. Tarling, E. J., and P. A. Edwards. 2012. Dancing with the sterols: Critical roles for ABCG1, ABCA1, miRNAs, and nuclear and cell surface receptors in controlling cellular sterol homeostasis. *Biochim. Biophys. Acta.* **1821**: 386–395.
105. Sankaranarayanan, S., J. F. Oram, B. F. Asztalos, A. M. Vaughan, S. Lund-Katz, M. P. Adorni, M. C. Phillips, and G. H. Rothblat. 2009. Effects of acceptor composition and mechanism of ABCG1-mediated cellular free cholesterol efflux. *J. Lipid Res.* **50**: 275–284.
106. Tarling, E. J., and P. A. Edwards. 2011. ATP binding cassette transporter G1 (ABCG1) is an intracellular sterol transporter. *Proc. Natl. Acad. Sci. U.S.A.* **108**: 19719–19724.
107. Adorni, M. P., F. Zimetti, J. T. Billheimer, N. Wang, D. J. Rader, M. C. Phillips, and G. H. Rothblat. 2007. The roles of different pathways in the release of cholesterol from macrophages. *J. Lipid Res.* **48**: 2453–2462.
108. Ji, Y., B. Jian, N. Wang, Y. Sun, M. L. Moya, M. C. Phillips, G. H. Rothblat, J. B. Swaney, and A. R. Tall. 1997. Scavenger receptor BI promotes high density lipoprotein-mediated cellular cholesterol efflux. *J. Biol. Chem.* **272**: 20982–20985.
109. Jian, B., M. de la Llera-Moya, Y. Ji, N. Wang, M. C. Phillips, J. B. Swaney, A. R. Tall, and G. H. Rothblat. 1998. Scavenger receptor class B type I as a mediator of cellular cholesterol efflux to lipoproteins and phospholipid acceptors. *J. Biol. Chem.* **273**: 5599–5606.
110. la Llera-Moya, de, M., M. A. Connelly, D. Drazul, S. M. Klein, E. Favari, P. G. Yancey, D. L. Williams, and G. H. Rothblat. 2001. Scavenger receptor class B type I affects cholesterol homeostasis by magnifying cholesterol flux between cells and HDL. *J. Lipid Res.* **42**: 1969–1978.
111. Zimetti, F., G. K. Weibel, M. Duong, and G. H. Rothblat. 2006. Measurement of cholesterol bidirectional flux between cells and lipoproteins. *J. Lipid Res.* **47**: 605–613.
112. Haberland, M. E., and J. A. Reynolds. 1973. Self-association of cholesterol in aqueous solution. *Proc. Natl. Acad. Sci. U.S.A.* **70**: 2313–2316.
113. Phillips, M. C., W. J. Johnson, and G. H. Rothblat. 1987. Mechanisms and

- consequences of cellular cholesterol exchange and transfer. *Biochim. Biophys. Acta.* **906**: 223–276.
114. Jonas, A. 2000. Lecithin cholesterol acyltransferase. *Biochim. Biophys. Acta.* **1529**: 245–256.
115. Fielding, C. J., and P. E. Fielding. 1971. Purification and substrate specificity of lecithin-cholesterol acyl transferase from human plasma. *FEBS Lett.* **15**: 355–358.
116. Barter, P. J., M. Caulfield, M. Eriksson, S. M. Grundy, J. J. P. Kastelein, M. Komajda, J. Lopez-Sendon, L. Mosca, J.-C. Tardif, D. D. Waters, C. L. Shear, J. H. Revkin, K. A. Buhr, M. R. Fisher, A. R. Tall, B. Brewer, and ILLUMINATE Investigators. 2007. Effects of torcetrapib in patients at high risk for coronary events. *N. Engl. J. Med.* **357**: 2109–2122.
117. Nissen, S. E., J.-C. Tardif, S. J. Nicholls, J. H. Revkin, C. L. Shear, W. T. Duggan, W. Ruzyllo, W. B. Bachinsky, G. P. Lasala, G. P. Lasala, E. M. Tuzcu, and ILLUSTRATE Investigators. 2007. Effect of torcetrapib on the progression of coronary atherosclerosis. *N. Engl. J. Med.* **356**: 1304–1316.
118. Rader, D. J. 2007. Illuminating HDL—is it still a viable therapeutic target? *N. Engl. J. Med.* **357**: 2180–2183.
119. Rader, D. J. 2007. Mechanisms of disease: HDL metabolism as a target for novel therapies. *Nat. Clin. Pract. Cardiovasc. Med.* **4**: 102–109.
120. Lewis, G. F., and D. J. Rader. 2005. New insights into the regulation of HDL metabolism and reverse cholesterol transport. *Circ. Res.* **96**: 1221–1232.
121. Albers, J. J., S. Vuletic, and M. C. Cheung. 2012. Role of plasma phospholipid transfer protein in lipid and lipoprotein metabolism. *Biochim. Biophys. Acta.* **1821**: 345–357.
122. Lusa, S., M. Jauhiainen, J. Metso, P. Somerharju, and C. Ehnholm. 1996. The mechanism of human plasma phospholipid transfer protein-induced enlargement of high-density lipoprotein particles: evidence for particle fusion. *Biochem. J.* **313** (Pt 1): 275–282.
123. Settasatian, N., M. Duong, L. K. Curtiss, C. Ehnholm, M. Jauhiainen, J. Huuskonen, and K. A. Rye. 2001. The mechanism of the remodeling of high density lipoproteins by phospholipid transfer protein. *J. Biol. Chem.* **276**: 26898–26905.
124. Wolfbauer, G., J. J. Albers, and J. F. Oram. 1999. Phospholipid transfer protein enhances removal of cellular cholesterol and phospholipids by high-density lipoprotein apolipoproteins. *Biochim. Biophys. Acta.* **1439**: 65–76.
125. Oram, J. F., G. Wolfbauer, A. M. Vaughan, C. Tang, and J. J. Albers. 2003.

- Phospholipid transfer protein interacts with and stabilizes ATP-binding cassette transporter A1 and enhances cholesterol efflux from cells. *J. Biol. Chem.* **278**: 52379–52385.
126. Badellino, K. O., M. L. Wolfe, M. P. Reilly, and D. J. Rader. 2006. Endothelial lipase concentrations are increased in metabolic syndrome and associated with coronary atherosclerosis. *PLoS Med.* **3**: e22.
127. Badellino, K. O., M. L. Wolfe, M. P. Reilly, and D. J. Rader. 2008. Endothelial lipase is increased in vivo by inflammation in humans. *Circulation.* **117**: 678–685.
128. Qiu, G., and J. S. Hill. 2009. Endothelial lipase promotes apolipoprotein AI-mediated cholesterol efflux in THP-1 macrophages. *Arterioscler. Thromb. Vasc. Biol.* **29**: 84–91.
129. Santamarina-Fojo, S., H. González-Navarro, L. Freeman, E. Wagner, and Z. Nong. 2004. Hepatic lipase, lipoprotein metabolism, and atherogenesis. *Arterioscler. Thromb. Vasc. Biol.* **24**: 1750–1754.
130. Connelly, P. W., and R. A. Hegele. 1998. Hepatic lipase deficiency. *Crit. Rev. Clin. Lab. Sci.* **35**: 547–572.
131. Brunzell, J. D., and S. S. Deeb. *In Scriver's Online Metabolic and Molecular Bases of Inherited Disease* (Valle, D., Beaudet, A. L., Vogelstein, B., Kinzler, K. W., Antonarakis, S. E., and Ballabio, A., eds.). pp. 1–60., McGraw-Hill.
132. Jeon, H., and S. C. Blacklow. 2005. Structure and physiologic function of the low-density lipoprotein receptor. *Annu. Rev. Biochem.* **74**: 535–562.
133. Goldstein, J. L., and M. S. Brown. 2009. The LDL receptor. *Arterioscler. Thromb. Vasc. Biol.* **29**: 431–438.
134. Davis, C. G., J. L. Goldstein, T. C. Südhof, R. G. Anderson, D. W. Russell, and M. S. Brown. 1987. Acid-dependent ligand dissociation and recycling of LDL receptor mediated by growth factor homology region. *Nature.* **326**: 760–765.
135. Brown, M. S., R. G. Anderson, and J. L. Goldstein. 1983. Recycling receptors: the round-trip itinerary of migrant membrane proteins. *Cell.* **32**: 663–667.
136. Luzio, J. P., P. R. Pryor, and N. A. Bright. 2007. Lysosomes: fusion and function. *Nat. Rev. Mol. Cell Biol.* **8**: 622–632.
137. Infante, R. E., M. L. Wang, A. Radhakrishnan, H. J. Kwon, M. S. Brown, and J. L. Goldstein. 2008. NPC2 facilitates bidirectional transfer of cholesterol between NPC1 and lipid bilayers, a step in cholesterol egress from lysosomes. *Proc. Natl. Acad. Sci. U.S.A.* **105**: 15287–15292.

138. Kwon, H. J., L. Abi-Mosleh, M. L. Wang, J. Deisenhofer, J. L. Goldstein, M. S. Brown, and R. E. Infante. 2009. Structure of N-terminal domain of NPC1 reveals distinct subdomains for binding and transfer of cholesterol. *Cell*. **137**: 1213–1224.
139. Ikonen, E. 2008. Cellular cholesterol trafficking and compartmentalization. *Nat. Rev. Mol. Cell Biol.* **9**: 125–138.
140. Rigotti, A., B. L. Trigatti, M. Penman, H. Rayburn, J. Herz, and M. Krieger. 1997. A targeted mutation in the murine gene encoding the high density lipoprotein (HDL) receptor scavenger receptor class B type I reveals its key role in HDL metabolism. *Proc. Natl. Acad. Sci. U.S.A.* **94**: 12610–12615.
141. Varban, M. L., F. Rinninger, N. Wang, V. Fairchild-Huntress, J. H. Dunmore, Q. Fang, M. L. Gosselin, K. L. Dixon, J. D. Deeds, S. L. Acton, A. R. Tall, and D. Huszar. 1998. Targeted mutation reveals a central role for SR-BI in hepatic selective uptake of high density lipoprotein cholesterol. *Proc. Natl. Acad. Sci. U.S.A.* **95**: 4619–4624.
142. Wang, N., T. Arai, Y. Ji, F. Rinninger, and A. R. Tall. 1998. Liver-specific overexpression of scavenger receptor BI decreases levels of very low density lipoprotein ApoB, low density lipoprotein ApoB, and high density lipoprotein in transgenic mice. *J. Biol. Chem.* **273**: 32920–32926.
143. Zhang, Y., J. R. Da Silva, M. Reilly, J. T. Billheimer, G. H. Rothblat, and D. J. Rader. 2005. Hepatic expression of scavenger receptor class B type I (SR-BI) is a positive regulator of macrophage reverse cholesterol transport in vivo. *J. Clin. Invest.* **115**: 2870–2874.
144. Schwartz, C. C., L. G. Halloran, Z. R. Vlahcevic, D. H. Gregory, and L. Swell. 1978. Preferential utilization of free cholesterol from high-density lipoproteins for biliary cholesterol secretion in man. *Science*. **200**: 62–64.
145. Bloch, K. 1992. Sterol molecule: structure, biosynthesis, and function. *Steroids*. **57**: 378–383.
146. Bloch, K. 1965. The biological synthesis of cholesterol. *Science*. **150**: 19–28.
147. Goldstein, J. L., and M. S. Brown. 1990. Regulation of the mevalonate pathway. *Nature*. **343**: 425–430.
148. Yu, L., J. Li-Hawkins, R. E. Hammer, K. E. Berge, J. D. Horton, J. C. Cohen, and H. H. Hobbs. 2002. Overexpression of ABCG5 and ABCG8 promotes biliary cholesterol secretion and reduces fractional absorption of dietary cholesterol. *J. Clin. Invest.* **110**: 671–680.
149. Yu, L., S. Gupta, F. Xu, A. D. B. Liverman, A. Moschetta, D. J. Mangelsdorf, J. J. Repa, H. H. Hobbs, and J. C. Cohen. 2005. Expression of ABCG5 and ABCG8 is required for

- regulation of biliary cholesterol secretion. *J. Biol. Chem.* **280**: 8742–8747.
150. Wang, H. H., S. B. Patel, M. C. Carey, and D. Q.-H. Wang. 2007. Quantifying anomalous intestinal sterol uptake, lymphatic transport, and biliary secretion in *Abcg8(-/-)* mice. *Hepatology*. **45**: 998–1006.
151. Berge, K. E., K. Von Bergmann, D. Lutjohann, R. Guerra, S. M. Grundy, H. H. Hobbs, and J. C. Cohen. 2002. Heritability of plasma noncholesterol sterols and relationship to DNA sequence polymorphism in *ABCG5* and *ABCG8*. *J. Lipid Res.* **43**: 486–494.
152. Altmann, S. W., H. R. Davis, L.-J. Zhu, X. Yao, L. M. Hoos, G. Tetzloff, S. P. N. Iyer, M. Maguire, A. Golovko, M. Zeng, L. Wang, N. Murgolo, and M. P. Graziano. 2004. Niemann-Pick C1 Like 1 protein is critical for intestinal cholesterol absorption. *Science*. **303**: 1201–1204.
153. Davis, H. R., L.-J. Zhu, L. M. Hoos, G. Tetzloff, M. Maguire, J. Liu, X. Yao, S. P. N. Iyer, M.-H. Lam, E. G. Lund, P. A. Detmers, M. P. Graziano, and S. W. Altmann. 2004. Niemann-Pick C1 Like 1 (*NPC1L1*) is the intestinal phytosterol and cholesterol transporter and a key modulator of whole-body cholesterol homeostasis. *J. Biol. Chem.* **279**: 33586–33592.
154. Ge, L., J. Wang, W. Qi, H.-H. Miao, J. Cao, Y.-X. Qu, B.-L. Li, and B.-L. Song. 2008. The cholesterol absorption inhibitor ezetimibe acts by blocking the sterol-induced internalization of *NPC1L1*. *Cell Metab.* **7**: 508–519.
155. Garcia-Calvo, M., J. Lisnock, H. G. Bull, B. E. Hawes, D. A. Burnett, M. P. Braun, J. H. Crona, H. R. Davis, D. C. Dean, P. A. Detmers, M. P. Graziano, M. Hughes, D. E. Macintyre, A. Ogawa, K. A. O'Neill, S. P. N. Iyer, D. E. Shevell, M. M. Smith, Y. S. Tang, A. M. Makarewicz, F. Ujjainwalla, S. W. Altmann, K. T. Chapman, and N. A. Thornberry. 2005. The target of ezetimibe is Niemann-Pick C1-Like 1 (*NPC1L1*). *Proc. Natl. Acad. Sci. U.S.A.* **102**: 8132–8137.
156. Repa, J. J., K. K. Buhman, R. V. Farese, J. M. Dietschy, and S. D. Turley. 2004. *ACAT2* deficiency limits cholesterol absorption in the cholesterol-fed mouse: impact on hepatic cholesterol homeostasis. *Hepatology*. **40**: 1088–1097.
157. Buhman, K. K., M. Accad, S. Novak, R. S. Choi, J. S. Wong, R. L. Hamilton, S. Turley, and R. V. Farese. 2000. Resistance to diet-induced hypercholesterolemia and gallstone formation in *ACAT2*-deficient mice. *Nat. Med.* **6**: 1341–1347.
158. Yen, C., M. Cheong, C. Grueter, P. Zhou, J. Moriwaki, J. Wong, B. Hubbard, S. Marmor, and R. Farese. 2009. Deficiency of the intestinal enzyme acyl CoA:monoacylglycerol acyltransferase-2 protects mice from metabolic disorders induced by high-fat feeding. *Nat. Med.*
159. Wetterau, J. R., L. P. Aggerbeck, M. E. Bouma, C. Eisenberg, A. Munck, M. Hermier,

- J. Schmitz, G. Gay, D. J. Rader, and R. E. Gregg. 1992. Absence of microsomal triglyceride transfer protein in individuals with abetalipoproteinemia. *Science*. **258**: 999–1001.
160. Jamil, H., J. K. Dickson, C. H. Chu, M. W. Lago, J. K. Rinehart, S. A. Biller, R. E. Gregg, and J. R. Wetterau. 1995. Microsomal triglyceride transfer protein. Specificity of lipid binding and transport. *J. Biol. Chem.* **270**: 6549–6554.
161. Hussain, M. M., J. Shi, and P. Dreizen. 2003. Microsomal triglyceride transfer protein and its role in apoB-lipoprotein assembly. *J. Lipid Res.* **44**: 22–32.
162. Guo, Q., R. K. Avramoglu, and K. Adeli. 2005. Intestinal assembly and secretion of highly dense/lipid-poor apolipoprotein B48-containing lipoprotein particles in the fasting state: evidence for induction by insulin resistance and exogenous fatty acids. *Metab. Clin. Exp.* **54**: 689–697.
163. Magun, A. M., B. Mish, and R. M. Glickman. 1988. Intracellular apoA-I and apoB distribution in rat intestine is altered by lipid feeding. *J. Lipid Res.* **29**: 1107–1116.
164. Ginsberg, H. N., and E. A. Fisher. 2009. The ever-expanding role of degradation in the regulation of apolipoprotein B metabolism. *J. Lipid Res.* **50**: S162–S166.
165. Fisher, E. A., N. A. Khanna, and R. S. McLeod. 2011. Ubiquitination regulates the assembly of VLDL in HepG2 cells and is the committing step of the apoB-100 ERAD pathway. *J. Lipid Res.* **52**: 1170–1180.
166. Pan, M., V. Maitin, S. Parathath, U. Andreo, S. X. Lin, C. St Germain, Z. Yao, F. R. Maxfield, K. J. Williams, and E. A. Fisher. 2008. Presecretory oxidation, aggregation, and autophagic destruction of apoprotein-B: a pathway for late-stage quality control. *Proc. Natl. Acad. Sci. U.S.A.* **105**: 5862–5867.
167. Fisher, E. A. 2012. The degradation of apolipoprotein B100: Multiple opportunities to regulate VLDL triglyceride production by different proteolytic pathways. *Biochim. Biophys. Acta.*
168. Neeli, I., S. A. Siddiqi, S. Siddiqi, J. Mahan, W. S. Lagakos, B. Binas, T. Gheyi, J. Storch, and C. M. Mansbach. 2007. Liver fatty acid-binding protein initiates budding of pre-chylomicron transport vesicles from intestinal endoplasmic reticulum. *J. Biol. Chem.* **282**: 17974–17984.
169. Cartwright, I. J., D. Plonné, and J. A. Higgins. 2000. Intracellular events in the assembly of chylomicrons in rabbit enterocytes. *J. Lipid Res.* **41**: 1728–1739.
170. Cartwright, I. J., and J. A. Higgins. 2001. Direct evidence for a two-step assembly of ApoB48-containing lipoproteins in the lumen of the smooth endoplasmic reticulum of rabbit enterocytes. *J. Biol. Chem.* **276**: 48048–48057.

171. Iqbal, J., and M. M. Hussain. 2005. Evidence for multiple complementary pathways for efficient cholesterol absorption in mice. *J. Lipid Res.* **46**: 1491–1501.
172. Dassa, E., and P. Bouige. 2001. The ABC of ABCs: a phylogenetic and functional classification of ABC systems in living organisms. *Res. Microbiol.* **152**: 211–229.
173. Dean, M., A. Rzhetsky, and R. Allikmets. 2001. The human ATP-binding cassette (ABC) transporter superfamily. *Genome Res.* **11**: 1156–1166.
174. Eckford, P. D. W., and F. J. Sharom. 2009. ABC efflux pump-based resistance to chemotherapy drugs. *Chem. Rev.* **109**: 2989–3011.
175. Dean, M. 2002. The Human ATP-Binding Cassette (ABC) Transporter Superfamily. National Center for Biotechnology Information (US), Baltimore, MD. [online] <http://www.ncbi.nlm.nih.gov/books/NBK3/>.
176. Aller, S. G., J. Yu, A. Ward, Y. Weng, S. Chittaboina, R. Zhuo, P. M. Harrell, Y. T. Trinh, Q. Zhang, I. L. Urbatsch, and G. Chang. 2009. Structure of P-glycoprotein reveals a molecular basis for poly-specific drug binding. *Science.* **323**: 1718–1722.
177. Juliano, R. L., and V. Ling. 1976. A surface glycoprotein modulating drug permeability in Chinese hamster ovary cell mutants. *Biochim. Biophys. Acta.* **455**: 152–162.
178. Beck, W. T., T. J. Mueller, and L. R. Tanzer. 1979. Altered surface membrane glycoproteins in Vinca alkaloid-resistant human leukemic lymphoblasts. *Cancer Res.* **39**: 2070–2076.
179. Gros, P., J. Croop, and D. Housman. 1986. Mammalian multidrug resistance gene: complete cDNA sequence indicates strong homology to bacterial transport proteins. *Cell.* **47**: 371–380.
180. Chen, C. J., J. E. Chin, K. Ueda, D. P. Clark, I. Pastan, M. M. Gottesman, and I. B. Roninson. 1986. Internal duplication and homology with bacterial transport proteins in the *mdr1* (P-glycoprotein) gene from multidrug-resistant human cells. *Cell.* **47**: 381–389.
181. Thiebaut, F., T. Tsuruo, H. Hamada, M. M. Gottesman, I. Pastan, and M. C. Willingham. 1987. Cellular localization of the multidrug-resistance gene product P-glycoprotein in normal human tissues. *Proc. Natl. Acad. Sci. U.S.A.* **84**: 7735–7738.
182. Sugawara, I., I. Kataoka, Y. Morishita, H. Hamada, T. Tsuruo, S. Itoyama, and S. Mori. 1988. Tissue distribution of P-glycoprotein encoded by a multidrug-resistant gene as revealed by a monoclonal antibody, MRK 16. *Cancer Res.* **48**: 1926–1929.
183. Cordon-Cardo, C., J. P. O'Brien, D. Casals, L. Rittman-Grauer, J. L. Biedler, M. R. Melamed, and J. R. Bertino. 1989. Multidrug-resistance gene (P-glycoprotein) is

- expressed by endothelial cells at blood-brain barrier sites. *Proc. Natl. Acad. Sci. U.S.A.* **86**: 695–698.
184. Schinkel, A. H., U. Mayer, E. Wagenaar, C. A. A. M. Mol, L. van Deemter, J. J. M. Smit, M. van der Valk, A. C. Voordouw, H. Spits, O. van Tellingen, J. M. J. M. Zijlmans, W. E. Fibbe, and P. Borst. 1997. Normal viability and altered pharmacokinetics in mice lacking *mdr1*-type (drug-transporting) P-glycoproteins. *Proc. Natl. Acad. Sci. U.S.A.* **94**: 4028–4033.
185. Penzotti, J. E., M. L. Lamb, E. Evensen, and P. D. J. Grootenhuis. 2002. A computational ensemble pharmacophore model for identifying substrates of P-glycoprotein. *J. Med. Chem.* **45**: 1737–1740.
186. Melchior, D. L., F. J. Sharom, R. Evers, G. E. Wright, J. W. K. Chu, S. E. Wright, X. Chu, and J. Yabut. 2012. Determining P-glycoprotein-drug interactions: evaluation of reconstituted P-glycoprotein in a liposomal system and LLC-MDR1 polarized cell monolayers. *J. Pharmacol. Toxicol. Methods.* **65**: 64–74.
187. Sharom, F. J. 2008. ABC multidrug transporters: structure, function and role in chemoresistance. *Pharmacogenomics.* **9**: 105–127.
188. Shapiro, A. B., K. Fox, P. Lam, and V. Ling. 1999. Stimulation of P-glycoprotein-mediated drug transport by prazosin and progesterone. Evidence for a third drug-binding site. *Eur. J. Biochem.* **259**: 841–850.
189. Dawson, R. J. P., and K. P. Locher. 2006. Structure of a bacterial multidrug ABC transporter. *Nature.* **443**: 180–185.
190. Ward, A., C. L. Reyes, J. Yu, C. B. Roth, and G. Chang. 2007. Flexibility in the ABC transporter MsbA: Alternating access with a twist. *Proc. Natl. Acad. Sci. U.S.A.* **104**: 19005–19010.
191. Sharom, F. J. 2006. pp. 979–992.
192. Szakács, G., J. K. Paterson, J. A. Ludwig, C. Booth-Genthe, and M. M. Gottesman. 2006. Targeting multidrug resistance in cancer. *Nat. Rev. Drug. Discov.* **5**: 219–234.
193. Szakács, G., J.-P. Annereau, S. Lababidi, U. Shankavaram, A. Arciello, K. J. Bussey, W. Reinhold, Y. Guo, G. D. Kruh, M. Reimers, J. N. Weinstein, and M. M. Gottesman. 2004. Predicting drug sensitivity and resistance: profiling ABC transporter genes in cancer cells. *Cancer Cell.* **6**: 129–137.
194. Niwa, R., and F. J. Slack. 2007. RNAi experimental controls. *ETBR.* 34–36. [online] <http://www.cell.com/cellpress/ETBR#>.
195. Zelcer, N., and P. Tontonoz. 2006. Liver X receptors as integrators of metabolic and inflammatory signaling. *J. Clin. Invest.* **116**: 607–614.

196. Van der Blik, A. M., F. Baas, T. Ten Houte de Lange, P. M. Kooiman, T. Van der Velde-Koerts, and P. Borst. 1987. The human *mdr3* gene encodes a novel P-glycoprotein homologue and gives rise to alternatively spliced mRNAs in liver. *EMBO J.* **6**: 3325–3331.
197. Smit, J. J., A. H. Schinkel, R. P. Oude Elferink, A. K. Groen, E. Wagenaar, L. van Deemter, C. A. Mol, R. Ottenhoff, N. M. van der Lugt, and M. A. van Roon. 1993. Homozygous disruption of the murine *mdr2* P-glycoprotein gene leads to a complete absence of phospholipid from bile and to liver disease. *Cell.* **75**: 451–462.
198. Smith, A. J., J. L. Timmermans-Hereijgers, B. Roelofsen, K. W. Wirtz, W. J. van Blitterswijk, J. J. Smit, A. H. Schinkel, and P. Borst. 1994. The human MDR3 P-glycoprotein promotes translocation of phosphatidylcholine through the plasma membrane of fibroblasts from transgenic mice. *FEBS Lett.* **354**: 263–266.
199. van Helvoort, A., A. J. Smith, H. Sprong, I. Fritzsche, A. H. Schinkel, P. Borst, and G. van Meer. 1996. MDR1 P-glycoprotein is a lipid translocase of broad specificity, while MDR3 P-glycoprotein specifically translocates phosphatidylcholine. *Cell.* **87**: 507–517.
200. de Vree, J. M., E. Jacquemin, E. Sturm, D. Cresteil, P. J. Bosma, J. Aten, J. F. Deleuze, M. Desrochers, M. Burdelski, O. Bernard, R. P. Oude Elferink, and M. Hadchouel. 1998. Mutations in the MDR3 gene cause progressive familial intrahepatic cholestasis. *Proc. Natl. Acad. Sci. U.S.A.* **95**: 282–287.
201. Wasmuth, H. E., A. Glantz, H. Keppeler, E. Simon, C. Bartz, W. Rath, L.-A. Mattsson, H.-U. Marschall, and F. Lammert. 2007. Intrahepatic cholestasis of pregnancy: the severe form is associated with common variants of the hepatobiliary phospholipid transporter ABCB4 gene. *Gut.* **56**: 265–270.
202. Rosmorduc, O., B. Hermelin, P.-Y. Boelle, R. Parc, J. Taboury, and R. Poupon. 2003. ABCB4 gene mutation-associated cholelithiasis in adults. *Gastroenterology.* **125**: 452–459.
203. Childs, S., R. L. Yeh, E. Georges, and V. Ling. 1995. Identification of a sister gene to P-glycoprotein. *Cancer Res.* **55**: 2029–2034.
204. Strautnieks, S. S., L. N. Bull, A. S. Knisely, S. A. Kocoshis, N. Dahl, H. Arnell, E. Sokal, K. Dahan, S. Childs, V. Ling, M. S. Tanner, A. F. Kagalwalla, A. Németh, J. Pawlowska, A. Baker, G. Mieli-Vergani, N. B. Freimer, R. M. Gardiner, and R. J. Thompson. 1998. A gene encoding a liver-specific ABC transporter is mutated in progressive familial intrahepatic cholestasis. *Nat. Genet.* **20**: 233–238.
205. Hofmann, A. F. 2007. Biliary secretion and excretion in health and disease: current concepts. *Ann. Hepatol.* **6**: 15–27.

206. Strautnieks, S. S., J. A. Byrne, L. Pawlikowska, D. Cebecauerová, A. Rayner, L. Dutton, Y. Meier, A. Antoniou, B. Stieger, H. Arnell, F. Ozçay, H. F. Al-Hussaini, A. F. Bassas, H. J. Verkade, B. Fischler, A. Németh, R. Kotalová, B. L. Shneider, J. Cielecka-Kuszyk, P. McClean, P. F. Whittington, E. Sokal, M. Jirsa, S. H. Wali, I. Jankowska, J. Pawłowska, G. Mieli-Vergani, A. S. Knisely, L. N. Bull, and R. J. Thompson. 2008. Severe bile salt export pump deficiency: 82 different ABCB11 mutations in 109 families. *Gastroenterology*. **134**: 1203–1214.
207. Wang, R., P. Lam, L. Liu, D. Forrest, I. M. Yousef, D. Mignault, M. J. Phillips, and V. Ling. 2003. Severe cholestasis induced by cholic acid feeding in knockout mice of sister of P-glycoprotein. *Hepatology*. **38**: 1489–1499.
208. Byrne, J. A., S. S. Strautnieks, G. Mieli-Vergani, C. F. Higgins, K. J. Linton, and R. J. Thompson. 2002. The human bile salt export pump: characterization of substrate specificity and identification of inhibitors. *Gastroenterology*. **123**: 1649–1658.
209. Gerloff, T., B. Stieger, B. Hagenbuch, J. Madon, L. Landmann, J. Roth, A. F. Hofmann, and P. J. Meier. 1998. The sister of P-glycoprotein represents the canalicular bile salt export pump of mammalian liver. *J. Biol. Chem.* **273**: 10046–10050.
210. Green, R. M., F. Hoda, and K. L. Ward. 2000. Molecular cloning and characterization of the murine bile salt export pump. *Gene*. **241**: 117–123.
211. Noe, J., B. Hagenbuch, P. J. Meier, and M. V. St-Pierre. 2001. Characterization of the mouse bile salt export pump overexpressed in the baculovirus system. *Hepatology*. **33**: 1223–1231.
212. Heuman, D. M. 1989. Quantitative estimation of the hydrophilic-hydrophobic balance of mixed bile salt solutions. *J. Lipid Res.* **30**: 719–730.
213. Eckford, P. D. W., and F. J. Sharom. 2008. Interaction of the P-glycoprotein multidrug efflux pump with cholesterol: effects on ATPase activity, drug binding and transport. *Biochemistry*. **47**: 13686–13698.
214. Orlowski, S., S. Martin, and A. Escargueil. 2006. P-glycoprotein and “lipid rafts”: some ambiguous mutual relationships (floating on them, building them or meeting them by chance?). *Cell. Mol. Life Sci.* **63**: 1038–1059.
215. Kimura, Y., N. Kioka, H. Kato, M. Matsuo, and K. Ueda. 2007. Modulation of drug-stimulated ATPase activity of human MDR1/P-glycoprotein by cholesterol. *Biochem. J.* **401**: 597–605.
216. Garrigues, A., A. E. Escargueil, and S. Orlowski. 2002. The multidrug transporter, P-glycoprotein, actively mediates cholesterol redistribution in the cell membrane. *Proc. Natl. Acad. Sci. U.S.A.* **99**: 10347–10352.

217. Wang, E., C. N. Casciano, R. P. Clement, and W. W. Johnson. 2000. Cholesterol interaction with the daunorubicin binding site of P-glycoprotein. *Biochem. Biophys. Res. Commun.* **276**: 909–916.
218. Troost, J., H. Lindenmaier, W. E. Haefeli, and J. Weiss. 2004. Modulation of cellular cholesterol alters P-glycoprotein activity in multidrug-resistant cells. *Mol. Pharmacol.* **66**: 1332–1339.
219. Radeva, G., J. Perabo, and F. J. Sharom. 2005. P-Glycoprotein is localized in intermediate-density membrane microdomains distinct from classical lipid rafts and caveolar domains. *FEBS J.* **272**: 4924–4937.
220. Metherall, J. E., K. Waugh, and H. Li. 1996. Progesterone inhibits cholesterol biosynthesis in cultured cells. Accumulation of cholesterol precursors. *J. Biol. Chem.* **271**: 2627–2633.
221. Metherall, J. E., H. Li, and K. Waugh. 1996. Role of multidrug resistance P-glycoproteins in cholesterol biosynthesis. *J. Biol. Chem.* **271**: 2634–2640.
222. Debry, P., E. A. Nash, D. W. Neklason, and J. E. Metherall. 1997. Role of multidrug resistance P-glycoproteins in cholesterol esterification. *J. Biol. Chem.* **272**: 1026–1031.
223. Field, F. J., E. Born, H. Chen, S. Murthy, and S. N. Mathur. 1995. Esterification of plasma membrane cholesterol and triacylglycerol-rich lipoprotein secretion in CaCo-2 cells: possible role of p-glycoprotein. *J. Lipid Res.* **36**: 1533–1543.
224. Field, F. J., E. Born, S. Murthy, and S. N. Mathur. 1998. Transport of cholesterol from the endoplasmic reticulum to the plasma membrane is constitutive in CaCo-2 cells and differs from the transport of plasma membrane cholesterol to the endoplasmic reticulum. *J. Lipid Res.* **39**: 333–343.
225. Luker, G. D., K. R. Nilsson, D. F. Covey, and D. Piwnica-Worms. 1999. Multidrug resistance (MDR1) P-glycoprotein enhances esterification of plasma membrane cholesterol. *J. Biol. Chem.* **274**: 6979–6991.
226. Tessner, T. G., and W. F. Stenson. 2000. Overexpression of MDR1 in an intestinal cell line results in increased cholesterol uptake from micelles. *Biochem. Biophys. Res. Commun.* **267**: 565–571.
227. Le Goff, W., M. Settle, D. J. Greene, R. E. Morton, and J. D. Smith. 2006. Reevaluation of the role of the multidrug-resistant P-glycoprotein in cellular cholesterol homeostasis. *J. Lipid Res.* **47**: 51–58.
228. Kavallaris, M., J. Madafiglio, M. D. Norris, and M. Haber. 1993. Resistance to tetracycline, a hydrophilic antibiotic, is mediated by P-glycoprotein in human

- multidrug-resistant cells. *Biochem. Biophys. Res. Commun.* **190**: 79–85.
229. Luker, G. D., J. L. Dahlheimer, R. E. Ostlund, and D. Piwnica-Worms. 2001. Decreased hepatic accumulation and enhanced esterification of cholesterol in mice deficient in mdr1a and mdr1b P-glycoproteins. *J. Lipid Res.* **42**: 1389–1394.
230. Thornton, S. J., E. Wong, S. D. Lee, and K. M. Wasan. 2008. Effect of dietary fat on hepatic liver X receptor expression in P-glycoprotein deficient mice: implications for cholesterol metabolism. *Lipids Health Dis.* **7**: 21.
231. Wagner, M., G. Zollner, and M. Trauner. 2009. New molecular insights into the mechanisms of cholestasis. *J. Hepatol.* **51**: 565–580.
232. Radhakrishnan, A., J. L. Goldstein, J. G. McDonald, and M. S. Brown. 2008. Switch-like control of SREBP-2 transport triggered by small changes in ER cholesterol: a delicate balance. *Cell Metab.* **8**: 512–521.
233. Goldstein, J. L., R. A. DeBose-Boyd, and M. S. Brown. 2006. Protein sensors for membrane sterols. *Cell.* **124**: 35–46.
234. Repa, J. J., S. D. Turley, J. A. Lobaccaro, J. Medina, L. Li, K. Lustig, B. Shan, R. A. Heyman, J. M. Dietschy, and D. J. Mangelsdorf. 2000. Regulation of absorption and ABC1-mediated efflux of cholesterol by RXR heterodimers. *Science.* **289**: 1524–1529.
235. Tontonoz, P. 2011. Transcriptional and Posttranscriptional Control of Cholesterol Homeostasis by Liver X Receptors. *Cold Spring Harb. Symp. Quant. Biol.*
236. Russell, D. W. 2000. Oxysterol biosynthetic enzymes. *Biochim. Biophys. Acta.* **1529**: 126–135.
237. Björkhem, I. 2002. Do oxysterols control cholesterol homeostasis? *J. Clin. Invest.* **110**: 725–730.
238. Björkhem, I., and U. Diczfalusy. 2002. Oxysterols: friends, foes, or just fellow passengers? *Arterioscler. Thromb. Vasc. Biol.* **22**: 734–742.
239. Gill, S., R. Chow, and A. J. Brown. 2008. Sterol regulators of cholesterol homeostasis and beyond: the oxysterol hypothesis revisited and revised. *Prog. Lipid Res.* **47**: 391–404.
240. Schroepfer, G. J. 2000. Oxysterols: modulators of cholesterol metabolism and other processes. *Physiol. Rev.* **80**: 361–554.
241. Nelson, J. A., S. R. Steckbeck, and T. A. Spencer. 1981. Biosynthesis of 24,25-epoxycholesterol from squalene 2,3;22,23-dioxide. *J. Biol. Chem.* **256**: 1067–1068.

242. Chawla, A., J. J. Repa, R. M. Evans, and D. J. Mangelsdorf. 2001. Nuclear receptors and lipid physiology: opening the X-files. *Science*. **294**: 1866–1870.
243. Peet, D. J., S. D. Turley, W. Ma, B. A. Janowski, J. M. Lobaccaro, R. E. Hammer, and D. J. Mangelsdorf. 1998. Cholesterol and bile acid metabolism are impaired in mice lacking the nuclear oxysterol receptor LXR alpha. *Cell*. **93**: 693–704.
244. Alberti, S., G. Schuster, P. Parini, D. Feltkamp, U. Diczfalusy, M. Rudling, B. Angelin, I. Björkhem, S. Pettersson, and J. A. Gustafsson. 2001. Hepatic cholesterol metabolism and resistance to dietary cholesterol in LXRbeta-deficient mice. *J. Clin. Invest.* **107**: 565–573.
245. Hong, C., M. N. Bradley, X. Rong, X. Wang, A. Wagner, V. Grijalva, L. W. Castellani, J. Salazar, S. Realegeno, R. Boyadjian, A. M. Fogelman, B. J. Van Lenten, S. T. Reddy, A. J. Lusis, R. K. Tangirala, and P. Tontonoz. 2012. LXRA is uniquely required for maximal reverse cholesterol transport and atheroprotection in ApoE-deficient mice. *J. Lipid Res.*
246. Bradley, M. N., C. Hong, M. Chen, S. B. Joseph, D. C. Wilpitz, X. Wang, A. J. Lusis, A. Collins, W. A. Hseuh, J. L. Collins, R. K. Tangirala, and P. Tontonoz. 2007. Ligand activation of LXR beta reverses atherosclerosis and cellular cholesterol overload in mice lacking LXR alpha and apoE. *J. Clin. Invest.* **117**: 2337–2346.
247. Janowski, B. A., P. J. Willy, T. R. Devi, J. R. Falck, and D. J. Mangelsdorf. 1996. An oxysterol signalling pathway mediated by the nuclear receptor LXR alpha. *Nature*. **383**: 728–731.
248. Lehmann, J. M., S. A. Kliewer, L. B. Moore, T. A. Smith-Oliver, B. B. Oliver, J. L. Su, S. S. Sundseth, D. A. Winegar, D. E. Blanchard, T. A. Spencer, and T. M. Willson. 1997. Activation of the nuclear receptor LXR by oxysterols defines a new hormone response pathway. *J. Biol. Chem.* **272**: 3137–3140.
249. Fu, X., J. G. Menke, Y. Chen, G. Zhou, K. L. MacNaul, S. D. Wright, C. P. Sparrow, and E. G. Lund. 2001. 27-hydroxycholesterol is an endogenous ligand for liver X receptor in cholesterol-loaded cells. *J. Biol. Chem.* **276**: 38378–38387.
250. Tontonoz, P., and D. J. Mangelsdorf. 2003. Liver X receptor signaling pathways in cardiovascular disease. *Mol. Endocrinol.* **17**: 985–993.
251. Glass, C. K., and M. G. Rosenfeld. 2000. The coregulator exchange in transcriptional functions of nuclear receptors. *Genes Dev.* **14**: 121–141.
252. Willy, P. J., K. Umesono, E. S. Ong, R. M. Evans, R. A. Heyman, and D. J. Mangelsdorf. 1995. LXR, a nuclear receptor that defines a distinct retinoid response pathway. *Genes Dev.* **9**: 1033–1045.

253. Bensinger, S. J., and P. Tontonoz. 2008. Integration of metabolism and inflammation by lipid-activated nuclear receptors. *Nature*. **454**: 470–477.
254. Calkin, A. C., and P. Tontonoz. 2012. Transcriptional integration of metabolism by the nuclear sterol-activated receptors LXR and FXR. *Nat. Rev. Mol. Cell Biol.* **13**: 213–224.
255. Kalaany, N. Y., and D. J. Mangelsdorf. 2006. LXRS and FXR: the yin and yang of cholesterol and fat metabolism. *Annu. Rev. Physiol.* **68**: 159–191.
256. Costet, P., Y. Luo, N. Wang, and A. R. Tall. 2000. Sterol-dependent transactivation of the ABC1 promoter by the liver X receptor/retinoid X receptor. *J. Biol. Chem.* **275**: 28240–28245.
257. Kennedy, M. A., A. Venkateswaran, P. T. Tarr, I. Xenarios, J. Kudoh, N. Shimizu, and P. A. Edwards. 2001. Characterization of the human ABCG1 gene: liver X receptor activates an internal promoter that produces a novel transcript encoding an alternative form of the protein. *J. Biol. Chem.* **276**: 39438–39447.
258. Repa, J. J., K. E. Berge, C. Pomajzl, J. A. Richardson, H. Hobbs, and D. J. Mangelsdorf. 2002. Regulation of ATP-binding cassette sterol transporters ABCG5 and ABCG8 by the liver X receptors alpha and beta. *J. Biol. Chem.* **277**: 18793–18800.
259. Hummasti, S., B. A. Laffitte, M. A. Watson, C. Galardi, L. C. Chao, L. Ramamurthy, J. T. Moore, and P. Tontonoz. 2004. Liver X receptors are regulators of adipocyte gene expression but not differentiation: identification of apoD as a direct target. *J. Lipid Res.* **45**: 616–625.
260. Laffitte, B. A., J. J. Repa, S. B. Joseph, D. C. Wilpitz, H. R. Kast, D. J. Mangelsdorf, and P. Tontonoz. 2001. LXRs control lipid-inducible expression of the apolipoprotein E gene in macrophages and adipocytes. *Proc. Natl. Acad. Sci. U.S.A.* **98**: 507–512.
261. Luo, Y., and A. R. Tall. 2000. Sterol upregulation of human CETP expression in vitro and in transgenic mice by an LXR element. *J. Clin. Invest.* **105**: 513–520.
262. Laffitte, B. A., S. B. Joseph, M. Chen, A. Castrillo, J. Repa, D. Wilpitz, D. Mangelsdorf, and P. Tontonoz. 2003. The phospholipid transfer protein gene is a liver X receptor target expressed by macrophages in atherosclerotic lesions. *Mol. Cell. Biol.* **23**: 2182–2191.
263. Malerød, L., L. K. Juvet, A. Hanssen-Bauer, W. Eskild, and T. Berg. 2002. Oxysterol-activated LXRA/RXR induces hSR-BI-promoter activity in hepatoma cells and preadipocytes. *Biochem. Biophys. Res. Commun.* **299**: 916–923.
264. Mak, P. A., B. A. Laffitte, C. Desrumaux, S. B. Joseph, L. K. Curtiss, D. J. Mangelsdorf,

- P. Tontonoz, and P. A. Edwards. 2002. Regulated expression of the apolipoprotein E/C-I/C-IV/C-II gene cluster in murine and human macrophages. A critical role for nuclear liver X receptors alpha and beta. *J. Biol. Chem.* **277**: 31900–31908.
265. Agellon, L. B., V. A. B. Drover, S. K. Cheema, G. F. Gbaguidi, and A. Walsh. 2002. Dietary cholesterol fails to stimulate the human cholesterol 7alpha-hydroxylase gene (CYP7A1) in transgenic mice. *J. Biol. Chem.* **277**: 20131–20134.
266. Zhang, Y., J. J. Repa, K. Gauthier, and D. J. Mangelsdorf. 2001. Regulation of lipoprotein lipase by the oxysterol receptors, LXRA and LXRbeta. *J. Biol. Chem.* **276**: 43018–43024.
267. Laffitte, B. A., S. B. Joseph, R. Walczak, L. Pei, D. C. Wilpitz, J. L. Collins, and P. Tontonoz. 2001. Autoregulation of the human liver X receptor alpha promoter. *Mol. Cell. Biol.* **21**: 7558–7568.
268. Zelcer, N., C. Hong, R. Boyadjian, and P. Tontonoz. 2009. LXR regulates cholesterol uptake through Idol-dependent ubiquitination of the LDL receptor. *Science*. **325**: 100–104.
269. Repa, J. J., G. Liang, J. Ou, Y. Bashmakov, J. M. Lobaccaro, I. Shimomura, B. Shan, M. S. Brown, J. L. Goldstein, and D. J. Mangelsdorf. 2000. Regulation of mouse sterol regulatory element-binding protein-1c gene (SREBP-1c) by oxysterol receptors, LXRA and LXRbeta. *Genes Dev.* **14**: 2819–2830.
270. Sun, Y., M. Hao, Y. Luo, C.-P. Liang, D. L. Silver, C. Cheng, F. R. Maxfield, and A. R. Tall. 2003. Stearoyl-CoA desaturase inhibits ATP-binding cassette transporter A1-mediated cholesterol efflux and modulates membrane domain structure. *J. Biol. Chem.* **278**: 5813–5820.
271. Joseph, S. B., B. A. Laffitte, P. H. Patel, M. A. Watson, K. E. Matsukuma, R. Walczak, J. L. Collins, T. F. Osborne, and P. Tontonoz. 2002. Direct and indirect mechanisms for regulation of fatty acid synthase gene expression by liver X receptors. *J. Biol. Chem.* **277**: 11019–11025.
272. Lichtenstein, L., and S. Kersten. 2010. Modulation of plasma TG lipolysis by Angiopoietin-like proteins and GPIHBP1. *Biochim. Biophys. Acta.* **1801**: 415–420.
273. Hua, X., A. Nohturfft, J. L. Goldstein, and M. S. Brown. 1996. Sterol resistance in CHO cells traced to point mutation in SREBP cleavage-activating protein. *Cell.* **87**: 415–426.
274. Zanetti, G., K. B. Pahuja, S. Studer, S. Shim, and R. Schekman. 2012. COPII and the regulation of protein sorting in mammals. *Nat. Cell Biol.* **14**: 20–28.
275. Sun, L.-P., L. Li, J. L. Goldstein, and M. S. Brown. 2005. Insig required for sterol-

- mediated inhibition of Scap/SREBP binding to COPII proteins in vitro. *J. Biol. Chem.* **280**: 26483–26490.
276. Sakai, J., E. A. Duncan, R. B. Rawson, X. Hua, M. S. Brown, and J. L. Goldstein. 1996. Sterol-regulated release of SREBP-2 from cell membranes requires two sequential cleavages, one within a transmembrane segment. *Cell.* **85**: 1037–1046.
277. Horton, J. D., J. L. Goldstein, and M. S. Brown. 2002. SREBPs: activators of the complete program of cholesterol and fatty acid synthesis in the liver. *J. Clin. Invest.* **109**: 1125–1131.
278. Radhakrishnan, A., L.-P. Sun, H. J. Kwon, M. S. Brown, and J. L. Goldstein. 2004. Direct binding of cholesterol to the purified membrane region of SCAP: mechanism for a sterol-sensing domain. *Mol. Cell.* **15**: 259–268.
279. Brown, A. J., L. Sun, J. D. Feramisco, M. S. Brown, and J. L. Goldstein. 2002. Cholesterol addition to ER membranes alters conformation of SCAP, the SREBP escort protein that regulates cholesterol metabolism. *Mol. Cell.* **10**: 237–245.
280. Adams, C. M., J. Reitz, J. K. De Brabander, J. D. Feramisco, L. Li, M. S. Brown, and J. L. Goldstein. 2004. Cholesterol and 25-hydroxycholesterol inhibit activation of SREBPs by different mechanisms, both involving SCAP and Insigs. *J. Biol. Chem.* **279**: 52772–52780.
281. Hua, X., C. Yokoyama, J. Wu, M. R. Briggs, M. S. Brown, J. L. Goldstein, and X. Wang. 1993. SREBP-2, a second basic-helix-loop-helix-leucine zipper protein that stimulates transcription by binding to a sterol regulatory element. *Proc. Natl. Acad. Sci. U.S.A.* **90**: 11603–11607.
282. Tréguier, M., C. Doucet, M. Moreau, C. Datchet, J. Thillet, M. J. Chapman, and T. Huby. 2004. Transcription factor sterol regulatory element binding protein 2 regulates scavenger receptor Cla-1 gene expression. *Arterioscler. Thromb. Vasc. Biol.* **24**: 2358–2364.
283. Alrefai, W. A., F. Annaba, Z. Sarwar, A. Dwivedi, S. Saksena, A. Singla, P. K. Dudeja, and R. K. Gill. 2007. Modulation of human Niemann-Pick C1-like 1 gene expression by sterol: Role of sterol regulatory element binding protein 2. *Am. J. Physiol. Gastrointest. Liver Physiol.* **292**: G369–76.
284. Rayner, K. J., Y. Suárez, A. Dávalos, S. Parathath, M. L. Fitzgerald, N. Tamehiro, E. A. Fisher, K. J. Moore, and C. Fernández-Hernando. 2010. MiR-33 contributes to the regulation of cholesterol homeostasis. *Science.* **328**: 1570–1573.
285. Scotti, E., C. Hong, Y. Yoshinaga, Y. Tu, Y. Hu, N. Zelcer, R. Boyadjian, P. J. de Jong, S. G. Young, L. G. Fong, and P. Tontonoz. 2011. Targeted disruption of the idol gene alters cellular regulation of the low-density lipoprotein receptor by sterols and liver

- x receptor agonists. *Mol. Cell. Biol.* **31**: 1885–1893.
286. Hong, C., S. Duit, P. Jalonen, R. Out, L. Scheer, V. Sorrentino, R. Boyadjian, K. W. Rodenburg, E. Foley, L. Korhonen, D. Lindholm, J. Nimpf, T. J. C. van Berkel, P. Tontonoz, and N. Zelcer. 2010. The E3 ubiquitin ligase IDOL induces the degradation of the low density lipoprotein receptor family members VLDLR and ApoER2. *J. Biol. Chem.* **285**: 19720–19726.
287. Zhang, L., L. Fairall, B. T. Goult, A. C. Calkin, C. Hong, C. J. Millard, P. Tontonoz, and J. W. R. Schwabe. 2011. The IDOL-UBE2D complex mediates sterol-dependent degradation of the LDL receptor. *Genes Dev.* **25**: 1262–1274.
288. Calkin, A. C., B. T. Goult, L. Zhang, L. Fairall, C. Hong, J. W. R. Schwabe, and P. Tontonoz. 2011. FERM-dependent E3 ligase recognition is a conserved mechanism for targeted degradation of lipoprotein receptors. *Proc. Natl. Acad. Sci. U.S.A.* **108**: 20107–20112.
289. Rayner, K. J., F. J. Sheedy, C. C. Esau, F. N. Hussain, R. E. Temel, S. Parathath, J. M. van Gils, A. J. Rayner, A. N. Chang, Y. Suárez, C. Fernández-Hernando, E. A. Fisher, and K. J. Moore. 2011. Antagonism of miR-33 in mice promotes reverse cholesterol transport and regression of atherosclerosis. *J. Clin. Invest.* **121**: 2921–2931.
290. Rayner, K. J., C. C. Esau, F. N. Hussain, A. L. McDaniel, S. M. Marshall, J. M. van Gils, T. D. Ray, F. J. Sheedy, L. Goedeke, X. Liu, O. G. Khatsenko, V. Kaimal, C. J. Lees, C. Fernández-Hernando, E. A. Fisher, R. E. Temel, and K. J. Moore. 2011. Inhibition of miR-33a/b in non-human primates raises plasma HDL and lowers VLDL triglycerides. *Nature.* **478**: 404–407.
291. Russell, D. W. 2003. The enzymes, regulation, and genetics of bile acid synthesis. *Annu. Rev. Biochem.* **72**: 137–174.
292. Hofmann, A. F., and D. M. Small. 1967. Detergent properties of bile salts: correlation with physiological function. *Annu. Rev. Med.* **18**: 333–376.
293. Wang, D. Q., B. Paigen, and M. C. Carey. 1997. Phenotypic characterization of Lith genes that determine susceptibility to cholesterol cholelithiasis in inbred mice: physical-chemistry of gallbladder bile. *J. Lipid Res.* **38**: 1395–1411.
294. Wang, D. Q., F. Lammert, D. E. Cohen, B. Paigen, and M. C. Carey. 1999. Cholic acid aids absorption, biliary secretion, and phase transitions of cholesterol in murine cholelithogenesis. *Am. J. Physiol.* **276**: G751–60.
295. Chiang, J. Y. L. 2009. Bile acids: regulation of synthesis. *J. Lipid Res.* **50**: 1955–1966.
296. Schwarz, M., D. W. Russell, J. M. Dietschy, and S. D. Turley. 1998. Marked reduction in bile acid synthesis in cholesterol 7 α -hydroxylase-deficient mice does not

- lead to diminished tissue cholesterol turnover or to hypercholesterolemia. *J. Lipid Res.* **39**: 1833–1843.
297. Ishibashi, S., M. Schwarz, P. K. Frykman, J. Herz, and D. W. Russell. 1996. Disruption of cholesterol 7 α -hydroxylase gene in mice. I. Postnatal lethality reversed by bile acid and vitamin supplementation. *J. Biol. Chem.* **271**: 18017–18023.
298. Schwarz, M., E. G. Lund, K. D. Setchell, H. J. Kayden, J. E. Zerwekh, I. Björkhem, J. Herz, and D. W. Russell. 1996. Disruption of cholesterol 7 α -hydroxylase gene in mice. II. Bile acid deficiency is overcome by induction of oxysterol 7 α -hydroxylase. *J. Biol. Chem.* **271**: 18024–18031.
299. Chiang, J. Y. L. 2004. Regulation of bile acid synthesis: pathways, nuclear receptors, and mechanisms. *J. Hepatol.* **40**: 539–551.
300. Makishima, M., A. Y. Okamoto, J. J. Repa, H. Tu, R. M. Learned, A. Luk, M. V. Hull, K. D. Lustig, D. J. Mangelsdorf, and B. Shan. 1999. Identification of a nuclear receptor for bile acids. *Science*. **284**: 1362–1365.
301. Parks, D. J., S. G. Blanchard, R. K. Bledsoe, G. Chandra, T. G. Consler, S. A. Kliewer, J. B. Stimmel, T. M. Willson, A. M. Zavacki, D. D. Moore, and J. M. Lehmann. 1999. Bile acids: natural ligands for an orphan nuclear receptor. *Science*. **284**: 1365–1368.
302. Lu, T. T., M. Makishima, J. J. Repa, K. Schoonjans, T. A. Kerr, J. Auwerx, and D. J. Mangelsdorf. 2000. Molecular basis for feedback regulation of bile acid synthesis by nuclear receptors. *Mol. Cell.* **6**: 507–515.
303. Goodwin, B., S. A. Jones, R. R. Price, M. A. Watson, D. D. McKee, L. B. Moore, C. Galardi, J. G. Wilson, M. C. Lewis, M. E. Roth, P. R. Maloney, T. M. Willson, and S. A. Kliewer. 2000. A regulatory cascade of the nuclear receptors FXR, SHP-1, and LXR-1 represses bile acid biosynthesis. *Mol. Cell.* **6**: 517–526.
304. Hayhurst, G. P., Y. H. Lee, G. Lambert, J. M. Ward, and F. J. Gonzalez. 2001. Hepatocyte nuclear factor 4 α (nuclear receptor 2A1) is essential for maintenance of hepatic gene expression and lipid homeostasis. *Mol. Cell. Biol.* **21**: 1393–1403.
305. Kerr, T. A., S. Saeki, M. Schneider, K. Schaefer, S. Berdy, T. Redder, B. Shan, D. W. Russell, and M. Schwarz. 2002. Loss of nuclear receptor SHP impairs but does not eliminate negative feedback regulation of bile acid synthesis. *Dev. Cell.* **2**: 713–720.
306. Holt, J. A., G. Luo, A. N. Billin, J. Bisi, Y. Y. McNeill, K. F. Kozarsky, M. Donahee, D. Y. Wang, T. A. Mansfield, S. A. Kliewer, B. Goodwin, and S. A. Jones. 2003. Definition of a novel growth factor-dependent signal cascade for the suppression of bile acid biosynthesis. *Genes Dev.* **17**: 1581–1591.

307. Potthoff, M. J., S. A. Kliewer, and D. J. Mangelsdorf. 2012. Endocrine fibroblast growth factors 15/19 and 21: from feast to famine. *Genes Dev.* **26**: 312–324.
308. Kir, S., S. A. Kliewer, and D. J. Mangelsdorf. 2011. Roles of FGF19 in Liver Metabolism. *Cold Spring Harb. Symp. Quant. Biol.*
309. Dawson, P. A., T. Lan, and A. Rao. 2009. Bile acid transporters. *J. Lipid Res.* **50**: 2340–2357.
310. Trauner, M., and J. L. Boyer. 2003. Bile salt transporters: molecular characterization, function, and regulation. *Physiol. Rev.* **83**: 633–671.
311. Jonker, J. W., C. Liddle, and M. Downes. 2011. FXR and PXR: Potential therapeutic targets in cholestasis. *J. Steroid Biochem. Mol. Biol.*
312. Neimark, E., F. Chen, X. Li, and B. L. Schneider. 2004. Bile acid-induced negative feedback regulation of the human ileal bile acid transporter. *Hepatology.* **40**: 149–156.
313. Insull, W. 2006. Clinical utility of bile acid sequestrants in the treatment of dyslipidemia: a scientific review. *South. Med. J.* **99**: 257–273.
314. van Heek, M., D. S. Compton, C. F. France, R. P. Tedesco, A. B. Fawzi, M. P. Graziano, E. J. Sybertz, C. D. Strader, and H. R. Davis. 1997. Diet-induced obese mice develop peripheral, but not central, resistance to leptin. *J. Clin. Invest.* **99**: 385–390.
315. Wang, D. Q.-H., and M. C. Carey. 2003. Measurement of intestinal cholesterol absorption by plasma and fecal dual-isotope ratio, mass balance, and lymph fistula methods in the mouse: an analysis of direct versus indirect methodologies. *J. Lipid Res.* **44**: 1042–1059.
316. Hyogo, H., S. Roy, B. Paigen, and D. E. Cohen. 2002. Leptin promotes biliary cholesterol elimination during weight loss in ob/ob mice by regulating the enterohepatic circulation of bile salts. *J. Biol. Chem.* **277**: 34117–34124.
317. Bustin, S. A., V. Benes, J. A. Garson, J. Hellems, J. Huggett, M. Kubista, R. Mueller, T. Nolan, M. W. Pfaffl, G. L. Shipley, J. Vandesompele, and C. T. Wittwer. 2009. The MIQE guidelines: minimum information for publication of quantitative real-time PCR experiments. *Clin. Chem.* **55**: 611–622.
318. VanPatten, S., N. Ranginani, S. Shefer, L. B. Nguyen, L. Rossetti, and D. E. Cohen. 2001. Impaired biliary lipid secretion in obese Zucker rats: leptin promotes hepatic cholesterol clearance. *Am. J. Physiol. Gastrointest. Liver Physiol.* **281**: G393–404.
319. Towbin, H., T. Staehelin, and J. Gordon. 1979. Electrophoretic transfer of proteins from polyacrylamide gels to nitrocellulose sheets: procedure and some applications. *Proc. Natl. Acad. Sci. U.S.A.* **76**: 4350–4354.

320. Folch, J., M. Lees, and G. H. S. Stanley. 1957. A simple method for the isolation and purification of total lipides from animal tissues. *J. Biol. Chem.* **226**: 497–509.
321. Schinkel, A. H., J. J. Smit, O. van Tellingen, J. H. Beijnen, E. Wagenaar, L. van Deemter, C. A. Mol, M. A. van der Valk, E. C. Robanus-Maandag, and H. P. te Riele. 1994. Disruption of the mouse *mdr1a* P-glycoprotein gene leads to a deficiency in the blood-brain barrier and to increased sensitivity to drugs. *Cell.* **77**: 491–502.
322. Schinkel, A. H., E. Wagenaar, L. van Deemter, C. A. Mol, and P. Borst. 1995. Absence of the *mdr1a* P-Glycoprotein in mice affects tissue distribution and pharmacokinetics of dexamethasone, digoxin, and cyclosporin A. *J. Clin. Invest.* **96**: 1698–1705.
323. Jeannesson, E., G. Siest, B. Bastien, L. Albertini, C. Aslanidis, G. Schmitz, and S. Visvikis-Siest. 2009. Association of ABCB1 gene polymorphisms with plasma lipid and apolipoprotein concentrations in the STANISLAS cohort. *Clin. Chim. Acta.* **403**: 198–202.
324. Carstea, E. D., J. A. Morris, K. G. Coleman, S. K. Loftus, D. Zhang, C. Cummings, J. Gu, M. A. Rosenfeld, W. J. Pavan, D. B. Krizman, J. Nagle, M. H. Polymeropoulos, S. L. Sturley, Y. A. Ioannou, M. E. Higgins, M. Comly, A. Cooney, A. Brown, C. R. Kaneski, E. J. Blanchette-Mackie, N. K. Dwyer, E. B. Neufeld, T. Y. Chang, L. Liscum, J. F. Strauss, K. Ohno, M. Zeigler, R. Carmi, J. Sokol, D. Markie, R. R. O'Neill, O. P. van Diggelen, M. Elleder, M. C. Patterson, R. O. Brady, M. T. Vanier, P. G. Pentchev, and D. A. Tagle. 1997. Niemann-Pick C1 disease gene: homology to mediators of cholesterol homeostasis. *Science.* **277**: 228–231.
325. Naureckiene, S., D. E. Sleat, H. Lackland, A. Fensom, M. T. Vanier, R. Wattiaux, M. Jadot, and P. Lobel. 2000. Identification of HE1 as the second gene of Niemann-Pick C disease. *Science.* **290**: 2298–2301.
326. Patel, S. B., G. Salen, H. Hidaka, P. O. Kwiterovich, A. F. Stalenhoef, T. A. Miettinen, S. M. Grundy, M. H. Lee, J. S. Rubenstein, M. H. Polymeropoulos, and M. J. Brownstein. 1998. Mapping a gene involved in regulating dietary cholesterol absorption. The sitosterolemia locus is found at chromosome 2p21. *J. Clin. Invest.* **102**: 1041–1044.
327. de Vogel-van den Bosch, H. M., N. J. W. de Wit, G. J. E. J. Hooiveld, H. Vermeulen, J. N. van der Veen, S. M. Houten, F. Kuipers, M. Müller, and R. van der Meer. 2008. A cholesterol-free, high-fat diet suppresses gene expression of cholesterol transporters in murine small intestine. *Am. J. Physiol. Gastrointest. Liver Physiol.* **294**: G1171–80.
328. Nissinen, M. J., H. Gylling, and T. A. Miettinen. 2008. Responses of surrogate markers of cholesterol absorption and synthesis to changes in cholesterol metabolism during various amounts of fat and cholesterol feeding among healthy

- men. *Br. J. Nutr.* **99**: 370–378.
329. Hofmann, A. F. 2001. Bile secretion in mice and men. *Hepatology*. **34**: 848–850.
330. Miedema, B. W., and J. O. Johnson. 2003. Methods for decreasing postoperative gut dysmotility. *Lancet Oncol.* **4**: 365–372.
331. Steinbrook, R. A. 1998. Epidural anesthesia and gastrointestinal motility. *Anesth. Analg.* **86**: 837–844.
332. Nilsson, A., and D. B. Zilversmit. 1972. Fate of intravenously administered particulate and lipoprotein cholesterol in the rat. *J. Lipid Res.* **13**: 32–38.
333. Nilsson, A., and D. B. Zilversmit. 1972. Release of phagocytosed cholesterol by liver macrophages and spleen cells. *Biochim. Biophys. Acta.* **260**: 479–491.
334. Repa, J. J., and D. J. Mangelsdorf. 2002. The liver X receptor gene team: potential new players in atherosclerosis. *Nat. Med.* **8**: 1243–1248.
335. Hozoji, M., Y. Munehira, Y. Ikeda, M. Makishima, M. Matsuo, N. Kioka, and K. Ueda. 2008. Direct interaction of nuclear liver X receptor-beta with ABCA1 modulates cholesterol efflux. *J. Biol. Chem.* **283**: 30057–30063.
336. Hozoji-Inada, M., Y. Munehira, K. Nagao, N. Kioka, and K. Ueda. 2011. Liver X receptor beta (LXRbeta) interacts directly with ATP-binding cassette A1 (ABCA1) to promote high density lipoprotein formation during acute cholesterol accumulation. *J. Biol. Chem.* **286**: 20117–20124.
337. Chisaki, I., M. Kobayashi, S. Itagaki, T. Hirano, and K. Iseki. 2009. Liver X receptor regulates expression of MRP2 but not that of MDR1 and BCRP in the liver. *Biochim. Biophys. Acta.* **1788**: 2396–2403.
338. Chan, G. N. Y., M. T. Hoque, C. L. Cummins, and R. Bendayan. 2011. Regulation of P-glycoprotein by orphan nuclear receptors in human brain microvessel endothelial cells. *J. Neurochem.* **118**: 163–175.
339. Tachibana, S., K. Yoshinari, T. Chikada, T. Toriyabe, K. Nagata, and Y. Yamazoe. 2009. Involvement of Vitamin D receptor in the intestinal induction of human ABCB1. *Drug Metab. Dispos.* **37**: 1604–1610.
340. Scotto, K. W. 2003. Transcriptional regulation of ABC drug transporters. *Oncogene.* **22**: 7496–7511.
341. Xie, W., A. Radomska-Pandya, Y. Shi, C. M. Simon, M. C. Nelson, E. S. Ong, D. J. Waxman, and R. M. Evans. 2001. An essential role for nuclear receptors SXR/PXR in detoxification of cholestatic bile acids. *Proc. Natl. Acad. Sci. U.S.A.* **98**: 3375–3380.

342. Staudinger, J. L., B. Goodwin, S. A. Jones, D. Hawkins-Brown, K. I. MacKenzie, A. LaTour, Y. Liu, C. D. Klaassen, K. K. Brown, J. Reinhard, T. M. Willson, B. H. Koller, and S. A. Kliewer. 2001. The nuclear receptor PXR is a lithocholic acid sensor that protects against liver toxicity. *Proc. Natl. Acad. Sci. U.S.A.* **98**: 3369–3374.
343. Geick, A., M. Eichelbaum, and O. Burk. 2001. Nuclear receptor response elements mediate induction of intestinal MDR1 by rifampin. *J. Biol. Chem.* **276**: 14581–14587.
344. Kliewer, S. A., B. Goodwin, and T. M. Willson. 2002. The nuclear pregnane X receptor: a key regulator of xenobiotic metabolism. *Endocr. Rev.* **23**: 687–702.
345. Xie, W., J. L. Barwick, C. M. Simon, A. M. Pierce, S. Safe, B. Blumberg, P. S. Guzelian, and R. M. Evans. 2000. Reciprocal activation of xenobiotic response genes by nuclear receptors SXR/PXR and CAR. *Genes Dev.* **14**: 3014–3023.
346. Radhakrishnan, A., Y. Ikeda, H. J. Kwon, M. S. Brown, and J. L. Goldstein. 2007. Sterol-regulated transport of SREBPs from endoplasmic reticulum to Golgi: oxysterols block transport by binding to Insig. *Proc. Natl. Acad. Sci. U.S.A.* **104**: 6511–6518.
347. Lange, Y., J. Ye, M. Rigney, and T. L. Steck. 1999. Regulation of endoplasmic reticulum cholesterol by plasma membrane cholesterol. *J. Lipid Res.* **40**: 2264–2270.
348. Lange, Y., J. Ye, and T. L. Steck. 2004. How cholesterol homeostasis is regulated by plasma membrane cholesterol in excess of phospholipids. *Proc. Natl. Acad. Sci. U.S.A.* **101**: 11664–11667.
349. Roberts, M. S., B. M. Magnusson, F. J. Burczynski, and M. Weiss. 2002. Enterohepatic circulation: physiological, pharmacokinetic and clinical implications. *Clin. Pharmacokinet.* **41**: 751–790.
350. Henikoff, S., and J. G. Henikoff. 1992. Amino acid substitution matrices from protein blocks. *Proc. Natl. Acad. Sci. U.S.A.* **89**: 10915–10919.
351. Schatton, T., G. F. Murphy, N. Y. Frank, K. Yamaura, A.-M. Waaga-Gasser, M. Gasser, Q. Zhan, S. Jordan, L. M. Duncan, C. Weishaupt, R. C. Fuhlbrigge, T. S. Kupper, M. H. Sayegh, and M. H. Frank. 2008. Identification of cells initiating human melanomas. *Nature.* **451**: 345–349.
352. Frank, N. Y., and M. H. Frank. 2009. ABCB5 gene amplification in human leukemia cells. *Leuk. Res.* **33**: 1303–1305.
353. Wilson, B. J., T. Schatton, Q. Zhan, M. Gasser, J. Ma, K. R. Saab, R. Schanche, A.-M. Waaga-Gasser, J. S. Gold, Q. Huang, G. F. Murphy, M. H. Frank, and N. Y. Frank. 2011. ABCB5 identifies a therapy-refractory tumor cell population in colorectal cancer patients. *Cancer Res.* **71**: 5307–5316.

354. Moitra, K., M. Scally, K. McGee, G. Lancaster, B. Gold, and M. Dean. 2011. Molecular evolutionary analysis of ABCB5: the ancestral gene is a full transporter with potentially deleterious single nucleotide polymorphisms. *PLoS ONE*. **6**: e16318.
355. Plösch, T., T. Kok, V. W. Bloks, M. J. Smit, R. Havinga, G. Chimini, A. K. Groen, and F. Kuipers. 2002. Increased hepatobiliary and fecal cholesterol excretion upon activation of the liver X receptor is independent of ABCA1. *J. Biol. Chem.* **277**: 33870–33877.
356. Romsicki, Y., and F. J. Sharom. 2001. Phospholipid flippase activity of the reconstituted P-glycoprotein multidrug transporter. *Biochemistry*. **40**: 6937–6947.
357. Jung, D., D. J. Mangelsdorf, and U. A. Meyer. 2006. Pregnane X receptor is a target of farnesoid X receptor. *J. Biol. Chem.* **281**: 19081–19091.
358. Lange, Y., and T. L. Steck. 1994. Cholesterol homeostasis. Modulation by amphiphiles. *J. Biol. Chem.* **269**: 29371–29374.
359. Buzza, M. S., S. Netzel-Arnett, T. Shea-Donohue, A. Zhao, C.-Y. Lin, K. List, R. Szabo, A. Fasano, T. H. Bugge, and T. M. Antalis. 2010. Membrane-anchored serine protease matriptase regulates epithelial barrier formation and permeability in the intestine. *Proc. Natl. Acad. Sci. U.S.A.* **107**: 4200–4205.
360. Issandou, M., and T. Grand-Perret. 2000. Multidrug resistance P-glycoprotein is not involved in cholesterol esterification. *Biochem. Biophys. Res. Commun.* **279**: 369–377.
361. Pinto, M., S. Robine-Leon, M. Appay, M. Kedubger, N. Triadou, E. Dussaulx, B. Lacroix, P. Simon-Assmann, K. Haffen, J. Fogh, and A. Zweibaum. 1983. Enterocyte-Like Differentiation and Polarization of the Human-Colon Carcinoma Cell-Line Caco-2 in Culture. *Biol. Cell*. **47**: 323–330.
362. Hauri, H. P., E. E. Sterchi, D. Bienz, J. A. Fransen, and A. Marxer. 1985. Expression and intracellular transport of microvillus membrane hydrolases in human intestinal epithelial cells. *J. Cell Biol.* **101**: 838–851.
363. Rousset, M. 1986. The human colon carcinoma cell lines HT-29 and Caco-2: two in vitro models for the study of intestinal differentiation. *Biochimie*. **68**: 1035–1040.
364. Lisanti, M. P., I. W. Caras, M. A. Davitz, and E. Rodriguez-Boulan. 1989. A glycopospholipid membrane anchor acts as an apical targeting signal in polarized epithelial cells. *J. Cell Biol.* **109**: 2145–2156.
365. Hubatsch, I., E. G. E. Ragnarsson, and P. Artursson. 2007. Determination of drug permeability and prediction of drug absorption in Caco-2 monolayers. *Nat. Protoc.* **2**: 2111–2119.

366. Bartlett, D. W., and M. E. Davis. 2006. Insights into the kinetics of siRNA-mediated gene silencing from live-cell and live-animal bioluminescent imaging. *Nucleic Acids Res.* **34**: 322–333.
367. Bartlett, D. W., and M. E. Davis. 2007. Effect of siRNA nuclease stability on the in vitro and in vivo kinetics of siRNA-mediated gene silencing. *Biotechnol. Bioeng.* **97**: 909–921.
368. Grès, M. C., B. Julian, M. Bourrié, V. Meunier, C. Roques, M. Berger, X. Boulenc, Y. Berger, and G. Fabre. 1998. Correlation between oral drug absorption in humans, and apparent drug permeability in TC-7 cells, a human epithelial intestinal cell line: comparison with the parental Caco-2 cell line. *Pharm. Res.* **15**: 726–733.
369. Sambuy, Y., I. De Angelis, G. Ranaldi, M. L. Scarino, A. Stamatii, and F. Zucco. 2005. The Caco-2 cell line as a model of the intestinal barrier: influence of cell and culture-related factors on Caco-2 cell functional characteristics. *Cell Biol. Toxicol.* **21**: 1–26.
370. Clayburgh, D. R., S. Rosen, E. D. Witkowski, F. Wang, S. Blair, S. Dudek, J. G. N. Garcia, J. C. Alverdy, and J. R. Turner. 2004. A differentiation-dependent splice variant of myosin light chain kinase, MLCK1, regulates epithelial tight junction permeability. *J. Biol. Chem.* **279**: 55506–55513.
371. Stevenson, B. R., J. D. Siliciano, M. S. Mooseker, and D. A. Goodenough. 1986. Identification of ZO-1: a high molecular weight polypeptide associated with the tight junction (zonula occludens) in a variety of epithelia. *J. Cell Biol.* **103**: 755–766.
372. Farquhar, M. G., and G. E. Palade. 1963. Junctional complexes in various epithelia. *J. Cell Biol.* **17**: 375–412.
373. Anderson, J. M., C. M. Van Itallie, M. D. Peterson, B. R. Stevenson, E. A. Carew, and M. S. Mooseker. 1989. ZO-1 mRNA and protein expression during tight junction assembly in Caco-2 cells. *J. Cell Biol.* **109**: 1047–1056.
374. Hunziker, W., M. Spiess, G. Semenza, and H. F. Lodish. 1986. The sucrase-isomaltase complex: primary structure, membrane-orientation, and evolution of a stalked, intrinsic brush border protein. *Cell.* **46**: 227–234.
375. Peterson, M. D., W. M. Bement, and M. S. Mooseker. 1993. An in vitro model for the analysis of intestinal brush border assembly. II. Changes in expression and localization of brush border proteins during cell contact-induced brush border assembly in Caco-2BBE cells. *J. Cell. Sci.* **105 (Pt 2)**: 461–472.
376. Muller, C., G. Laurent, and V. Ling. 1995. P-glycoprotein stability is affected by serum deprivation and high cell density in multidrug-resistant cells. *J. Cell. Physiol.* **163**: 538–544.

377. Zhang, W., and V. Ling. 2000. Cell-cycle-dependent turnover of P-glycoprotein in multidrug-resistant cells. *J. Cell. Physiol.* **184**: 17–26.
378. Xie, Y., M. Burcu, D. E. Linn, Y. Qiu, and M. R. Baer. 2010. Pim-1 kinase protects P-glycoprotein from degradation and enables its glycosylation and cell surface expression. *Mol. Pharmacol.* **78**: 310–318.
379. Zhang, Y., I. Zanotti, M. P. Reilly, J. M. Glick, G. H. Rothblat, and D. J. Rader. 2003. Overexpression of apolipoprotein A-I promotes reverse transport of cholesterol from macrophages to feces in vivo. *Circulation.* **108**: 661–663.
380. Calpe-Berdiel, L., N. Rotllan, C. Fiévet, R. Roig, F. Blanco-Vaca, and J. C. Escolà-Gil. 2008. Liver X receptor-mediated activation of reverse cholesterol transport from macrophages to feces in vivo requires ABCG5/G8. *J. Lipid Res.* **49**: 1904–1911.
381. Graf, G. A., W.-P. Li, R. D. Gerard, I. Gelissen, A. White, J. C. Cohen, and H. H. Hobbs. 2002. Coexpression of ATP-binding cassette proteins ABCG5 and ABCG8 permits their transport to the apical surface. *J. Clin. Invest.* **110**: 659–669.
382. Zhao, B., J. Song, and S. Ghosh. 2008. Hepatic overexpression of cholesteryl ester hydrolase enhances cholesterol elimination and in vivo reverse cholesterol transport. *J. Lipid Res.* **49**: 2212–2217.